

## ABSTRACT

Nonwovens are utilized in health, hygiene, and outdoor applications where uncontaminated and antibiofouling surfaces are crucial to sustain performance. Biofouling is the structured accumulation of unwanted, biological materials, self-encapsulated in a multilayered protective matrix, which adheres to porous and nonporous surfaces in the form of biofilm. Most commonly bacterial accumulation causes biofouling. The presence of antimicrobial drugs can inhibit bacterial growth, but the exposed bacteria tend to develop resistance against those agents over time. Biocides like antimicrobial agents (e. g. silver nanoparticles, chitosan, zinc particles etc.) are toxic and harmful to the ecology of some beneficial organisms. Hydrophilic coatings of polyethylene oxide or polyethylene glycol can deter the irreversible adhesion of microbes onto medical products. Further, it is known that nanoscale features can hinder bacterial attachment more readily than microscale features. Therefore, antibiofouling nonwovens that exhibit self-cleaning behaviors against bacterial and fungal microbes can be achieved through the careful tuning of surface chemistry and roughness. Hydrophobins are biological surfactants that aid in the adhesion of microbes onto surfaces. An understanding of hydrophobin assembly along fibrous structures (with and without modification) may give fundamental insight on how to prevent microbial adhesion.

The first objective of this study was to identify bacterial growth regimes that correlate to the most aggressive periods of nonwoven adhesion and to examine the correlation between bacteria cell wall nature and suspending liquid media chemistry with the surface chemistry of meltblown nonwovens to phenomenon governing bacterial adhesion.

The second research objective was to evaluate the performance of meltblown nonwovens tuned by the assembly of amphiphilic surfactants: Pluronic and bacterial hydrophobin against both the adhesion of both the gram negative and gram positive bacteria.

The third research objective was to analyze the role of surface modified nonwovens against bacterial adhesion under both the static and continuous flow conditions.

Meltblown Polypropylene (PP) nonwovens were chosen in this study for their performance against biofouling due to two reasons: highly porous structure easily contaminated by microorganisms and the meltblown fibers have similar fiber size as the typical size of bacteria (1 - 2  $\mu\text{m}$ ). Surface uniformity and porosity of meltblown nonwovens were varied using two different die geometries (BIAX and REICOFIL) to produce meltblown PP nonwoven samples. Fifteen samples were prepared having average fiber diameter of 1.2  $\mu\text{m}$  and basis weights of 15 - 25 gsm. Higher basis weight Reicofil fabrics having uniform fiber distribution showed more bacterial adhesion than Biax samples.

The growth cycle for two bacteria: gram negative - *Escherichia coli* (*E. coli*) and gram positive - *Bacillus cereus* (*B. cereus*) was characterized to ensure comparisons of microbial adhesion along growth phases. To analyze the effect of variable media chemistry over adhesion, four solvents: one pair of polar (chloroform-ethyl acetate) and one pair of nonpolar (hexadecane-decane) were used to characterize the hydrophilicity of bacterial cell wall. The results showed that within a fixed medium, the partitioning of both the bacteria at different solvents: water interface depends on their cell wall nature. Conventional surface analysis techniques are expensive to sterilize after testing with different bacteria. We have found an affordable tool which can be easily autoclave sterilized for continuous bacterial studies. Capillary surface tensiometer was used to measure the surface tension (ST) values of the suspending media for *E. coli* and *B. cereus*. Nutrient broth with varying concentrations of polar and apolar solvents were used as suspending media for both the bacteria. ST of liquid media were then correlated with the extent of bacterial adhesion (total no of viable bacteria). Within a fixed media and at various solvent- water interface, the migration of both the bacteria was governed by the electrostatic interaction between cell wall and solvent. The interaction between *E. coli* and *B. cereus* and neat meltblown PP nonwovens was imaged using scanning electron microscope (SEM).

The efficacy of hydrophilic coatings of polyethylene oxide-polypropylene oxide triblock copolymer (Pluronic) on meltblown PP nonwovens as deterrents against bacteria was investigated using X-ray photoelectron microscope. The change in hydrophilicity of nonwoven fabrics after coating with varying concentrations of Pluronic F-108 was evaluated by water

contact angles. The nonwoven surfaces were modified with varying concentrations of hydrophobin: H\* B protein and were exposed to continuous flow conditions inside a flow chamber. The extent of bacterial adhesion on these surface modified nonwovens were characterized in terms of change in hydrophilicity and surface roughness. Both hydrophobin modification and continuous flow increased *E. coli* adhesion than the control.

The findings provided insights of how the change in hydrophilicity and surface roughness after modification with amphiphilic Pluronic and hydrophobin influences the bacterial adhesion on meltblown PP nonwovens. The presence of Vistamaxx™ 8880 additive was found to improve the surface roughness of PP1550-Vista-RI. Surface tensions of untreated PP nonwoven fabrics range from 31 mN/m and cannot prevent the initial attachment of hydrophilic *E. coli* and *B. cereus* bacteria from the environment. SEM images showed maximum surface coverage after coating with 5 w/v % Pluronic. This resulted in pore blocking and decrease in RMS roughness by 33 % and also a decrease in water contact angles from 137.9 ° to 121.9 °. The SEM images of PP1550-RI and PP1550-Vista-RI showed increase in roughness due to wrinkling on the fibers after the Pluronic modification. This increase in surface roughness and moderate pore blockage after modification also resulted in slight decrease in water contact angles. The RMS roughness value associated with this 3%-plu-PP1550-Vista-RI was found to be intermediate ( $8.5 \pm 1.05 \mu\text{m}$ ) between roughness values for untreated and treated nonwovens. PP500-BX showed maximum drop in RMS roughness after 5w/v % Pluronic Treatment ( $7.5 \pm 0.44 \mu\text{m}$ ). PP1550-Vista-RI showed the maximum drop in water contact angle ( $\sim 28^\circ$ ) due to treatment with 3 w/v % of Pluronic.

Before Pluronic treatment and under static condition, higher resolution SEM image confirmed the presence of higher no of viable cells of *E. coli* on unmodified PP1550-Vista-RI. Under continuous flow conditions, the same trend for *E. coli* and *B. cereus* colonies on PP1550-Vista-RI was observed. Irrespective of the type of bacteria, PP-1550-Vista-RI had the maximum bacterial accumulation over time. After pluronic treatment, Between *E. coli* and *B. cereus*, the growth of the latter was more influenced by the Pluronic treatment. Under continuous flow conditions, the same trend for *E. coli* and *B. cereus* cells on PP1550-Vista-RI was observed. Irrespective of the type of bacteria, PP-1550-Vista-RI had the maximum bacterial accumulation over time ( $\sim 3.80 \text{ cfu/cm}^2$ ). PEO blocks of Pluronic copolymers tend to hinder the cell attachment and hence with

5 w/v % Pluronic in aqueous solution, PP1550-Vista-RI has almost zero bacteria. It is evident that the highest growth has been found on 5%-PP1550-RI in comparison to 1%-PP1550-RI. This drastic increase in *E. coli* growth may be due to the highest decrease in water contact angle (from 143 ° to 109 °). Also, there was negligible amount of *E. coli* on both 1 w/v % and 5 w/v % treated PP-1550-Vista-RI. Whereas 3%-plu-PP1550-Vista-RI has the maximum amount of *E. coli* among all three treated samples which again can be explained by the decrease in water contact angle after treatment with Pluronic solution (~ 105 °). Hydrophobic textiles with smaller pores might promote *E. coli* adhesion. All the nonwoven samples were still hydrophobic (lowest contact angle achieved ~ 105 °) even after 5 % Pluronic modification, but the combined effect of reduced pore sizes on modified nonwovens also contributed to more bacterial adhesion. In the case of *B. cereus*, the size of *B. cereus* bacteria may also play a key role in cell accumulation.

*E. coli* adhesion increased with the increase in concentration of hydrophobin due to the combined effect from increased roughness (~ 41 %) and wettability (~ 42 °). The assembly of hydrophobin onto nonwovens tuned the adhesion as such at 5 w/w % conc., adhesion was more than doubled from the number of initially attached bacteria. In case of continuous flow, growth continued till there was supply of nutrients even after 240 minutes. The number of colonies of *E. coli* was much higher in case of continuous flow than in static study. Both hydrophobin modification and continuous flow increased *E. coli* adhesion than the control. The results of this study are beneficial to design nonwoven surfaces with controlled parameters affecting the adhesion of commonly found pathogens.

© Copyright 2023 by Nahida Sultana  
All Rights Reserved

Nonwoven Surface Modification to Resist Particulate Attachment

by

Nahida Sultana

A dissertation submitted to the Graduate Faculty of

North Carolina State University

in partial fulfillment of the

requirements for the Degree of

Doctor of Philosophy

Fiber and Polymer Science

Raleigh, North Carolina

2023

APPROVED BY:

---

Dr. Ericka Ford

---

Dr. Mohamed Bourham

---

Dr. Jessica Gluck

---

Dr. Saad Khan

---

Chair of Advisory Committee

Dr. Ericka Ford

## **DEDICATION**

This work is dedicated to my family, my son Mohammad Usman Waasi, my mother, Hazera Begum and my father, Nazir Hossain and my husband, Md Mehedi Hasnat, for their endless love, support, and sacrifice to help me reach this milestone. This work is inspired by my beloved sister Nadia Sultana.

## **BIOGRAPHY**

Nahida Sultana was born in Dhaka, Bangladesh, to Hazera Begum, and Nazir Hossain. She received her BS in Applied Chemistry & Chemical Engineering in 2013 and MS in Applied Chemistry & Chemical Engineering in 2015 from the University of Dhaka. Before coming to the United States for her higher education, Nahida Sultana taught undergraduate courses as a lecturer in the Textile Engineering Department of Daffodil International University. She also worked as a Research Fellow in the Center for Advanced Research in Sciences in the University of Dhaka from 2015 to 2016. She started as a Ph.D. student at NC State in August 2017.



## **ACKNOWLEDGEMENTS**

I would like to express my deepest gratitude to my advisor, Dr. Ericka Ford, for her continuous guidance and support. Dr. Ford showed me how to overcome critical challenges in diverse research projects and grow as an individual researcher. I am grateful to Dr. Mohamed Bourham, Dr. Terrence Gardner, Dr. Jessica Gluck, Dr. Saad Khan for their support and valuable feedback on this dissertation. I am so grateful to Dr. Gluck for her immense patience in reviewing this dissertation.

I would like to thank Dr. Shuang Liu, Dr. Juan Frene, Dr. Debjyoti Biswas, Hannah Dedmon, Dr. Sachin Hiwale for helping me in my research.

Thanks to my husband, Md Mehedi Hasnat, who has been my mental strength throughout the challenging times of my Ph.D. studies. I am immensely lucky for my newborn son Usman Waasi. Despite being only 2 months old, Waasi has been my biggest strength to finish this work strong. I will remember those nights when I was awake breastfeeding my son and also editing this dissertation. I am thankful to my friends from home and abroad who believed and pushed me to achieve the best.

Finally, I would like to acknowledge the funding and support of this dissertation by the Nonwovens Institute, North Carolina State University.

## TABLE OF CONTENTS

LIST OF TABLES .....	viii
LIST OF FIGURES .....	x
CHAPTER 1.....	1
INTRODUCTION .....	1
1.1 Particulate Adhesion.....	1
1.1.2 Effects of Particulate Adhesion .....	1
1.1.3 Biofouling .....	2
1.1.4 Common Microorganisms Responsible for Biofouling .....	5
1.1.5 Range of Biofouling Occurrences .....	7
1.1.6 Prevention of Biofouling .....	10
1.1.7 Prevention of Nonwoven Biofouling.....	11
1.1.8 Hydrophobins.....	12
1.1.8.1 Background of Hydrophobins .....	12
1.1.8.2 Applications of Hydrophobins .....	13
1.1.9 Nonwovens.....	14
1.1.9.1 Why Nonwovens? .....	14
1.1.9.2 Meltblown Technology .....	14
1.1.9.3 Surface Modification of Nonwovens .....	16
1.2 Summary and Objectives .....	19
CHAPTER 2.....	20
PERSPECTIVE ON HOW THE FLUID CARRIER INDIRECTLY INFLUENCE THE BACTERIAL ADHESION ONTO NONWOVENS .....	20
2.1 Abstract.....	20
2.2 Introduction .....	21
2.3 Materials and Methods.....	24
2.3.1 Materials .....	24
2.3.2 Methods.....	24
2.3.2.1 Bacterial Cell Wall Chemistry Based on MATS Testing.....	25

2.3.2.2 Bacteria Count in Fluid Carriers .....	26
2.3.2.3 Fluid Surface Tension -Capillary Rise Technique .....	26
2.4 Results and Discussion .....	27
2.4.1 Bacterial Growth Cycles .....	27
2.4.2 Bacterial Cell Wall Affinity According to MATS Testing .....	28
2.4.3 Role of Bacteria Solution Surface Tension to Bacterial Growth .....	30
2.5 Conclusions.....	33
Acknowledgements.....	33
CHAPTER 3.....	34
BACTERIAL ADHESION ONTO PLURONIC TREATED, MELTBLOWN NONWOVENS UNDER STATIC AND CONTINUOUS FLOW MEDIA .....	34
3.1 Abstract.....	34
3.2 Introduction .....	34
3.3 Materials and Methods.....	38
3.3.1 Materials .....	38
3.3.2 Methods .....	38
3.3.2.1 Meltblowing of PP Nonwoven Fabrics.....	38
3.3.2.2 Pluronic Modification of PP Meltblown Nonwovens .....	40
3.3.2.3 Structure of Meltblown PP Nonwovens .....	40
3.3.2.4 Surface Characterization of Meltblown PP Nonwovens.....	41
3.3.2.5 Bacterial Suspension & Growth Media.....	41
3.3.2.6 Bacteria Count on PP Meltblown Nonwovens Under Static and Flow Conditions....	42
3.4 Results and Discussion .....	43
3.4.1 Meltblowing Die Effect on the Structure of Nonwovens.....	43
3.4.2 Effect of PP Nonwoven Structure on Bacterial Adhesion .....	47
3.4.3 Characterization of Pluronic Treated Meltblown PP Nonwovens .....	50
3.4.4 Effect of Pluronic Treatment on Bacterial Adhesion .....	52
3.5 Conclusions .....	56
Acknowledgments.....	57

CHAPTER 4.....	58
BACTERIAL ADHESION ONTO HYDROPHOBIN TREATED MELTBLOWN POLYPROPYLENE NONWOVENS UNDER STATIC AND CONTINUOUS FLOW CONDITION .....	58
4.1 Abstract.....	58
4.2 Introduction .....	59
4.3 Materials and Methods.....	63
4.3.1 Materials .....	63
4.3.2 Methods .....	63
4.3.2.1 Meltblowing of PP Nonwoven Fabrics.....	63
4.3.2.2 Characterization of Meltblown PP Nonwovens.....	64
4.3.2.3 Bacteria Count on PP Nonwovens at Static Conditions.....	65
4.3.2.4 Bacteria Count on PP Nonwovens Under Flow Conditions .....	65
4.3.2.5 Modification of Meltblown PP Nonwovens with Hydrophobin .....	66
4.3.2.6 Surface Characterization of Modified PP Nonwovens.....	66
4.4 Results and Discussion .....	67
4.4.1 Hydrophobin on Structure of Meltblown PP Nonwovens .....	67
4.4.1.1 Surface Wettability and Roughness of Modified Nonwovens.....	67
4.4.2 Bacteria Count on PP Nonwovens Under Static and Flow Conditions.....	69
4.4.1.2 Characterization of Hydrophobin Modification by XPS.....	72
4.5 Conclusions .....	74
Acknowledgements.....	75
CHAPTER 5.....	76
SUMMARY & CONCLUSIONS.....	76
APPENDICES .....	79
REFERENCES .....	81

## LIST OF TABLES

Table 1.1	Summary of numerous surface modification techniques applied to study bacterial adhesion and biofilm formation. . . . .	7
Table 2.1	Surface free energies of commonly found carriers and bacteria in medical and healthcare environments . . . . .	22
Table 2.2	Surface energy values of commonly used formulation in cosmetic liquids . . .	23
Table 2.3	Surface components of four solvents used in MATS test from literature . . . . .	29
Table 2.4	Mean surface tension values of carrier fluid during the growth of <i>E. coli</i> and <i>B. cereus</i> . . . . .	31
Table 2.5	Surface tension of bacteria at room temperature from literature . . . . .	31
Table 3.1	Meltblowing of PP nonwoven fabrics using different dies . . . . .	39
Table 3.2	Naming scheme of modified nonwovens . . . . .	40
Table 3.3	Nonwoven structures varied by manufacturing conditions . . . . .	44
Table 3.4	Surface properties of PP meltblown nonwovens loaded with the Pluronic copolymer . . . . .	46
Table 3.5	<i>E. coli</i> and <i>B. cereus</i> (log cfu/cm <sup>2</sup> ) cells adhered to nonwovens under static conditions . . . . .	47
Table 3.6	<i>E. coli</i> and <i>B. cereus</i> (log cfu/cm <sup>2</sup> ) cells adhered to nonwovens at a shear rate of 50 s <sup>-1</sup> . . . . .	49
Table 3.7	Mean colony forming units attached to modified nonwovens under static conditions . . . . .	55
Table 4.1	Change in mass and ninhydrin test before and after hydrophobin modification	67
Table 4.2	Mean surface hydrophobicity and roughness of Meltblown PP nonwovens before and after hydrophobin treatment . . . . .	68
Table 4.3	Mean <i>E. coli</i> attachment at static condition on unmodified and modified PP nonwovens . . . . .	69

Table 4.4 Mean *E. coli* attachment at 0.11 cm<sup>3</sup> s<sup>-1</sup> flowrate inside flow cell at time intervals ..... 70

Table 4.5 Comparison of static vs continuous study via t-test ..... 71

Table 4.6 Elemental composition of the unmodified and modified PP nonwovens ..... 74

Table 5.1 Varying degrees of bacterial adhesion on polypropylene nonwoven fabrics .. 77

Table A1 Probe liquids and their surface tension components from literature ..... 79

Table B1 Nonwoven surface tensions measured from the contact angle study show no trend ..... 80

## LIST OF FIGURES

Figure 1.1	Length scale of micro and nanomaterials . . . . .	1
Figure 1.2	Presence of biofilm on the inner surface of a polyurethane stent . . . . .	2
Figure 1.3	The major steps in biofilm formation; A: Adsorption of conditioning film components; B: microbial transport and coaggregation; C: (reversible) adhesion of single organisms and of microbial coaggregates; D: co-adhesion between microbial pairs; E: anchoring or the establishment of firm, irreversible adhesion through exopolymer production; F: growth . . .	4
Figure 1.4	Process of meltblown technique . . . . .	16
Figure 2.1	Surface tension of fluids using capillary surface tension analyzer . . . . .	27
Figure 2.2	Growth of a) <i>B. cereus</i> , and b) <i>E. coli</i> by plate inoculation method . . . . .	28
Figure 2.3	Optical density measurements of (a) <i>B. cereus</i> , (b) <i>E. coli</i> at 600 nm in nutrient broth media with time; incubated at 37 °C at 150 rpm . . . . .	28
Figure 2.4	The percentage affinity of <i>E. coli</i> and <i>B. cereus</i> suspended in control potassium phosphate buffer solution to polar (chloroform, ethyl acetate) and non-polar (decane, hexadecane) solvent interfaces, * = $p < 0.05$ . . . .	30
Figure 2.5	Growth of <i>E. coli</i> and <i>B. cereus</i> upon diluting nutrient broth fluids with organic, carrier liquids. The surface tension of each solvent is shown relative to each other . . . . .	32
Figure 3.1	Chemical structure of (a) PP and (b) Pluronic F-108 . . . . .	36
Figure 3.2	Schematics of the (a) meltblowing process, (b) meltblown PP nonwoven, die cross-sections: (c) Reifenhauser Reicofil™ and (d) Biax Fiberfilm . . . .	39
Figure 3.3	(a) Convertible flow cell assembly, (b) Phase contrast microscope, 40X objective lens . . . . .	43
Figure 3.4	Pore size distribution vs pore diameter, basis weight of (a) PP500-BX, (b) PP1550-RI and (b) PP1550-Vista-RI . . . . .	45

Figure 3.5	Topography of PP500-BX, PP1550-RI, and PP1550-Vista-RI before (a), (b), (c) and after modification with 5 w/v % aqueous pluronic solution (d), (e), (f) respectively . . . . .	45
Figure 3.6	Water contact angles of (i) PP500-BX, (ii) PP1550-RI and (iii) PP1550-Vista-RI before and after 0, 1 %, 3 % and 5 % Pluronic treatment; highlighted panels indicate most hydrophobic (PP1550-RI, ~ 143 °) and most hydrophilic (PP1550-Vista-RI ~ 105.6 °) surfaces. . . . .	46
Figure 3.7	<i>E. coli</i> and <i>B. cereus</i> (log cfu/cm <sup>2</sup> ) cells adhered to nonwovens under static conditions (aerobic incubation at 80 rpm at 30 °C for about 48 h), error bars indicate standard deviation, *p < 0.05 . . . . .	47
Figure 3.8	Scanning electron micrographs of PP meltblown nonwovens after 48 h of static incubation with <i>E. coli</i> : (a), (d): PP500-BX, 17 gsm; (b), (e): PP1550-RI, 25 gsm; (c), (f): PP1550-Vista-RI, 25 gsm . . . . .	48
Figure 3.9	<i>E. coli</i> and <i>B. cereus</i> (log cfu/cm <sup>2</sup> ) cells adhered to nonwovens at a shear rate of 50 s <sup>-1</sup> , error bars indicate standard deviation. . . . .	50
Figure 3.10	Representative XPS spectra of nonwoven fabrics (PP500-BX, PP1550-RI, PP1550-Vista-RI) after 0 %, 1 % and c) 5 % Pluronic treatment . . . . .	52
. . . . .		
Figure 3.11	<i>E. coli</i> and <i>B. cereus</i> attachment to modified nonwovens under static conditions, error bars indicate standard deviation, *p < 0.05 . . . . .	54
Figure 3.12	Scanning electron micrographs of Pluronic treated PP meltblown nonwovens after 48 h of static incubation with <i>E. coli</i> lowest (0.34 cfu/cm <sup>2</sup> ) and highest (0.98 cfu/cm <sup>2</sup> ) count on 1%-PP1550-RI and 5%-PP1550-RI respectively) . . . . .	56
Figure 4.1	Crystal structure of hydrophobin . . . . .	62
Figure 4.2	The (a) meltblowing process, (b) a meltblown PP nonwoven, and (c) the cross-section of a Reifenhauser Reicofil™ die . . . . .	64



Figure 4.3	a) Convertible flow cell assembly, b) Phase contrast microscope, 40X objective lens . . . . .	66
Figure 4.4	SEM images of nonwoven fabrics PP1550-RI before and after hydrophobin treatment . . . . .	68
Figure 4.5	<i>E. coli</i> adhesion by No of <i>E. coli</i> ( $10^6$ /cm <sup>2</sup> ) $\pm$ 0.05 as influenced by the hydrophobin treatment at static conditions, error bars indicate standard deviation, *p < 0.05 . . . . .	70
Figure 4.6	The number of <i>E. coli</i> adhering to PP meltblown nonwovens as a function of time in a 40 mM potassium phosphate buffer (pH 7.0) during exposure to 50 s <sup>-1</sup> shear rate in a flow chamber, error bars indicate standard deviation . . . . .	71
Figure 4.7	<i>E. Coli</i> adhesion onto meltblown PP nonwovens (a) with (i. e. 5%-HB-PP1550-RI) and (b) without 5% hydrophobin under static and continuous flow conditions . . . . .	73
Figure 4.8	Schematic of hydrophobin coated PP nonwovens. . . . .	73
Figure 4.9	XPS spectra of nonwoven fabrics PP1550-RI after hydrophobin treatment . . . . .	73

# CHAPTER 1

## INTRODUCTION

### 1.1 Particulate Adhesion

The attachment of soil, dust, microorganisms, and/or chemical particulates onto polymeric surfaces results in soiling or fouling. Adhesion of particulates to any surface or to themselves is a result of attractive forces between different surfaces. Particles which have submicron dimensions (Figure 1.1), are causing serious problems related to fouling and the adhesion on any surface.<sup>1</sup>

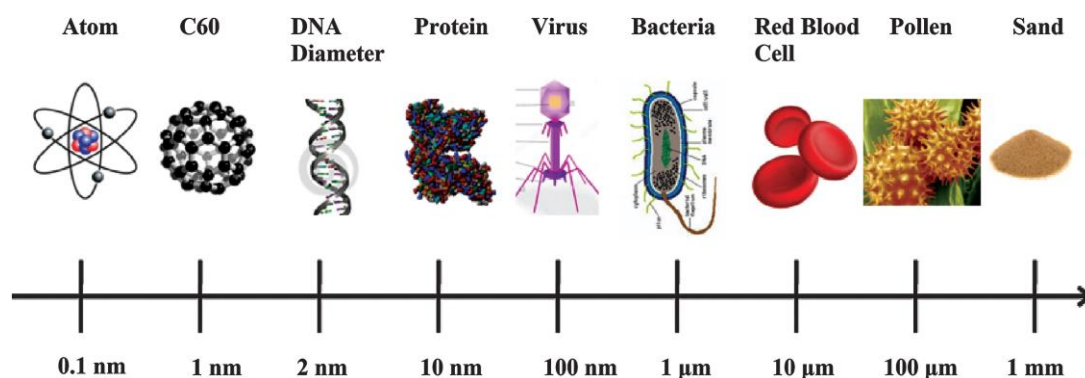


Figure 1.1. Length scale of micro and nanomaterials.<sup>2</sup>

In both air and water, adhesion of submicron particles depends on Van der Waals forces of attraction. In an aqueous environment the particles adhesion is determined by the electrostatic double layer force of repulsion in addition to the Van der Waals force of attraction.

The adhesion of both living and non-living particulates onto the surface of polymers, biomaterials, medical devices, and textiles has been studied intensively for years as fouling affects various aspects of our life. A detailed understanding of effects produced by the attachment of particles on surfaces can only lead us to realize real controlling strategies.

#### 1.1.2 Effects of Particulate Adhesion

Particulate adhesion can be either desirable (e. g. paints, print industry) or undesirable (filter beds, membranes). Adsorption of organic compounds present in the effluent cause membrane

fouling in a textile effluent plant. Fouling of membranes during filtration causes higher operational costs due to frequent cleaning required. Protein adsorption on biological implants may lead to biofilm formation as a result of conditioning layer of organic compounds formed on the implants.<sup>3</sup> Therefore, it is essential to design polymeric fibers or films or membranes which are less susceptible to fouling. Fouling at the surface of porous textiles or films can mar their performance- in terms of breathability, air permittivity, and even their filtration efficiency. Textile scientists are dedicated to developing newer fibers and textiles with inherent antibiofouling properties. Self-cleaning textiles mimicking the lotus leaf effect is an example of such scientific study incorporating a surface with antibiofouling features.<sup>4</sup>

### **1.1.3 Biofouling**

The detrimental bioadhesion between materials is known as biofouling. Among all kinds of attachments, adhesion of microorganisms or biofouling is the most crucial form in terms of their effects and mechanism of adhesion. Once microorganisms are attached to a substratum surface, a multistep process starts leading to the formation of a complex, adhering microbial community that is termed as 'biofilm'. A biofilm is a complex heterogeneous structure in which microorganisms are protected from harsh environments like nutrient deficient and hydrodynamic conditions. Biofilms are resistant to antibiotics and drugs and may lead to infections and diseases.<sup>5, 6</sup>

### **Mechanism of Biofouling**

The phenomenon by which bacteria adhere to most surfaces by forming a layer of complex and heterogeneous microbial communities is called biofilm formation.<sup>7</sup>

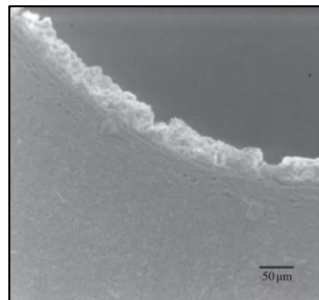


Figure 1.2. Presence of biofilm on the inner surface of a polyurethane stent.<sup>8</sup>

Biofilm formation is facilitated by different types of interactions which can be specific, for example through a protein film that might have formed on the surface, or through nonspecific interactions.<sup>3</sup> The buildup of bacterial community on a polyurethane stent<sup>8</sup> (Figure 1.2) and dental plaques caused by more than 500 bacterial strains are classic examples of biofilms.<sup>9</sup>

Figure 1.3 schematically presents the initial steps in the formation of a complex, multispecies biofilm. When microorganisms and substratum surfaces are in an aqueous environment, in which organic matter is present (e. g. sea water, milk, tear fluid, urine, blood or saliva etc.), substratum surfaces will first become covered with a layer of adsorbed, organic molecules, generally called "conditioning film", prior to microorganisms adhere, simply because transport and adsorption of molecules to a substratum proceed relatively fast compared to that of microorganisms. Transport of microorganisms towards a substratum surface, as the second step in biofilm formation can occur by different mechanisms, depending on the system, and may include Brownian motion, gravitation, diffusion, convection, or the intrinsic motility of a microorganism. Alternatively, microorganisms in suspension can be transported towards each other and microbial co-aggregates can be formed. Subsequently, microbial adhesion to a substrate (either of single organisms or of co-aggregates) may occur which is often initially reversible and becomes irreversible after certain time period through the excretion of exopolymeric substances (EPS) by the adhering microorganisms. Time period from initial adhesion to irreversibility will depend on the interaction between the EPS and the substrate (favorable interactions are steric interactions)<sup>10</sup> and in situ EPS secretion may strengthen adhesion resulting in irreversible adhesion. Sometimes the excreted, exopolymeric substance adsorbs to a substratum surface to form a microbially derived conditioning film, as opposed to host or environmentally derived conditioning films. When a conditioning film is present, an adhering microorganism is usually not in contact with the actual substratum surface and the strength of biofilm formation becomes dependent upon the cohesiveness of the conditioning film, rather than upon its direct interaction with the bare substratum surface. Only a few adhering, sessile microorganisms can stimulate the adhesion of other, still suspended planktonic microorganisms. This may occur by sessile microorganisms slowing down an approaching, planktonic microorganism, thus increasing its

chance of adhering to the substratum surface, as is frequently observed under flow or through strong attractive interactions between sessile and planktonic microorganisms, a phenomenon known as co-adhesion. Eventually, adhering microorganisms start growing, which the major factor is contributing to the accumulation of a high number of cells on a substratum surface.

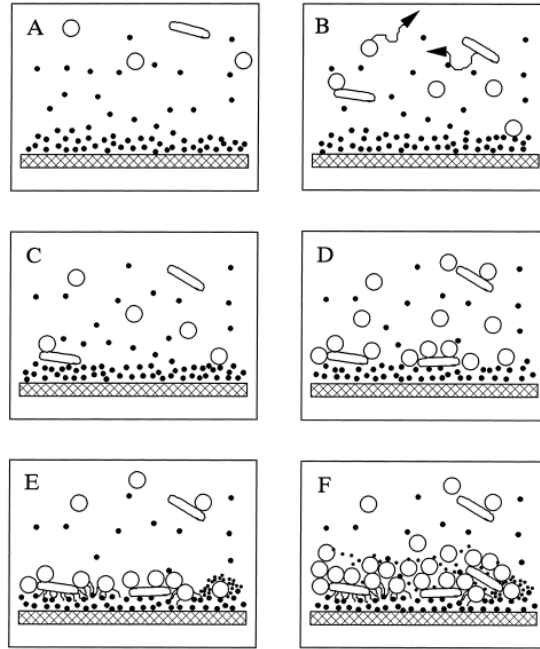


Figure 1.3. The major steps in biofilm formation; A: Adsorption of conditioning film components; B: microbial transport and coaggregation; C: (reversible) adhesion of single organisms and of microbial coaggregates; D: co-adhesion between microbial pairs; E: anchoring or the establishment of firm, irreversible adhesion through exopolymer production; F: growth.<sup>7</sup>

Roughness has an influence on biofilm formation but regarding initial adhesion roughness appears to be a minor factor. The influence of surface roughness on biofilm formation is more related to the difficulties involved in cleaning the rough surfaces, resulting in rapid re-growth of a biofilm, rather than to being a contributing factor on its own. From a physico-chemical, mechanistic point of view, a rough surface is a folded, flat surface with an extended surface area from which similar interaction forces arise as from a smooth surface.

Although microbial adhesion to inert substratum surfaces as well as to other microbial cell surfaces (i.e. co-aggregation or co-adhesion) is frequently described in terms of specific

interactions between localized, specific molecular groups and sometimes even in terms of specific forces as being a separate class of fundamental interaction forces, it is important to realize that all interaction forces originate from the same fundamental forces, including the ever present Van der Waals forces, electrostatic forces, and acid-base interactions. Moreover, whereas specific interactions are highly directional, spatially concerned between molecular groups and consequently operative over small distances, say smaller than 5 nm, the so-called non-specific association in microbial adhesion arises from interaction forces between all molecules of the entire cell and substratum and are consequently of a more long-range character. Therefore, to adequately describe microbial adhesive interactions, either between two microbial species or between a microorganism and a substratum surface, both the overall, long-range, and non-specific fundamental interaction forces and short-range, specific interactions, as a corollary of the same fundamental forces, now between microscopic stereo-chemical groups, must be taken into consideration. Proper identification of receptor/ligand partnership is very crucial for disruption of bacteria adhesion. Specific molecules such as lactoferrin<sup>11</sup>, lysozymes<sup>12</sup>, prebiotic oligosaccharides<sup>13</sup> are used to mediate the interaction between host cell and bacteria as they can change the host response by consistently pairing with the host receptors.<sup>14</sup>

#### **1.1.4 Common Microorganisms Responsible for Biofouling**

##### **Bacteria**

Nonwoven fabrics (NWF) have become popular for filtration applications due to their low cost, easy processability and good filtration efficiency.<sup>15</sup> NWF used as filtration membrane require bacteria free surface since bacterial adhesion limits their potential applications in water treatment. Most common strains are *Escherichia coli* (*E. coli*), *Streptococcus* sp., *Staphylococcus* sp. which readily form biofilms on membrane surface.

Bacterial adhesion on biomaterial surfaces and subsequent colonization lead to infection which is the one of the major causes for failure of medical devices and implants. *Staphylococcus epidermidis* and *Staphylococcus aureus* are two major species responsible for biomaterials infections.<sup>16</sup> *E. coli* has been found on catheters as infectious biofilms.<sup>17</sup>

Bacterial attachment depends on their growth phase. Understanding the relationship between bacterial growth curves and attachment will allow us to compare bacterial adhesion across the same or most aggressive growth phases for adhesion. The attachment of bacteria to a substratum surface depends on two events: when the bacteria get close to a surface enough for attachment and then when the interaction of bacterial surface and the substratum surface occurs by their adhesive properties. The probability of bacteria encountering a substratum surface depends on the nature of culture and bacteria motility.<sup>18</sup> The rate of bacterial attachment was found to be the greatest within the exponential phase than the stationary and death-phase cultures. There was a progressive decrease in adhesion with the latter two phases.<sup>18</sup> The properties of bacteria that influence the colonization and finally the biofilm formation of bacteria on a surface are cell surface properties. Cell surface properties such as cell components, appendages<sup>19</sup>, motility<sup>19</sup>, cell surface hydrophobicity<sup>20</sup>, colony spreading<sup>20</sup>, and slime production<sup>20</sup> are found to be influenced by the life-cycle of the microorganisms and most importantly on their growth phase within closed system.<sup>21</sup> Motile bacteria can actively search, sense and accumulate toward a favorable environment by using a flagellum, a surface appendage while non-motile bacteria deposition is mainly governed by the gravitational sedimentation as they lack appendages.<sup>19</sup> Non-motile bacteria with no appendages use fluid flow to attach to a surface.<sup>22</sup> Whereas flagella help to firmly attach cells to any substrate surface by electrostatic attraction and thus work as an anchor for motile bacteria. *E. coli* with flagellum showed increased adhesion to PDMS surface than the strain of *E. coli* without flagellum.<sup>23</sup> The diffusion coefficient for motile bacteria is 3 times higher than that of non-motile bacteria which increases the adhesion rate and eventually increases the total number of adherent cells per unit volume.<sup>19</sup> Gram positive bacteria have long glycan chains which make them negatively charged and hydrophilic and hence attach easily onto hydrophobic surfaces.<sup>19</sup> Most of the natural and manmade systems are exposed to a combination of various microorganisms with different size, shape, motility, and cell types resulting complex reactions toward environment. Therefore, it is especially important to study details of bacteria surface properties to understand complex interactions.

### 1.1.5 Range of Biofouling Occurrences

Biofouling is relevant in numerous applications such as textiles, food packaging and storage, surgical and protective equipment in hospital, biological implants, health and hygiene products, water and beverage filtration systems.<sup>3</sup>

Most literature shows tuning hydrophilicity of the surface would reduce bacterial and fungal adhesion. Several approaches have been made to analyze the factors affecting biofouling to membranes and polymer surfaces whereas biofouling to porous nonwovens lacks any extensive work. Since nonwovens are utilized in health, hygiene, and outdoor applications, comprehensive studies should be done to enhance their ability to deter or reverse microbial attachment. Nonwoven textiles comprise an interconnected pore structure that would undergo blockage when their surfaces are soiled. Particulate attachment is often the result of nonspecific binding that is often associated with hydrophobic or nonspecific intermolecular attraction. Therefore, nonwoven surfaces that deter particulate attachment or prevent irreversible adhesion are desired. Studies have been limited to only protein fouling of textiles, nonwoven membranes.

**Table 1.1** Summary of numerous surface modification techniques applied to study bacterial adhesion and biofilm formation.

Modification technique	Literature	Summary/Result
Surface abrasion	Siddiquie et al., 2020 <sup>24</sup>	Highly regular and single scale submicron laser induced periodic surface structures (LIPSS) and multiscale structures (MSs) containing both submicron- and micron-scale features. Both LIPSS and MS topographies on PDMS and PU elastomeric surfaces reduced (> 89%) the adhesion of Gram-negative <i>Escherichia coli</i> bacteria.



**Table 1.1** (continued).

	Chien et al., 2020 <sup>25</sup>	The microscale topography of shark skin slightly promoted bacterial attachment at an early stage but prevented bacteria from developing biofilms. Induced shark skin structure provided a physical barrier, preventing the expansion into microcolonies of small bacterial clusters present in the recesses, and interfering with quorum sensing.
	Epperlein et al., 2017 <sup>26</sup>	Periodic surface structure with a spatial period of 700 nm induced by femtosecond laser technique leads to an increase in surface area. The contact area for <i>E. coli</i> was reduced, diminishing colonization on the laser induced periodic surface structures (LIPSS) areas. The distance between the LIPSS ridges was less than 300 nm, which prevented <i>E. coli</i> adhesion within LIPSS. In contrast, <i>S. aureus</i> adhered to the structure, possibly because of its coccoid geometry.
	Xu et al., 2014 <sup>27</sup>	Submicron and micron textured polyurethane surfaces featuring ordered arrays of pillars were modified by air plasma to have different wettabilities. All the textured surfaces were originally hydrophobic and showed significant reductions in <i>Staphylococcus epidermidis</i> adhesion.
	Morgan et al., 2001 <sup>28</sup>	The type of acrylic used, and its roughness, affects the initial stages of biofilm formation by <i>Streptococcus oralis</i> . The number of bacteria adhering to heat-cure and cold-cure acrylic increased linearly with mean surface roughness after 2 h incubation, the increase being greater for the cold-cure than the heat-cure acrylic. After 4 h incubation, surface roughness had no effect on the number of adherent bacteria.

**Table 1.1** (continued).

	Pasmore et al., 2001 <sup>29</sup>	Biofilm initiation by a strain of <i>Pseudomonas aeruginosa</i> increases with increase in surface roughness and fouling was minimal when surface charge increases, whether positive or negative.
Chemical coating	Harris et al., 2004 <sup>30</sup>	Coating titanium with sodium hyaluronate significantly decreased the density of <i>Staphylococcus aureus</i> adhering to the surfaces.
Chemical grafting	Terada et al., 2012 <sup>31</sup>	Polyethylene (PE) sheets were modified by radiation-induced graft polymerization (RIGP) of an epoxy-group containing monomer glycidyl methacrylate (GMA). <i>E. coli</i> density and viability depended on sheet surface electrostatic property.
	Nejadnik et al., 2008 <sup>32</sup>	Brush-coatings made of a tri-block copolymer of polyethylene oxide (PEO) and polypropylene oxide (PPO) prevented adhesion of <i>Staphylococci</i> to below $5 \times 10^5 \text{ cm}^{-2}$ after 30 min of incubation. Biofilms on brush-coatings are more viable and easily removed by the application of fluid shear.
	Park et al., 1998 <sup>33</sup>	Polyethylene glycol (PEG) modified surfaces reduced bacterial adhesion significantly and the degree of adhesion differs depending on surfaces as well as media.
Chemical grafting	Roosjen et al., 2004 <sup>34</sup>	Bacterial adhesion to Polyethylene oxide (PEO) brushes in a parallel plate flow chamber was decreased with respect to adhesion to bare glass, except for hydrophobic bacteria. This decrease was caused by attenuation in Van der Waals attractive energies.

A study revealed that the modification of commercial polypropylene nonwoven fabric (PP-NWF) membranes with hydrophilic graphene oxide (GO) nanosheets improved water permeability.<sup>29</sup> The -OH groups from the immobilized GO nanosheets enhanced water permeability by improving membrane hydrophilicity which consequently resulted in improved antifouling property.

In another study coating of NWF membranes with chitosan enhanced the antifouling property as the resistance to irreversible fouling was decreased.<sup>30</sup> Grafting of poly(N-vinyl-2-pyrrolidone) (PNVP) on PP-NWF resulted in reversible bacterial adhesion due to improved hydrophilicity.<sup>31</sup>

In another approach of surface modification of polypropylene NWF by polyvinyl alcohol (PVA) led to improved antifouling property by decreasing bovine serum albumin adsorption.<sup>32</sup>

Self-cleaning behavior or reversible particulate attachment is challenging to achieve among nonwoven textiles, especially against biofouling. At the root of biofouling is the attachment of microorganisms that are less than 10 micrometers in length onto the surface of nonwovens. Applications where self-cleaning, anti-biofouling nonwovens are desirable include water purification and beverage filtration. Especially since the use of chemical disinfectants are less than desirable and a notable increase in the hours of filter operation would improve filtration efficiency. Therefore, nonwoven surfaces that deter microorganism attachment or prevent irreversible bioadhesion are desired.

### **1.1.6 Prevention of Biofouling**

Anti-fouling researchers have proposed methods to improve the resistance of surfaces to fouling. PVA-modified polypropylene NWF membranes by dip coating method resulted in membranes with improved antifouling properties.<sup>32</sup> Chemical grafting methods are found to be comparatively difficult to scale up; physical adsorption is another alternative anti-fouling treatment which is easily achieved, because the surface is directly immersed in a solution containing the hydrophilic polymer such as poly(ethylene glycol) (PEG) that will provide the antifouling properties to the surface.<sup>33</sup> Rapid motion of highly mobile and heavily hydrated PEG in aqueous solution possess few sites for binding and hence reject fouling by incoming protein molecule.

Another approach to combat bacterial adhesion on biomaterial surfaces is introduction of nano- or micro texture to the surface. Micro- or nano-size features like porosity and surface roughness were found to influence bacterial adhesion and biofilm formation significantly.<sup>34</sup> Surface roughness and hydrophobicity depend on the interaction between surface appendages of bacteria i. e. flagella, fimbria and topographical features.<sup>35</sup> Li-Chong Xu et al. developed a polyurethane surface consisting of submicron and micron textures with improved wettability.<sup>27</sup> Unmodified polyurethane surfaces were hydrophobic and after plasma treatment, bacterial adhesion was reduced and was directly dependent on size of the patterns present on the surfaces. The submicron patterns reduced bacterial adhesion, while the micron patterns caused an increase in *Staphylococcus epidermidis* adhesion.<sup>27</sup>

#### **1.1.7 Prevention of Nonwoven Biofouling**

NWF are very popular in filter applications<sup>30</sup> and wet-laid, meltblown and spunbonded NWF having micron sized fibers are used due to their low cost, easy processibility and good filtration efficiency.<sup>36</sup> NWF are also used as membranes in ultra or nanofiltration.<sup>37</sup> In liquid filtration, the potential application of hydrophobic NWF is limited due to severe fouling. The interaction between microbial cells, proteins and membrane materials with hydrophobic NWF membranes lead to extensive biofouling.<sup>38</sup> As a result, much attention has been made to reduce membrane fouling by modifying hydrophobic membranes to relative hydrophilic ones. Coating porous membrane with hydrophilic and functional polymer can enhance the performance of the membrane filtration<sup>39</sup> and thus it could be a suitable candidate to overcome its shortcomings. Yoon et al. has fabricated a high flux ultrafiltration membrane based on electrospun nanofibrous poly acrylonitrile (PAN) scaffolds and chitosan coating.<sup>40</sup> Zhang et al. has studied the permeability and antifouling property of the composite NWF membrane which was dip-coating by polyvinyl alcohol.<sup>32</sup> Recently, different methods have been proposed for functionalization of NWF membrane by polyvinyl alcohol/4-vinylpyridine copolymer to prepare antifouling membranes. Ranran Feng et al.<sup>31</sup> suggested that the hydrophilic modified membranes can effectively reduce the adhesion of bacteria on the membrane surfaces. However, the reversibility of attached bacteria on the membrane surface is also crucial. If the bacteria reversibly attached to the

membrane surface can be washed away by physical cleaning, it will be beneficial for the inhibition of the bacterial growth and subsequent biofilm formation. Therefore, hydrophilic and rougher membrane surface provided strong repulsive forces between the cells and membrane surface, and the cells near the membrane surface can be easily washed away by physical cleaning. In conclusion, the PNVP-modified membranes showed a much-suppressed number of adhered bacteria on the surface than the unmodified NWF membrane, and the bacteria adhered on the membrane surface were reversible, indicating that the anti-bacterial adhesion ability and antibiofouling property of NWF membranes can be improved by the immobilization of hydrophilic PNVP.

### **1.1.8 Hydrophobins**

#### **1.1.8.1 Background of Hydrophobins**

Bacterial and fungal microbes release amphiphilic proteins to aid their attachment onto hydrophobic surfaces and from the bulk of liquid media. These proteins called hydrophobin self-assemble as multilayers from which microorganisms can colonize into drug resistant biofilms. Hydrophobins are small proteins of about 100 to 150 amino acids which are characteristic of filamentous fungi, for example *Schizophyllum commune*. They have unique properties of stability against pH, temperature, solvents, detergents, and ability to modify surfaces and interphases (Teflon, Carbon, PP, PE, PET, Al, wood, SiO<sub>2</sub>). Even under in vitro or technical conditions hydrophobins can reverse the surface polarity by easily self-assembling at interfaces.<sup>41</sup>

BASF successfully produced two artificial hydrophobins called H\*Protein A and H\*Protein B in kilogram scale.<sup>42</sup> In nature, the fungi seem to use hydrophobins for altering their environment for themselves to thrive. At the air-water interface the SC3 hydrophobin from *Schizophyllum commune* self-assembles to form an amphiphilic coating which lowers the surface tension and allows the fungus to grow through it.<sup>43</sup> Hydrophobin surface layers also seem to mediate the attachment of pathogenic fungi to the host surface, such as plant or insect cuticle.<sup>44</sup> The SC3 hydrophobin has been found to form very stable coatings on hydrophobic materials such as Teflon and Parafilm, and thereby make them more hydrophilic.<sup>43</sup> Self-assembly of hydrophobins

change a surface from hydrophilic to hydrophobic, while hydrophobic material becomes hydrophilic. The water contact angle of the hydrophobic and hydrophilic side of the assembled hydrophobin was found to be in between 60° and 120° and between 22° and 60°, respectively.<sup>45</sup>

#### **1.1.8.2 Applications of Hydrophobins**

The novel properties of hydrophobins provide potential applications such as use in tissue engineering, particularly in coating of surfaces with a natural protein to increase the biocompatibility<sup>46</sup>. Hydrophobins affect the surface attachment of microbes and several studies have been done to understand the effect of hydrophobins on nonwovens surface. Hydrophilic surfaces are known to impede biofouling. Likewise, roughness along films reduces bacterial attachment and enables their removal under agitation.<sup>47</sup> Therefore, surficial modification of the device by coating with hydrophobin and multiscale roughness are posed as synergistic strategies for attachment deterring that inhibit the root cause of bacterial attachment: the self-assembly of hydrophobin multilayers. The increased hydrophilicity of surface when coated with hydrophobin layer proves to be a valuable property in applications where biofouling is undesirable.

By self-assembly hydrophobins change the wettability of surfaces. These proteins can be used to immobilize molecules at surfaces. In an analysis it has been reported that the presence of H\* Protein B (class I hydrophobin) prevents the adsorption of secondary proteins i. e. bovine serum albumin, casein, or collagen at low-salinity conditions and at pH 8.<sup>41</sup> Nonwovens are mostly hydrophobic polypropylenes and may have the similar phenomenon in the adsorption process of the H\* Protein B hydrophobin in similar conditions.

US 2006/0040349 A1 patent invented a hydrophobin derived from the thermophilic fungus *Talaromyces thermophiles*.<sup>48</sup> This patent also mentioned numerous applications of hydrophobins which include tissue engineering, drug delivery, stable foam formation etc. Another patent revealed a novel method for coating surfaces with hydrophobin.<sup>49</sup>

## **1.1.9 Nonwovens**

### **1.1.9.1 Why Nonwovens?**

Nonwovens are engineered fabrics manufactured by high speed, low-cost processes.<sup>50</sup> The first commercial use of nonwovens was to replace the expensive woven filters in automotive industry.<sup>51</sup> The most common nonwoven products listed by INDA, North America's Association of Nonwoven Industry include: sanitary napkins, sterile wraps, caps, gowns, wipes, apparel interlinings, padding and backing, wall and agricultural coverings, seed strips, automotive headliners and upholstery, filters, envelopes, tags, labels, insulation, house wraps, roofing products, and geotextiles.<sup>50</sup> Nonwovens on the basis of usage life time can be classified as disposable and durable or wetlaid, airlaid, or spunlaid on the basis of manufacturing process.<sup>52</sup>

In recent years, nonwoven filters have been given considerable attention due to their low cost, versatility in structures and diverse functionality. One of the major drawbacks of nonwoven filters is biofilm formation on the filter surfaces.<sup>53</sup> This leads to occasional cleaning of those filters increasing operational cost and decreasing filter life. Bacterial adhesion is one of the key steps of biofilm formation on surfaces. Bacteria are very prone to adhere to nonwoven surfaces due to ideal growth conditions like moderate temperature and humidity from the nonwoven processing. A patent on pluronic polymers (copolymers of ethylene glycol and propylene glycol) registered its use against microorganisms to prevent adhesion of microorganisms to textiles.<sup>54</sup> Therefore, we need to consider the development of antifouling nonwoven with better operational efficiency.

### **1.1.9.2 Meltblown Technology**

Meltblown is a web forming process of extruding and drawing molten polymer resins with hot, high velocity air to form fine filaments. The filaments are cooled and collected as a web onto a moving screen (Figure 1.4). This is a one step process requiring no bonding and is a continuous one. Carlton Francis in 1939 pictured a spray gun as a process in which microfibers can be developed.<sup>55</sup> In 1956, the meltblown concept was first introduced by Wente in Naval Research Laboratory's project to produce filters of microfibers to collect radioactive particles from

atmosphere during early years of cold war.<sup>56</sup> In meltblowing process polymer melt is extruded from a row of fine capillaries along the center of the die and are attenuated by very high velocity heated air before depositing on the conveyor belt to form a web.<sup>57</sup> The drag force caused by the high speed air jets attenuates the fiber rapidly and reduces the diameter by hundred times from the nozzle diameter.<sup>58</sup> The diameter of fibers produced from meltblown process is from 0.5-10 micron.<sup>52</sup> The web properties depend on the process parameters and the die configuration. The degree of fiber solidification will depend on the die to collector distance (DCD) and crystallization behavior of material. This process produces self-bonding nonwoven structures that derives strength from fiber to fiber contact.<sup>59</sup> Wentz in 1950's introduced a method to produce finer fibers from thermoplastic materials.<sup>60</sup> It is one of the fast growing processes for nonwoven production and has become an important industrial technique to produce microfiber fabric structures.<sup>61</sup> Meltblown nonwovens are produced directly from powder, granules or pellets of thermoplastic polymers.<sup>62</sup> This solid polymer is added into a hopper and is melted in the heated barrel called as extruder due to the movement of the screw; the polymer is further pushed into the meltblown die which consists of number of small capillaries through a metering pump.<sup>63</sup> A metering pump is a positive displacement constant volume device which is used to uniformly deliver polymer melt to the die assembly.<sup>63</sup> It is composed of two interlocking wheels which rotate in opposite direction. The design of the coat hanger die geometry is very important in meltblowing.<sup>61</sup> The air-gap and set back determine the angle and length of time the air hits the polymer stream.<sup>63</sup> Different air gap and setback leads to different web quality. The die geometry is normally adjusted for air gap and setback in the range of 0.2 - 2.5 mm but mostly used in the range of 0.5-2 mm. Finer fibers can be produced at 0.8 - 1 mm die geometry for polypropylene.<sup>64</sup> The manifold is located on the sides of the die tip; an air compressor is used to generate high velocity hot air which considerably decreases polymer melt viscosity.<sup>65</sup> Meltblown fabric is known for its high surface area per unit weight and excellent barrier properties<sup>66</sup> (preventing transfer of microorganisms from the environment to the man, or from man to man) hence most of the fiber membranes in nonwoven industry are made through meltblowing technology. These properties make meltblown fabrics an excellent applicant for making filters, medical garments, diapers where fluid barrier is extremely important.



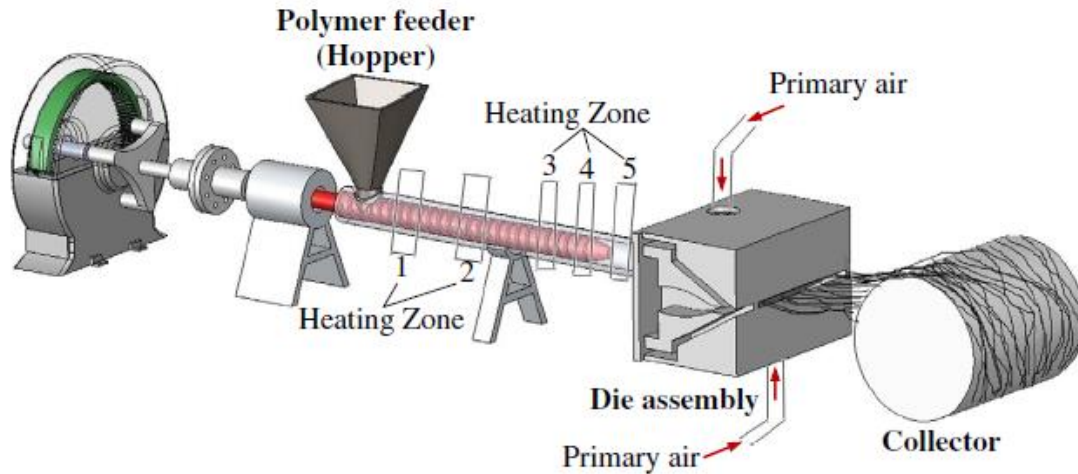


Figure 1.4. Process of meltblown technique.<sup>67</sup>

### 1.1.9.3 Surface Modification of Nonwovens

Nonwoven textiles have been widely used in medical and surgical applications, but large surface areas and the ability to retain moisture make these fabrics more prone to bacterial growth.<sup>68</sup> Especially surgical apparel made from nonwovens should not only provide protection against microbial attack but should also have blood barrier properties since most infections are caused by blood-borne pathogens. Huang et al. treated surgical gowns with antimicrobial agents and fluid repellent finishes through wet processing techniques.<sup>69</sup> However, there are some disadvantages to conventional fluid repellent finishes, such as the large amount of water consumed, the high cost of drying; emission of harmful chemicals presenting waste disposal problems, and the high cost of neutralizing chemical wastes. Low wet pick-up techniques have also been investigated, but they are limited due to non-uniform application of finishes. Moreover, traditional textile finishing operations change the bulk properties of the substrate. To prevent the change in bulk characteristics and to lower costs, surface treatments have often been investigated.

Plasma is an ionized gas in a neutral state with an equal density of positive and negative charges (physical definition of plasma). Plasma was defined as the “4th state of matter” (solid, liquid, gas and plasma) by Crookes in 1879.<sup>70</sup> Plasmas play an essential role in many industrial areas, particularly in electronic parts such as semiconductor microchip manufacturing, and in automotive and aerospace industries. Recently, plasma techniques are utilized in lighting and

large-screen televisions. Due to environmental regulations and concerns, the textile industry has become more interested in plasma applications as a novel finishing technology that significantly reduces toxic-chemical pollution. Plasma technology received enormous attention as a solution for environmental problems in textiles, and there has been rapid development and commercialization of plasma technology over the past decade. Plasma treatment is a dry process, i.e., it does not require water or wet chemicals. In addition, plasma can change substrate surface properties (such as micro-roughness and functionalization) without affecting bulk properties. Plasma surface modifications (such as desizing, wettability enhancement, water/soil-repellency, printability, dyeability, shrink-resistance, adhesion enhancement and sterilization etc.) can be achieved over large textile areas.

Plasma treatments are surface treatments that are cost efficient, environmentally friendly, uniform, and applicable to many materials, and they keep the bulk properties of the substrate intact. Plasma is an ionized gas composed of charged and neutral particles. When this plasma is applied to the substrate, the free electrons or other metastable particles, upon collision with the substrate, break the chemical bonds creating free radicals on the polymer surface.<sup>71</sup> These free radicals can undergo additional reactions depending on the gases in the atmosphere. Thus, the substrate can be coated with various kinds of gases without changing the fabric's bulk characteristics. Atmospheric pressure plasma techniques are becoming more popular due to the ease in incorporating them into continuous textile finishing operations.<sup>72</sup> Plasmas containing  $\text{CF}_4$ ,  $\text{C}_3\text{F}_6$ , argon, or other hydrocarbon gases can provide hydrophobicity to the fabric.<sup>73</sup> Rajpreet k. et al. demonstrated that plasma treatment in conjunction with an antimicrobial finish provides a better barrier against blood and microbial activity in nonwoven surgical gown materials.<sup>74</sup> Another research showed the surface grafting polymerization of biocompatible monomer N-vinyl-2-pyrrolidone (NVP) onto a plasma-treated nonwoven poly-(ethylene terephthalate) (PET) substrate with ultraviolet (UV)-induced methods. This surface modification modified the hydrophobic surface of the nonwoven into a hydrophilic one. Also an antibacterial assessment using *Staphylococcus aureus* indicated that *S. aureus* was restrained from growing in NVP-grafted nonwoven PET.<sup>75</sup>

In a combined study of a pretreatment with ozone and chitosan coating and glutaraldehyde crosslinking was developed for providing polypropylene nonwoven membrane with an antifouling and antibacterial surface.<sup>76</sup> The hydrophilicity of the composite membrane surface was improved. The static adsorption of protein on the composite membrane significantly decreased compared with the original membrane. Furthermore, antibacterial properties of the composite membranes were investigated by staining and growth inhibition. The results indicated that there were less bacteria attached onto the composite membranes. The composite membrane was thus demonstrated to be very effective in preventing the formation of biofilm, especially for the membrane with glutaraldehyde crosslinking.<sup>76</sup>

Since nonwovens are utilized in health, hygiene, and outdoor applications, the ability to reverse microbial attachment has both societal and environmental merit. Therefore, innovation of surface modification techniques to deter microbial attachment is of great importance. We need to study the modification techniques and underlying factors to fully comprehend the process of microbial adhesion to nonwoven textiles.

Adhesion is a surface property which depends on surface energy and the near surface-region of the interacting surfaces can be modified by several techniques without compromising the desirable bulk properties. Several surface modification techniques have been used for years including mechanical treatments, wet chemical treatment, acid treatment, flame treatment, corona discharge plasma, glow discharge plasma etc.<sup>77</sup> Wet chemical treatments with solvents, acids or bases have serious environmental concerns. Mechanical treatments have low effectiveness in surface roughening to modify the adhesion. Also flame treatment is hazardous and has safety issues. Plasma treatments have become popular among all surface modification techniques due to their advantages over other processes mentioned above. A major advantage of plasma processes is the absence of any harmful byproducts from other treatment processes. The main byproducts of plasma process are CO, CO<sub>2</sub> and water vapor which are produced in manageable quantity. Corona discharge uses ambient air to discharge plasma at atmospheric pressure and hence become well established.<sup>78</sup>

## 1.2 Summary and Objectives

This work is focused on understanding the chemistry of nonwoven surfaces to resist microbial adhesion. The goal is to develop a fundamental knowledge of nonwoven surface phenomena occurring when exposed to microbial environments for different applications. The modification of the nonwoven's surface chemistry by incorporating multiscale roughness is posed as one of the significant synergistic strategies for attachment deterring, self-cleaning nonwovens that inhibit the root cause of bacterial attachment: the self-assembly of hydrophobin multilayers. Bacterial hydrophobin will be used to study the assembly of bacterial hydrophobin along the porous structure of surface modified meltblown nonwovens.

The ultimate objectives of this research work are as follows:

1. Quantify behaviors that explain varying degrees of bacterial adhesion to nonwoven.
  - Test and quantify the adhesive properties of bacteria
  - Develop protocols to quantify bacterial attachment
2. Understand the role of nonwoven surface chemistry and topography on bacterial adhesion
  - Effect of hydrophilic pluronic coating on adhesion
  - Study of adhesion in presence of hydrophobin assembly
3. Assess nonwoven performance against the irreversible attachment of bacteria
  - Asses the performance of modified nonwovens as deterrents against reversible adhesion under continuous flow conditions.

## CHAPTER 2

### PERSPECTIVE ON HOW THE FLUID CARRIER INDIRECTLY INFLUENCE THE BACTERIAL ADHESION ONTO NONWOVENS

#### 2.1 Abstract

Bacterial infection is caused by accumulation of bacteria into human body by direct (infected skin or mucous membranes) or indirect contact (contaminated food, water, and surfaces)<sup>79</sup>. In medical and healthcare environments textile products like surgical sheets, drapes, masks, aprons, gloves, gowns<sup>80</sup> are frequently exposed to cough, sneeze, urine, body fluids from infected patients.<sup>81,82</sup> These textile products are specially designed to shield both healthcare workers and patients from infecting each other and also from the contaminated surfaces.<sup>83</sup> But bacteria accumulation and proliferation may occur on porous textiles<sup>84,85</sup> and may cause secondary infections too. Bacteria adhesion to a porous surface and subsequent colonization causing recurring infections will depend on both the nature of the bacteria and the environment. In this study we investigated the influence of bacteria cell wall chemistry by microbial adhesion to solvents (MATS) Test upon their growth in media mixed with different carrier fluids such as organic solvents i. e. decane, hexadecane, ethyl acetate and chloroform. *E. coli* strain showed almost equal affinity toward both the acidic and basic solvent whereas 51.03 % of *B. cereus* colony forming units was found to grow in basic solvent ethyl acetate. By mapping the growth of *E. coli* and *B. cereus* in carrier fluids with varying surface tension values, we correlated their growth to surface tension. Surface tensions of growth media showed no trend with the *E. coli* colonization over their growth phase. But a decrease in media surface tension values is found to increase *E. coli* growth in hydrophilic chloroform media. The growth of hydrophilic bacteria will mostly depend on the surface chemistry of the media. Hydrophilic bacteria with a polar cell wall are expected to preferentially grow in a polar media to grow than a nonpolar media. Thus, the hydrophilic nature of media can influence the growth of bacteria onto a hydrophobic substrate. Growth and subsequent colonization can be prevented if the surface tension of the growth media does not promote bacteria transportation towards a substrate. From the results of this study, we

can predict the extent and why the bacterial growth is proliferated or hampered based on the chemistry of the carrier fluid.

## 2.2 Introduction

Bacterial infection is caused by accumulation of bacteria into human body by direct (infected skin or mucous membranes) or indirect contact (contaminated food, water, and surfaces)<sup>79</sup>. In medical and healthcare environments textile products like surgical sheets, drapes, masks, aprons, gloves, gowns<sup>80</sup> are frequently exposed to cough, sneeze, urine, body fluids from infected patients.<sup>81,82</sup> These textile products are specially designed to shield both healthcare workers and patients from infecting each other and also from the contaminated surfaces.<sup>83</sup> But bacteria accumulation and proliferation may occur on porous textiles<sup>84,85</sup> and may cause secondary infections too. People can be infected by contacting through skin (primary exposure) or by contacting an already contaminated surface with bacteria (secondary exposure).<sup>79,86</sup> Both of this primary and secondary type exposures are more common in hospital settings where non-pathogenic bacteria can cause more secondary exposure whereas pathogenic bacteria can cause diseases for example *Enterococcus*, *Staphylococcus* and *Streptococcus* cause wide variety of infections and diseases<sup>87</sup>. Bacteria adhesion to a porous surface and subsequent colonization causing recurring infections will depend on both the nature of the bacteria and the environment. The presence of very thick peptidoglycan (long strand of alternating N-acetylmuramic acid (NAM) and N-acetylglucosamine) layer reacts with gram stain in case of gram positive cells while gram negative cells have very thin peptidoglycan layer.<sup>88</sup> In order to consider the effect of bacteria structure on adherence both gram negative *Escherichia coli* (*E. coli*) (rod shaped, 1-2  $\mu\text{m}$ )<sup>89</sup>, and gram positive *Bacillus cereus* (*B. cereus*) (rod shaped, 3 - 5  $\mu\text{m}$  in length and 1  $\mu\text{m}$  in width)<sup>90</sup> were used in this study. *E. coli* was chosen as it is one of the most common bacteria present in the atmosphere and is a common gut microorganism and can be excreted very easily in fecal matter and hence can also be found in soil, water, plant, and food.<sup>91</sup> *E. coli* is a common pathogen for wound and urinary tract infections in humans.<sup>84,92</sup> *B. cereus* is mainly found in marine and freshwater, vegetables from which soil and food products are easily contaminated.<sup>93</sup> *B. cereus* is also a human pathogen and can cause gastrointestinal diseases by secreting wide array of

toxins.<sup>94</sup> Primary exposure of bacteria can be inhibited by frequently washing hands and using respiratory protective devices (FRPDs), masks, bacteria filters. Bacteria filters can trap bacteria, but the efficacy of filters depends on the antifouling performance. Secondary exposure can be minimized by cleaning contaminated surfaces with cleaning wipes either in dry or wet state. Bacteria can be transported by surrounding carriers like fluids, dust, liquids, respiratory droplets etc.<sup>79</sup> Katarzyna M. et al. showed the efficacy of FRPDs depends on the amount of accumulated moisture from breathing and microorganism type.<sup>95</sup> If liquid carriers, such as those listed in Table 2.1 are contaminated with bacteria, these can help to transmit bacteria through pores of textiles and fibrous materials that are on the order of 1 - 5  $\mu\text{m}$ .<sup>79</sup> Bacterial contamination of nonwovens used in diapers, surgical sets, wipes etc. should take into account the interaction between bacteria, carrier and the textiles.<sup>79</sup> Carrier fluids that we find in medical and healthcare environments have a very large range of surface energies (6 - 72 mN/m). The higher the difference between the surface tensions of carrier fluids with textile or nonwoven fabrics, the lower would be the adhesion of bacteria. For example, polypropylene nonwovens have low surface energy (27 mN/m)<sup>7</sup> and act as a repellent for liquid carriers like water and urine depending on the surface tension of bacteria present in the carrier.<sup>19</sup> The top sheet of diapers and inner filtering layer of FRPDs<sup>95</sup> and masks are made of meltblown PP nonwovens due to the uniform distribution of thinner fibers (1 - 2  $\mu\text{m}$ ). That is why meltblown PP nonwovens were chosen for this study to evaluate the indirect influence of fluid carriers upon the bacterial adhesion onto nonwovens.

**Table 2.1** Surface free energies of commonly found carrier and bacteria in medical and healthcare environments.<sup>6,96</sup>

Carrier Fluid	Surface Energy, mN/m	Bacteria	Surface Energy, mN/m
Water	72	<i>Staphylococcus aureus 049</i>	69.7 $\pm$ 0.4
Blood	52	<i>Escherichia coli 055</i>	69.7 $\pm$ 0.4
Alcohol	22	<i>Escherichia coli 049</i>	69.1 $\pm$ 0.6
Urine	6	<i>Bacillus cereus</i>	46.64 $\pm$ 0.3

**Table 2.2** lists surface energy values of commonly used formulation in cosmetic liquids.<sup>97</sup> The performance of cosmetic impregnated nonwoven fabrics such as wipes or masks depends on their efficacy of preservative. Yuko et al. found that preservative efficacy was reduced as a result of introducing cosmetic liquids into nonwoven fabrics.<sup>98</sup> Therefore, we need to carefully study the influence of liquids present in wet wipes or masks.

**Table 2.2** Surface energy values of commonly used formulation in cosmetic liquids.

Purpose	Ingredient name	Surface Energy, mN/m
Preservative	EtOH	22.10 <sup>99</sup>
	2-Phenoxyethanol	70.7 <sup>100</sup>
Surfactant	Polysorbate 80	38 <sup>101</sup>
Solubilizing agent	Dipropylene glycol	33.55 <sup>97</sup>
	Water	72 <sup>79</sup>

The effects of bacterial properties, like cell wall nature (whether gram negative or gram positive) and cell wall chemistry, on the adhesion to a substrate exposed to fluid can be studied by growing bacteria in different fluids. According to Zheng et al., the chemistry of liquid carriers can either aid or hamper contamination due to its influence on the rate of bacterial attachment and colonization.<sup>19</sup> Despite the fact that chemistry of the carrier fluids influences the interaction between bacteria and the substrate, there is no prior and effective research done in this matter. Previously researchers found that electron donor or electron acceptor behavior of bacteria cell wall can influence their growth in carrier fluid.<sup>102</sup> An understanding of bacterial proliferation in liquids can influence bacterial adhesion to fibrous substrate is known to a lesser degree.

In this study, the cell wall chemistries of both *E. coli* and *B. cereus* were characterized according to the microbial adhesion to solvents (MATS) test, which measures growth in a suspension of aqueous-growth media mixed with an organic carrier fluid, such as decane, hexadecane, ethyl acetate and chloroform. The objective of this study was to map the growth of model bacteria in common carrier fluids and to apply an understanding of cell wall chemistries to explain these growth behaviors.



## 2.3 Materials and Methods

### 2.3.1 Materials

*E. coli* and *B. cereus* stock culture was a gift from the Department of Crop and Soil Science at NCSU and was subcultured twice from the frozen stock before each experiment. BD Difco™ Plate Count Agar (BD 247940) was used as growth media for both the bacteria. Sodium chloride (NaCl, 99%, 7647-14-5) was used as the sterile suspending liquid. Ethanol (CH<sub>3</sub>CH<sub>2</sub>OH, 99.9 %, 64-17-5) was diluted up to 70 % with distilled water for cleaning purposes.

Chloroform (J67241.AP), n-Hexadecane, 99% (AAA10322AE), Ethyl acetate, 99.5+% (AA39177K2), n-Decane, 99% (AAA14732AE) solvents were used towards the Microbial Adhesion to Solvents (MATS) test and were procured from Fisher Scientific.

### 2.3.2 Methods

*E. coli* and *B. cereus* bacteria were first grown overnight at 37 °C on nutrient agar from a frozen stock. For each experiment, cells were inoculated in 10 ml of nutrient broth and cultured aerobically for 24 h. Bacteria were harvested by centrifugation at 3000 g for 5 min. Bacteria were then resuspended in nutrient broth to a concentration of 10<sup>7</sup> cfu/ml.

#### Bacteria Growth Cycles

*E. coli* and *B. cereus* were grown for 24 hr in nutrient agar petri dishes. 1000 ml of nutrient broth culture was prepared and was divided into four 250 ml flasks and was autoclaved at 121 °C. In the growth experiments, for each bacterium, three flasks were inoculated, and one was kept as control. Then three bottles were incubated at 37 °C with shaking at 150 rpm. For all shaken flask batch cultures, the optical densities (OD<sub>600</sub>) were determined using a spectrophotometer (GENESYS™ 30) at 600 nm. The growth rate of the cultures was determined from samples taken periodically (30 minute) over a total time of 96 h at OD<sub>600</sub> values from 0.05 to 0.75.<sup>103</sup>

Both t-test and one-way analysis of variance (ANOVA) was performed to determine significant differences between experimental data sets. The arithmetic mean and standard deviation for the number of bacteria in each medium were calculated. The t-test at 95 % confidence interval was

used to determine if two populations have different means. ANOVA was used to analyze the significant differences between more than two populations. In both tests, differences were considered significant at  $p < 0.05$ . All data were analyzed using the Origin 2022 statistical software program.

### **2.3.2.1 Bacterial Cell Wall Chemistry Based on MATS Testing**

The microbial adhesion to solvents method was first developed by M.-N. Bellon-Fontaine, J. Rault and C. J. Van Oss to characterize electron-donor/ electron-acceptor, i.e., the Lewis acid-base, nature of the bacterial cell wall.<sup>102</sup> This method is based on the comparison between microbial cell affinity to a monopolar solvent and an apolar solvent. The monopolar solvent can be electron-acceptor or electron-donor, but both solvents must have similar Van der Waals surface tension components. Suspensions are used to understand growth at the interface of the hydrophilic, aqueous media with organic solvents that vary in degrees of hydrophobicity.

*E. coli* cells were stored in a freezer prior to the experiments and were subcultured twice in nutrient agar medium and then cultivated for 24 h at 37 °C in nutrient broth medium under oxygenated conditions until the stationary stage was reached. To prepare the bacterial suspension, cells were harvested by centrifugation for 10 min at 7000 g and then washed twice with the suspending liquid ( $1.5 \times 10^{23}$  mol/l of aqueous NaCl) and then resuspended in the same liquid.

Two pairs of solvents were used -

- Chloroform, an acidic and electron acceptor-solvent with hexadecane, an apolar n-alkane.
- Ethyl acetate, a basic and strong electron-donor solvent with decane, an apolar n-alkane.

The aqueous solution of NaCl ( $1.5 \times 10^{23}$  M) was used as control. A suspension containing  $10^8$  cells in 2.4 ml control (NaCl  $1.5 \times 10^{23}$  M) was vortex-mixed for 60 s with 0.4 ml of the solvent under investigation. We waited for 15 min to ensure complete separation of two phases before a sample (1 ml) was carefully removed from the aqueous phase and then the optical density was

measured at 400 nm. The percentage affinity of bacterial cells to each solvent was calculated using Equation 1 –

$$\% \text{ Affinity} = (1 - A/A_0) \times 100 \dots\dots\dots (1)$$

Where  $A_0$  is the optical density measured at 400 nm of the bacterial suspension before mixing and  $A$  is the absorbance from the GENESYS™ 30 UV-vis spectrophotometer after mixing.

### **2.3.2.2 Bacteria Count in Fluid Carriers**

The standard plate count method<sup>104</sup> was used to quantify bacterial populations within the different liquids, some of which contained media and carrier liquid.<sup>105</sup> This method consists of diluting a sample with sterile phosphate buffer until the bacteria colonies could be counted accurately. That is, the final plates for counting after serial dilution should have between 30 and 300 colonies. Fewer than 30 colonies are not acceptable for statistical analysis (being that too few are not representative of the sample), and more than 300 colonies on a plate were likely to produce colonies that are too close to each other to be distinguished as a distinct colony-forming units (cfu). The assumption is that each bacterial cell is separate from all others and that these will develop into a single discrete colony (i. e. cfu). A wide series of dilutions (e.g.,  $10^{-4}$  to  $10^{-10}$ ) were plated because the exact number of bacteria is usually unknown. Greater accuracy was achieved by having two technical (plating duplicates of each dilution) repeats and five biological repeats (using 5 different bacterial clones). All data were analyzed using the Origin 2022 statistical software program.

### **2.3.2.3 Fluid Surface Tension -Capillary Rise Technique**

The surface tension of fluids with and without bacteria were measured using the DWK Life Sciences (Kimble) 14818 Tensiometer, Capillary Surface Tension Apparatus (Figure 2.1). Surface tension values for each fluid were calculated according to the rise of the fluid in the capillary; see Equation 2 where-

$$\gamma = \frac{1}{2} hr\rho g \dots\dots\dots (2)$$

Where  $\gamma$  = fluid surface tension (dynes/cm)

$h$  = height of the fluid in the capillary (cm)

$\mu$  = density of fluid (g/cm<sup>3</sup>)

$r$  = radius of the capillary (cm)

$g$  = acceleration due to gravity (cm/s<sup>2</sup>).

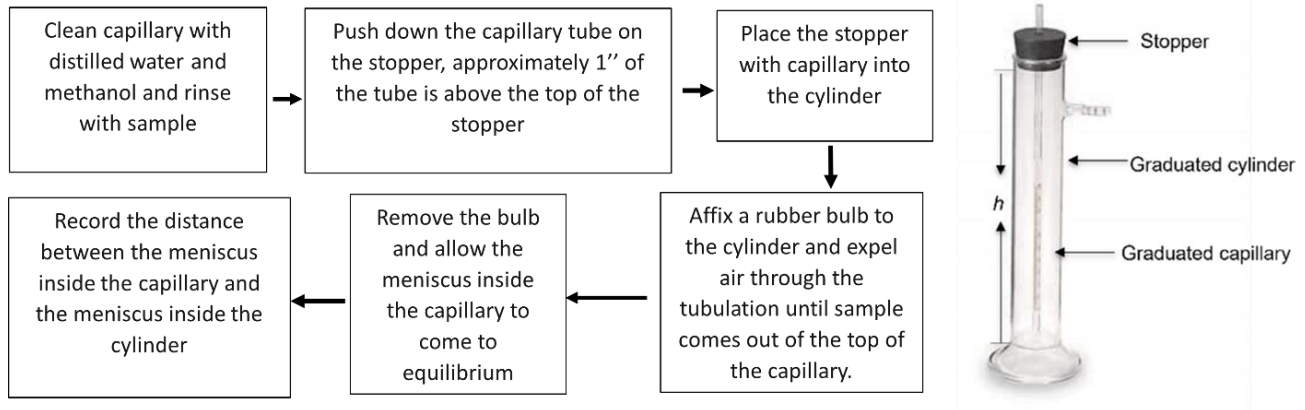


Figure 2.1. Surface tension of fluids using the capillary surface tension analyzer.

## 2.4 Results and Discussion

### 2.4.1 Bacterial Growth Cycles

Growth curves for *B. cereus*, and *E. coli* are shown in Figure 2.3. As seen from the cell growth curve in Figure 2.3(a) after cultivation for 60 h, cell density (OD<sub>600</sub>) of *B. cereus* increased rapidly to  $0.63 \pm 0.05$ . Cells entered the exponential phase since 10 h and in 70 h and onward, the cells were in death phase as cell density decreased. The growth of *E. coli* sustained until 3.5 h and the maximum optical density obtained is  $0.71 \pm 0.05$  as shown by Figure 2.3(b). *E. coli* reached the stationary phase in 3.5 h whereas *B. cereus* reached after 60 h.

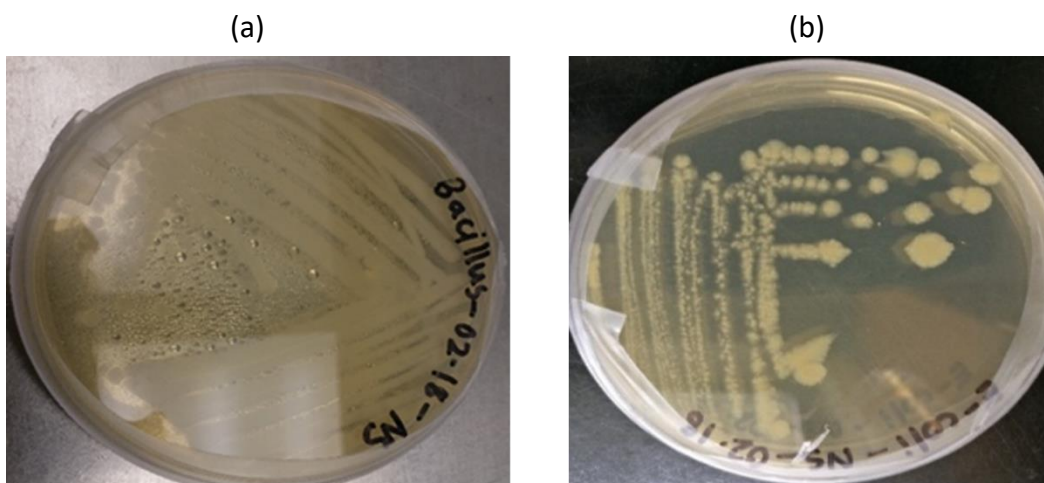


Figure 2.2. Growth of a) *B. cereus*, and b) *E. coli* by plate inoculation method.

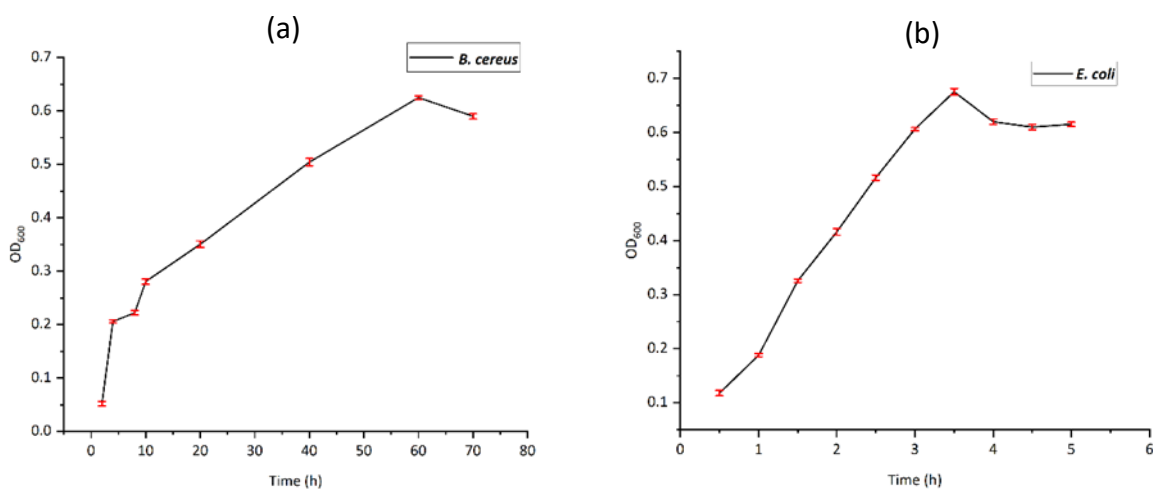


Figure 2.3. Optical density measurements of (a) *B. cereus*, (b) *E. coli* at 600 nm in nutrient broth media with time; incubated at 37 °C at 150 rpm.

#### 2.4.2 Bacterial Cell Wall Affinity According to MATS Testing

**Table 2.3** lists the surface components of the four solvents used in the MATS test.<sup>102</sup> Surface tension components of solvents help us to predict the trend of bacterial growth in those solvents. Figure 2.4 demonstrates the extent of growth of *E. coli* and *B. cereus* to four types of solvents. We can see that *E. coli* strain showed almost equal affinity toward both the acidic and basic solvent whereas 51.03 % *B. cereus* is found to grow in basic solvent ethyl acetate. Both of these

bacteria were found in greater quantity in polar solvents than the control indicative of their hydrophilic character.<sup>106</sup>

**Table 2.3** Surface components of four solvents used in MATS test from literature.<sup>102</sup>

Solvents	Van der Waals components (mJm <sup>-2</sup> )	Electron acceptor components (mJm <sup>-2</sup> )	Electron donor components (mJm <sup>-2</sup> )
Decane C <sub>10</sub> H <sub>22</sub>	23.9	0	0
Hexadecane C <sub>16</sub> H <sub>34</sub>	27.7	0	0
Ethyl acetate C <sub>4</sub> H <sub>10</sub> O	23.9	0	19.4
Chloroform CHCl <sub>3</sub>	27.2	3.8	0

Based on a t-test at 95 % confidence interval, significant differences ( $p < 0.05$ ) of percentage affinity of both the bacteria were observed between control and all four solvents: polar (chloroform, ethyl acetate) and non-polar (decane, hexadecane) as shown by \* in Figure 2.4. Also, % affinities were significantly different between *E. coli* and *B. cereus* bacteria irrespective of the medium. The maximum affinity of *E. coli* (50.3 %) toward chloroform (an electron acceptor solvent) than for hexadecane (a nonpolar solvent) indicates electron donor character of this hydrophilic bacteria. On the other hand, the maximum affinity of *B. cereus* (51.03 %) for ethyl acetate (an electron donor solvent) indicates electron acceptor nature.

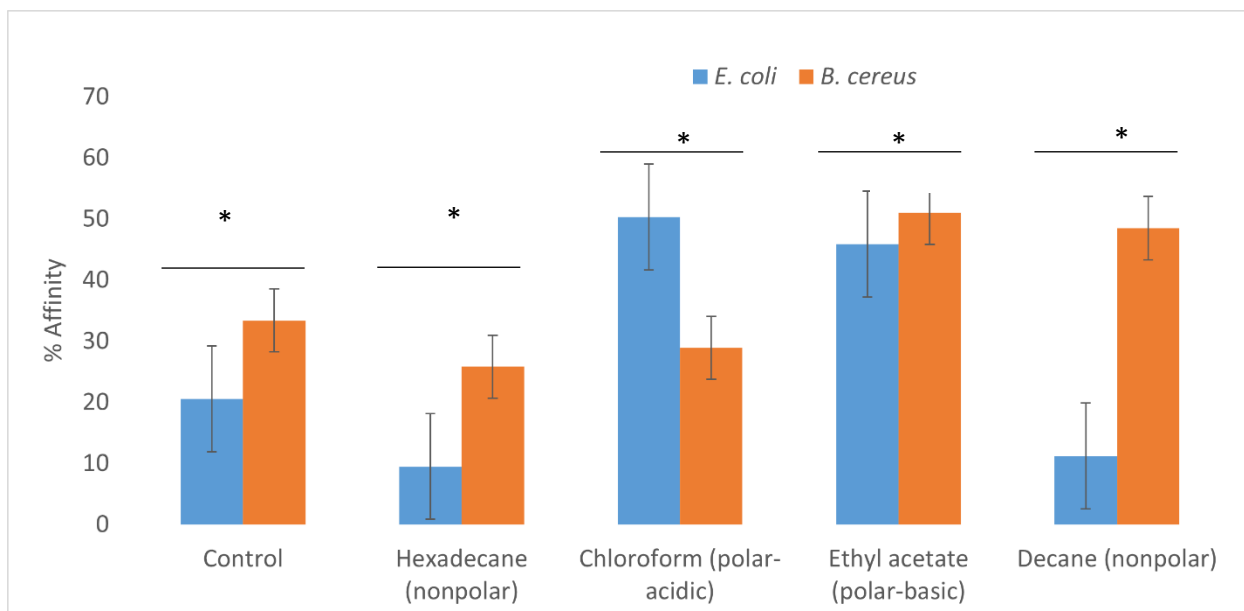


Figure 2.4. The percentage affinity of *E. coli* and *B. cereus* suspended in control - potassium phosphate buffer solution to polar (chloroform, ethyl acetate) and non-polar (decane, hexadecane) solvent interfaces, \* =  $p < 0.05$ .

### 2.4.3 Role of Bacteria Solution Surface Tension to Bacterial Growth

The bacterial growth data are reported in **Table 2.4** and Figure 2.5. The nutrient broth was diluted with concentrations of 0, 5, 10 and 50 % w/v organic solvent. The surface tensions of those fluids containing nutrient broth and an organic solvent (such as those used also for MATs testing) are also reported in **Table 2.5**. Surface tension values of *E. coli* and *B. cereus* bacteria reported in **Table 2.5**; these are collected from literature<sup>96,97,99</sup>.

When comparing the surface tensions of the *E. coli* and *B. cereus* to that of contaminated liquids, those values for inoculated liquids are lower (Figure 2.5). The effects of carrier liquid on the growth of *E. coli* and *B. cereus* are mapped in Figure 2.5. But the growth of *E. coli* and *B. cereus* did not trend with the addition of organic solvents.

**Table 2.4** Mean surface tension values of carrier fluid during the growth of *E. coli* and *B. cereus*.

Composition of Bacterial Carrier Fluid (% v/v)	Bacterial Carrier Fluid Surface Tension (N/m) $\pm$ 0.05 SD	No of <i>E. coli</i> / $10^4 \mu\text{m}^2$	No of <i>B. cereus</i> / $10^4 \mu\text{m}^2$
Nutrient Broth (NB)	0.057	89 $\pm$ 2E-3	110 $\pm$ 4E-3
Decane (D)	0.024	---	---
NB-D 5	0.055	85 $\pm$ 4E-3	111 $\pm$ 3E-3
NB-D 10	0.054	98 $\pm$ 4E-3	110 $\pm$ 3E-3
NB-D 50	0.054	78 $\pm$ 3E-3	112 $\pm$ 3E-3
Hexadecane (HexaD)	0.027	----	----
NB-HexaD 5	0.055	88 $\pm$ 3E-3	98 $\pm$ 3E-3
NB-HexaD 10	0.054	87 $\pm$ 5E-3	97 $\pm$ 2E-3
NB-HexaD 50	0.054	85 $\pm$ 6E-3	95 $\pm$ 2E-3
Chloroform (CHL)	0.027	----	----
NB-CHL 5	0.055	175 $\pm$ 4E-3	89 $\pm$ 2E-3
NB-CHL 10	0.054	167 $\pm$ 7E-3	91 $\pm$ 4E-3
NB-CHL 50	0.053	156 $\pm$ 6E-3	93 $\pm$ 5E-3
Ethyl acetate (EA)	0.024	----	----
NB-EA 5	0.055	144 $\pm$ 5E-3	111 $\pm$ 5E-3
NB-EA 10	0.055	155 $\pm$ 3E-3	115 $\pm$ 4E-3
NB-EA 50	0.056	145 $\pm$ 1E-3	114 $\pm$ 4E-3

**Table 2.5** Surface tension of bacteria at room temperature from literature.<sup>96,97,99</sup>

Bacteria	Surface Tension, $\gamma$ (N/m)
<i>Escherichia coli</i> 055	0.069 $\pm$ 4E-4
<i>Bacillus cereus</i>	0.047 $\pm$ 3E-4



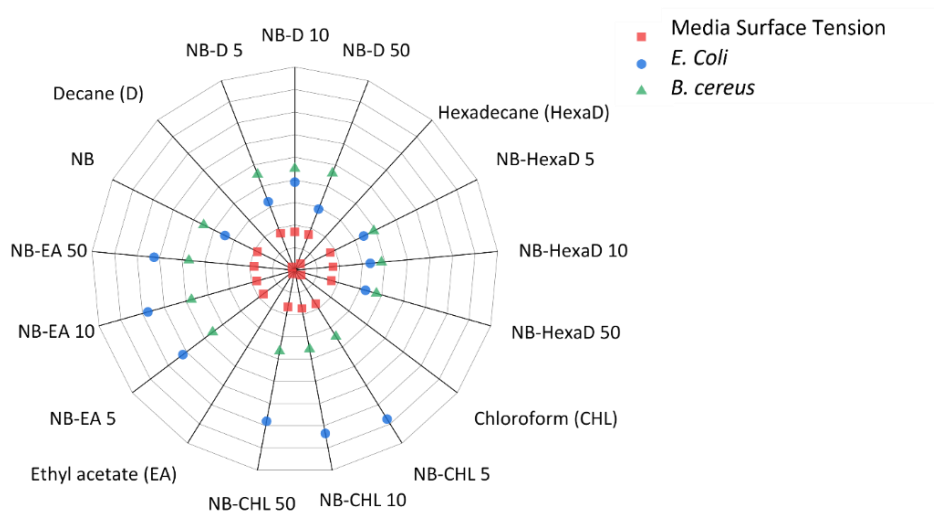


Figure 2.5. Growth of *E. coli* and *B. cereus* upon diluting nutrient broth fluids with organic, carrier liquids. The surface tension of each solvent is shown relative to each other.

From ANOVA analysis, substantial differences were observed between the growth of *E. coli* and *B. cereus* in sets of polar and nonpolar solvent media at 5 – 50 % v/v concentrations (**Table 2.4**). The growth of *E. coli* appeared to be more solvent dependent and number of cell directly correlates with its cell wall affinity for each solvent in accordance with the MATS test (Figure 2.5). The maximum growth of *E. coli* (50.3 %) in polar chloroform than nonpolar hexadecane confirms the hydrophilic cell wall nature as indicated by the hypothesis of MATS test<sup>102</sup>. Bacteria usually possess a net negative charge due to carboxyl, amino, and phosphate groups on their cell wall surfaces.<sup>107</sup> *E. coli* attachment in polar chloroform is mainly due to the electrostatic interaction between cell wall components and the medium. Based on Figure 2.5, chloroform and ethyl acetate exhibit polar acidic and basic behaviors, respectively. Maximum *E. coli* growth is found in a nutrient broth mixed with 5 % chloroform (Figure 2.5). Nutrient broth media surface tension is suppressed by the addition of chloroform which increases growth. Though the corresponding media surface tension values show no trend with the number of *E. coli* bacteria, a decrease in surface tension from the initial nutrient broth surface tension might help in the initial attachment of hydrophilic *E. coli*. Growth of *E. coli* in chloroform is mainly due to the electrostatic attraction between *E. coli* cell wall and chloroform. But as soon as media surface tension decreases, growth

is aided by the better transportation through the medium and therefore we saw a rise in growth of *E. coli* after mixing chloroform with nutrient broth.

In the case of *B. cereus*, maximum growth occurred in nutrient broth mixed with ethyl acetate, which is due to the polar basic behavior of its cell wall. Also, maximum growth of *B. cereus* occurred in nutrient broth mixed with 10 % ethyl acetate. This result also showed the polar basic cell wall nature is the most crucial factor for bacteria growth in media with varying surface tension values and polarity. Both *E. coli* and *B. cereus* adhesion do not show any trend with varying concentrations of different solvents.

## **2.5 Conclusions**

Surface tensions of growth media showed no trend with the *E. coli* colonization over their growth phase. But a decrease in media surface tension values was found to increase *E. coli* growth in hydrophilic chloroform media. The growth of hydrophilic bacteria will mostly depend on the surface chemistry of the media. Hydrophilic bacteria with a polar cell wall are expected to preferentially grow in a polar media to grow than a nonpolar media. Thus, the hydrophilic nature of media can influence the growth of bacteria onto a hydrophobic substrate. Growth and subsequent colonization can be prevented if the surface tension of the growth media does not promote bacteria transportation towards a substrate.

## **Acknowledgements**

Bacteria life cycle and adhesion study were carried out in the Department of Crop and Soil Science at North Carolina State University. The author is indebted to Dr. Shuang Liu and Dr. Juan Frene for their support in bacteria studies.

## CHAPTER 3

### BACTERIAL ADHESION ONTO PLURONIC TREATED, MELTBLOWN NONWOVENS UNDER STATIC AND CONTINUOUS FLOW MEDIA

#### 3.1 Abstract

The bacterial contamination of nonwovens (NW) is a significant issue for products utilized in healthcare, hygiene, and outdoor applications such that surfaces that are inherently resistant to contamination and biofouling are crucial to sustain performance. Polypropylene (PP) is the most commonly used polymer for nonwovens; this is due to their stability under thermal processing and low cost. However, PP nonwovens are susceptible to biofouling due to the relative ease by which bacteria can adhere to hydrophobic surfaces.<sup>108</sup> This study focuses on how the assembly of Pluronic affects bacterial adhesion onto meltblown PP nonwovens under both static and continuous flow conditions. The purpose of this study is to understand how differences in nonwovens uniformity, porosity, and structure affect Pluronic assembly followed by bacterial adhesion. We evaluated the performance of surface-modified nonwovens against adherence of two commonly found food-borne pathogens *Escherichia coli* (*E. coli* - gram negative, 1 - 2  $\mu\text{m}$ ) and *Bacillus cereus* (*B. cereus* - gram positive, 3 - 5  $\mu\text{m}$  in length and 1  $\mu\text{m}$  in width).

#### 3.2 Introduction

The bacterial contamination of nonwovens (NW) is a serious issue for products utilized in healthcare, hygiene, food and beverage, and outdoor applications such that surfaces that are inherently resistant to contamination and biofouling are crucial to sustaining performance.<sup>109-113</sup> Polypropylene (PP) is the most commonly used polymer for nonwovens; this is due to their stability under thermal processing<sup>114</sup> and relatively low cost<sup>80</sup>. However PP nonwovens are susceptible to biofouling due to the relative ease by which bacteria can adhere to hydrophobic surfaces.<sup>108</sup> The thinner fibers produced by meltblown technology (1-2  $\mu\text{m}$ , basis weight  $\sim 30 \text{ g/m}^2 \pm 10 \%$ ) are used as the filtering layers in filtering respiratory protective devices (FRPDs) due to their filtering efficiency.<sup>115</sup> To maintain the performance of FRPDs throughout their service, it

is important to protect their surface against the deposition and proliferation of microorganisms so that they are not a source of infection.

Strategies for limiting bacteria accumulation onto abiotic surfaces include the usage of biocides or surfaces that are inherently antifouling- but are also nonbiocidal. Biocides are chemical or biological substances which deter the harmful effect of microorganisms either by killing them or by inhibiting their growth. The most commonly used biocides are metals<sup>116,117</sup>, *N*-halamines<sup>118,119</sup>, chitosan<sup>120</sup>, quaternary ammonium compounds<sup>121</sup> or nanoparticles<sup>122</sup>. But there are growing concerns about the use of biocides due to the adaptability of bacteria<sup>123</sup> or bacterial induced resistance towards biocides<sup>79</sup>. Further, the toxicity<sup>113</sup> (presence of organic solvents, heavy metals, dioxins or furans) and cytotoxicity (DNA damage by interrupting with cell mitochondrial activity<sup>124</sup>) of biocides poses a risk to the ecology of beneficial microorganisms<sup>122</sup> and their natural environment<sup>125</sup>.

To avoid the use of biocides, researchers have focused on the development of surfaces that can repel microbes, so as to prevent microbial adhesion onto solids surfaces.<sup>126</sup> This approach eliminates the issues associated with microbial adaptation and the resistance of microbes to biocides. Antibiofouling surfaces are also popular due to their effectiveness against the accumulation of a wide variety of microorganisms.

Hydrophilic coatings of polyethylene oxide (PEO) and polyethylene glycol (PEG) have been applied to surfaces to make them inherently resistant to biofouling. Once applied to the hydrophobic surface of medical products, these coatings can deter the irreversible adhesion of microbes by adsorbing onto the microbial cells and creating a steric stabilized barrier to the incoming cells.<sup>127-129</sup> Pluronic surfactants having varying lengths of PEO and polypropylene oxide PPO blocks has the capability of self-assembling along the material's surface. Pluronic copolymers (as shown in Figure 3.1 consist of EO and PO arranged in a triblock structure of EO<sub>x</sub>-PO<sub>y</sub>-EO<sub>x</sub>) have generated great interest as it pertains to the chemical modification of a material's surface; as such, these amphiphilic polymers can repel interactions with the cell membranes of bacteria.<sup>130</sup> Dangling EO<sub>x</sub> blocks act as a barrier to incoming particles, due to their stronger interactions with the aqueous surroundings and leached surfactant molecules may subsequently adsorb to the

bacterial cells in the aqueous media and form a steric stabilized barrier to adsorption on the bacterial surfaces.<sup>131</sup> In aqueous solution, the two EO<sub>x</sub> protruding blocks face outwards so hydrogen bond with the oxygen atoms of ether groups or water molecules. The end result is a micellar corona (or shell) that confers solubility in water.<sup>132</sup> The PO<sub>x</sub> segment is confined to the hydrophobic core of the micelle. Further, the methyl units of the PO<sub>x</sub> segments might interact with hydrocarbon substrates through Van der Waals interactions. The coating of polystyrene with a variety of Pluronic surfactants has reduced the adhesion of *Staphylococcus epidermidis* to its surface by ~ 97%<sup>131</sup> under static conditions.

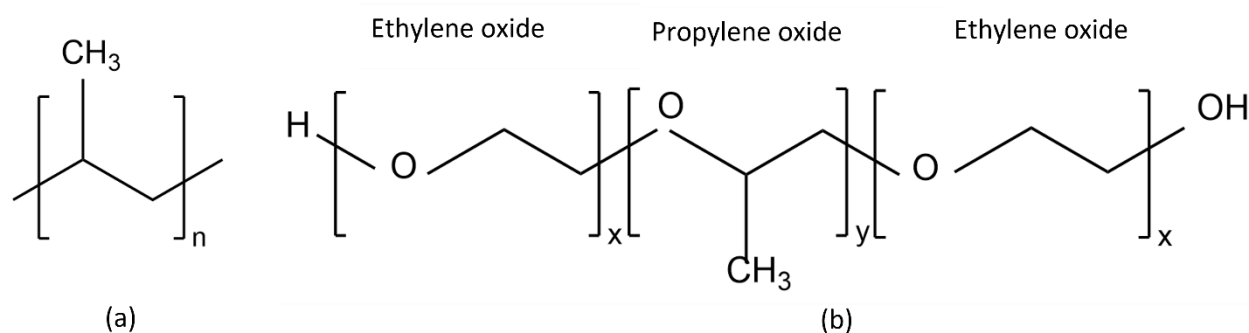


Figure 3.1. Chemical structure of (a) PP and (b) Pluronic F-108.

Several studies<sup>133–135</sup> showed after deliberately passing an air-liquid interface, both the deposition of bacteria and the desorption of bacterial adhesion are affected by shear rate and flow displacement. As the fluid flows, both the deposition and reversibility of bacterial adhesion can occur as the results of the shear rate and flow displacement. J. M. Meinders et al. ascribed the deposition and reversibility of bacterial adhesion onto inert polystyrene particles to the secondary interaction minimum, which infers an energy barrier to Gibbs interaction energy (the sum of the Van der Waals and the electrostatic interactions), at separation distances of several hundred Ångstroms from the substrate.<sup>93</sup> Both the adsorption and desorption phases were influenced by acid-base interactions in addition to Gibbs interaction energy, between a substrate and microorganisms for a hydrophobic substrate like fluoroethylenepropylene.<sup>93</sup> The desorption of *Staphylococcus epidermidis* HBH<sub>2</sub> 169, *Acinetobacter calcoaceticus* RAG-1, *Streptococcus thermophilus* from different substrates was provoked under conditions of fluid flow (namely, a flow volume of 0.11 cm<sup>3</sup> and shear rate at the wall of 50 s<sup>-1</sup>).<sup>93</sup> Collisions between

bacteria in the carrier liquid with bacteria adhered to the substrate had likely caused desorption.<sup>93</sup>

The objective of this study was to understand how the assembly of Pluronic surfactant onto meltblown PP nonwovens would affect bacterial adhesion under both static and continuous flow conditions. Differences in the uniformity, porosity, and structure of nonwoven fabrics were considered to understand their effects on Pluronic assembly, followed by bacterial adhesion. Bacteria adhesion to a porous surface and subsequent colonization will depend on both the nature of the bacteria and the environment. We evaluated the performance of Pluronic-modified, nonwoven fabrics against adherence by both gram negative *Escherichia coli* and gram positive *Bacillus cereus* bacteria. Both bacteria can form biofilms, which can entrap toxic microbes that are not capable of forming biofilms themselves.<sup>136</sup> The presence of very thick peptidoglycan (long strand of alternating N-acetylmuramic acid (NAM) and N-acetylglucosamine) layer reacts with gram stain in case of gram positive cells while gram negative cells have very thin peptidoglycan layer.<sup>88</sup> In order to consider the effect of bacteria structure on adherence both gram negative *E. coli* (rod shaped, 1 - 2  $\mu\text{m}$ )<sup>89</sup>, and gram positive *B. cereus* (rod shaped, 3 - 5  $\mu\text{m}$  in length and 1  $\mu\text{m}$  in width)<sup>90</sup> were used in this study. *E. coli* was chosen as it is one of the most common bacteria present in the atmosphere and is a common gut microorganism and can be excreted very easily in fecal matter and hence can also be found in soil, water, plant, and food.<sup>91</sup> *E. coli* is a common pathogen for wound and urinary tract infections in humans.<sup>84,92</sup> *E. coli* is a common gut microorganism and can be excreted very easily in fecal matter and hence can also be found in soil, water, plant, and food.<sup>91</sup> Several strains being pathogenic, *E. coli* is one of the frequent pathogens in hospital-related and healthcare associated infections.<sup>137</sup> *B. cereus* is mainly found in marine and freshwater, vegetables from which soil and food products are easily contaminated.<sup>90</sup> *B. cereus* is also a human pathogen and can cause gastrointestinal diseases by secreting wide array of toxins.<sup>94</sup>

### 3.3 Materials and Methods

#### 3.3.1 Materials

PP pellets were procured from Exxon Mobil (Achieve® Advanced PP 6035G1, 500MFR and 1550MFR). Melt flow rate (MFR) is the flow rate of 2.16 kg of polypropylene, in this case, that was extruded at a standard temperature of 230 °C through a die under set load over 10 min. Two Reicofil manufactured, meltblown PP nonwoven fabrics were supplied by Exxon Mobil. One nonwoven of 25 gram per square inch (gsm) was meltblown from Achieve™ Advanced PP6936G2, and the other was meltblown from Achieve™ Advanced PP6936G2 + 20% Vistamaxx™ 8880 at 25 gsm. Vistamaxx™ 8880 is a low-density isotactic PP polymer, having random distribution of ethylene monomer. Pluronic F-108, having a molecular weight of 14.6 kDa and 82.5 wt. % EO units was obtained from BASF. Distilled water, ethylene glycol, 99.5 % (295530010) (EG) and dimethyl sulfoxide, 99.9 % (032434.M1) (DMSO) were used as probe liquids for contact angle testing. Both EG and DMSO were obtained from Fisher Scientific.

#### Bacterial Growth and Characterization

*E. coli* and *B. cereus* stock culture was a gift from the Department of Crop and Soil Science at NCSU and was subcultured twice from the frozen stock before each experiment. BD Difco™ Plate Count Agar (BD 247940) was used as growth media for both the bacteria. Sodium chloride (NaCl, 99%, 7647-14-5) was used as the sterile suspending liquid. Ethanol (CH<sub>3</sub>CH<sub>2</sub>OH, 99.9 %, 64-17-5) was diluted with distilled water for cleaning purposes.

#### 3.3.2 Methods

##### 3.3.2.1 Meltblowing of PP Nonwoven Fabrics

In this research, three types of nonwovens were fabricated. PP500-BX was produced from Achieve® Advanced PP 6035G1, 500MFR) on the Biax meltblown die, which was 15' long with 736 capillary holes (diameter of 0.009 inch); see Figure 3.2. Fabric was produced at an 11-psi air flow rate. Die to collector distance (DCD) and throughput are set at 12 cm and 0.05 g/(h·m), respectively. The basis weight of the as-produced fiber was 16 gsm (PP500-BX).

PP1550-RI and PP1550-Vista-RI were supplied from Exxon Mobil: Reicofil Meltblown PP 25 gsm Achieve™ Advanced PP6936G2 (PP1550-RI) and 25 gsm Achieve™ Advanced PP6936G2 + 20% Vistamaxx™ 8880. These fabrics were produced on the Reifenhäuser Reicofil™ meltblown pilot line. The width of the Reicofil™ meltblown die is 1 m with 35 capillary holes per inch as shown in Figure 3.2(c) at these conditions: setback/air gap of 1.2 mm, DCD of 25 cm and throughput of 0.4 g/(h·m).

**Table 3.1** Meltblowing of PP nonwoven fabrics using different dies.

Nonwoven ID	Raw material (PP Composition)	Meltblown Fabrication Die
PP500-BX	Achieve® Advanced PP 6035G1, 500 MFR *	Biax
PP1550-RI	Achieve™ Advanced PP6936G2 (1550 MFR*)	Reifenhäuser Reicofil™
PP1550-Vista-RI	Achieve™ Advanced PP6936G2 + 20% Vistamaxx™ 8880* (1550 MFR*)	Reifenhäuser Reicofil™

\*MFR melt flow rate (flow value of the amount of material (2.16 kg for polypropylene) extruded at a standardized temperature (230 °C for polypropylene) through a die under pressure from a set mass over a period of 10 min).

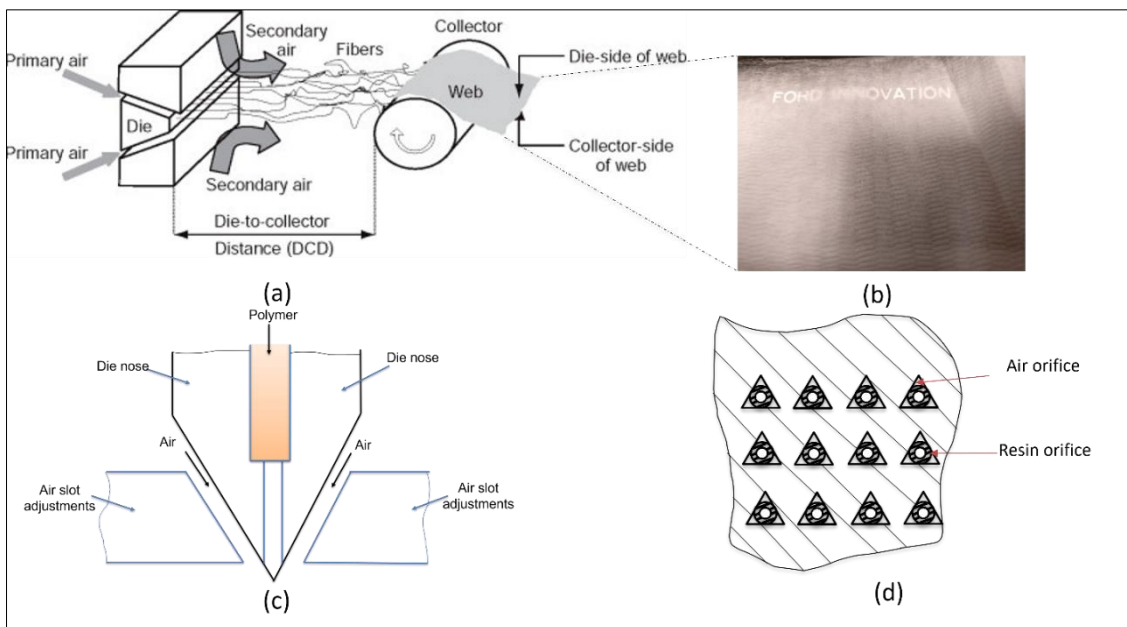


Figure 3.2. Schematics of the (a) meltblowing process <sup>138</sup>, (b) a meltblown PP nonwoven, and die cross-sections for (c) Reifenhäuser Reicofil™ <sup>139</sup> and (d) the Biax Fiberfilm <sup>140</sup> are shown.



### 3.3.2.2 Pluronic Modification of PP Meltblown Nonwovens

Nonwoven fabrics were cut into 5 cm x 5 cm samples and cleansed with sterile water twice before coating. All the cleansed samples were dipped into capped vials containing 50 ml of 1, 3 and 5 % w/v Pluronic F-108 solution in deionized water. The vials were shaken at medium speed for 5 h. Samples were removed from the vial and dried on aluminum foil inside a 1300 Series Class II, Type A2 Biological Safety Cabinet (1323TS) for a minimum of 8 h prior to characterization. The modified nonwovens were named based on the concentration of Pluronic solution used for modification as shown by **Table 3.2**.

**Table 3.2** Naming scheme of modified nonwovens.

Nonwoven ID	Modification Type (Pluronic w/v %)		
	1	3	5
	Modified Nonwoven ID		
PP500-BX	1%-plu-PP500-BX	3%-plu-PP500-BX	5%-plu-PP500-BX
PP1550-RI	1%-plu-PP1550-RI	3%-plu-PP1550-RI	5%-plu-PP1550-RI
PP1550-Vista-RI	1%-plu-PP1550-Vista-RI	3%-plu-PP1550-Vista-RI	5%-plu-PP1550-Vista-RI

### 3.3.2.3 Structure of Meltblown PP Nonwovens

#### Fiber Diameter and Basis Weight

LEXT O SL4000 3D confocal laser microscopic images were obtained for each meltblown fabric. The fiber diameter was measured using ImageJ image analysis software. The results were expressed as the average of 50 measurements per sample, and '±' indicates the standard deviations. The average basis weight (gsm) was measured from three circular samples that were 12 cm<sup>2</sup> in size, according to ASTM D3776<sup>141</sup> using James Heal's Sample Cutter (Model 230/38).

#### Porosity and Surface Roughness

Porosity distribution was determined using a CFP-1100-AEL capillary flow porometer by Porous Material, Inc. according to ASTM D737<sup>142</sup>. The fabric was immersed in Galwick<sup>TM</sup> wetting solution, which has a known surface tension of 15.9 dynes/cm. The sample was completely saturated with solution to give a 0° contact angle. Pore size was measured according to Equation 1, where  $d_p$  is

the pore diameter,  $\gamma$  is the surface tension of the wetting liquid,  $\Theta$  is the contact angle of the wetting liquid, and  $p$  is the extrusion pressure.<sup>143</sup>

$$dp = 4\gamma\cos\Theta/V \dots\dots\dots (1)$$

The surface roughness of the modified and unmodified nonwoven fabrics was measured by the LEXT-O-SL4000 3D confocal laser microscope. The root means square average ( $R_q$ ) of the profile heights over an evaluation length of 0.4 mm were determined. The 50X objective lens was used for measuring image sizes of 720  $\mu\text{m}$  over a minimum of five readings per sample and at least 3 samples of each type of nonwoven.

#### **3.3.2.4 Surface Characterization of Meltblown PP Nonwovens**

Static contact angles measurements for unmodified and modified nonwoven fabrics (sample size 6x6  $\text{cm}^2$ ) were measured using a contact angle goniometer (FTA1000) at room temperature. A droplet of distilled water, having a constant volume of 5  $\mu\text{l}$ , was dispensed using a micro-syringe. Measurements were taken at 5 s intervals for the unmodified, hydrophobic nonwoven since water droplets could remain stable on such surfaces for that length of time. Conversely, measurements were taken at 1 s intervals for the Pluronic modified nonwovens since water droplets were immediately absorbed by its surfaces. The contact angle values for the other three liquids were taken at intervals from 0 to 5 s.

X-ray photoelectron spectroscopy (XPS) was used to investigate the surface chemistry of nonwoven fabrics, especially those treated with Pluronic. XPS on the PHOBIOS 150 hemispherical energy analyzer (SPECS GmbH) was equipped with a monochromatic Mg  $K\alpha$  excitation source (1253.6 eV). Binding energies for O 1s and C 1s were reported for Pluronic segments.

#### **3.3.2.5 Bacterial Suspension & Growth Media**

*E. coli* and *B. cereus* bacteria were first grown overnight at 37 °C on nutrient agar from a frozen stock. For each experiment, cells were inoculated in 10 ml of nutrient broth and cultured

aerobically for 24 h. Bacteria were harvested by centrifugation at 3000 g for 5 min. Bacteria were then resuspended in nutrient broth to a concentration of  $10^7$  cfu/ml.

### **3.3.2.6 Bacteria Count on PP Meltblown Nonwovens Under Static and Flow Conditions**

#### **Under Static Conditions**

To analyze the possible interactions between microbial cells and PP meltblown nonwovens, the fabrics were incubated with cells of the *E. coli* and *B. cereus*. Before incubation with the fabrics, bacterial cultures from agar plates were pre-cultured (30 ml) overnight in nutrient broth media. Aliquots of bacteria pre-cultured cells were inoculated in Erlenmeyer flasks containing 25 ml of nutrient broth to obtain a suspension of  $0.8 \pm 0.02 \times 10^6$  cfu/ml (ensured by UV-vis spectrophotometer). The adhesion of bacterial cells onto PP meltblown nonwovens was then assessed by placing 1 cm<sup>2</sup> pieces of fabric into flasks of inoculant and then incubating them aerobically under orbital shaking at 80 rpm at 30 °C for about 48 h. After 48 h, the fabric mats were removed and rinsed with sterilized water to remove non-adhering bacterial cells. Afterward, each fabric sample was placed onto petri dishes and bacterial colonies were counted using a Quebec Colony Counter.

Bacterial adhesion onto exposed fabrics were qualitatively observed by scanning electron microscopic images. Fabric squares of approximately 7 mm<sup>2</sup> were fixed in 3 % glutaraldehyde in 0.1 M NaPO<sub>4</sub> (pH 7.4) on ice and held at 4 °C for 1 week. Samples are then washed in three 15-minute changes of cold 0.1 M NaPO<sub>4</sub> (pH 7.4) on ice followed by critical point drying (in liquid CO<sub>2</sub> for 7-minute in a Tousimis S-795). The fabrics were then mounted onto stubs with double-sided tape and silver paint. To obtain a better image, all samples were pre-coated in a Hummer 6.2 sputtering system (Anatech USA, Hayward CA) with Au/Pd of 20 Å thickness on top and were viewed in a JEOL JSM-5900LV at 15 kV.

#### **Under Flow Conditions**

A flow cell containing three parallel plate flow chambers of 7.7cm<sup>3</sup> (24mm x 40mm x 8mm) with air bubble traps, supply bottle and a damping bottle connected with a pump was used for continuous flow testing (Figure 3.3). During experiments, suspensions of bacteria were made to flow through a circuit, first passing through the flow chambers and then going into the

dampening bottle and the temperature was maintained at 37 °C. Pump speed can be adjusted to adjust shear rate and flow volume. Flow volume was set at  $0.11 \text{ cm}^3\text{s}^{-1}$  and wall shear rate was  $50\text{s}^{-1}$ . The deposition was continued for 24 h. A control fluid of nutrient broth without bacteria was first passed through the flow cell initially to purge air from the system. The number of adhering microorganisms were counted from the images captured by a phase contrast microscope using a 40X objective lens and each image is analyzed using ImageJ image analysis software.<sup>144</sup>

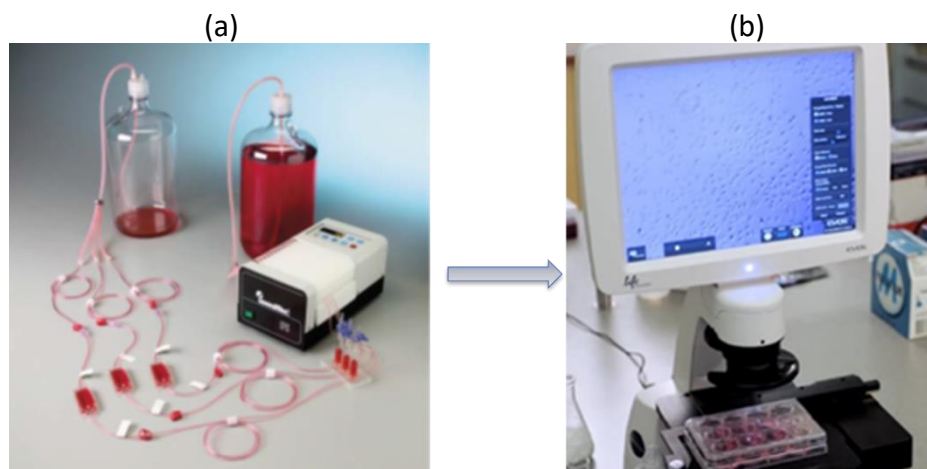


Figure 3.3. (a) Convertible flow cell assembly, (b) Phase contrast microscope, 40X objective lens.

### Statistical Analysis

T-tests were performed to determine significant differences between experimental data sets. The arithmetic mean and standard deviation for the number of bacteria were calculated. The t-test at 95 % confidence interval was used to determine if two populations have different means and the differences were considered significant at  $p < 0.05$ . All data were analyzed using the Origin 2022 statistical software program.

## 3.4 Results and Discussion

### 3.4.1 Meltblowing Die Effect on the Structure of Nonwovens

The characterization of fabric structure included mean fiber diameter, mean pore diameter, basis weight, and root mean square (RMS) roughness, as listed in **Table 3.3**. PP500-BX was more porous ( $15.04 \pm 0.4 \mu\text{m}$ ) with higher RMS roughness of  $11.21 \pm 0.44 \mu\text{m}$  than both PP1550-RI and PP1550-

Vista-RI. The structure of PP500-BX is attributed to the zigzag design of the Biax collector, whereas the commercial Reicofil die produced more uniform nonwoven structures. Also, larger size pores were distributed within PP500-BX, having a mean diameter of  $15.4 \pm 0.4 \mu\text{m}$  (Figure 3.4). PP1550-RI had moderate size pores ( $7.3 \pm 0.5 \mu\text{m}$ ) and moderate RMS roughness with maximum standard deviation ( $7.31 \pm 2.74 \mu\text{m}$ ).

**Table 3.3** Nonwoven structures varied by manufacturing conditions.

Fiber ID	Raw material (Polypropylene Composition)	Die used to manufacture	Mean Fiber Diameter ( $\mu\text{m}$ ) $\pm$ SD <sup>b</sup>	Mean pore diameter ( $\mu\text{m}$ ) $\pm$ SD <sup>b</sup>	Basis weight ( $\text{g}/\text{m}^2$ ) $\pm$ SD <sup>b</sup>	RMS roughness <sup>c</sup> ( $R_q$ ), $\mu\text{m}$ $\pm$ SD <sup>b</sup>
PP500-BX	Achieve® Advanced PP 6035G1, 500MFR <sup>a</sup>	Biax	$1.5 \pm 0.5$	$15.4 \pm 0.4$	$16 \pm 0.1$	$11.21 \pm 0.44$
PP1550-RI	Achieve™ Advanced PP6936G2 (1550 MFR <sup>a</sup> )	Reifenhäuser Reicofil™	$1.5 \pm 0.6$	$7.3 \pm 0.5$	$25 \pm 0.1$	$7.31 \pm 2.74$
PP1550-Vista-RI	Achieve™ Advanced PP6936G2 + 20% Vistamaxx™ 8880 (1550 MFR <sup>a</sup> )	Reifenhäuser Reicofil™	$1.8 \pm 0.3$	$8.2 \pm 0.5$	$25 \pm 0.1$	$8.41 \pm 0.05$

<sup>a</sup> MFR melt flow rate (flow value of the amount of material (2.16 kg for polypropylene) extruded at a standardized temperature (230 °C for polypropylene) through a die under pressure from a set mass over a period of 10 min); <sup>b</sup> SD Standard deviation; <sup>c</sup> Root mean square roughness,  $R_q$ , is the root mean square average of the profile heights over the evaluation length.

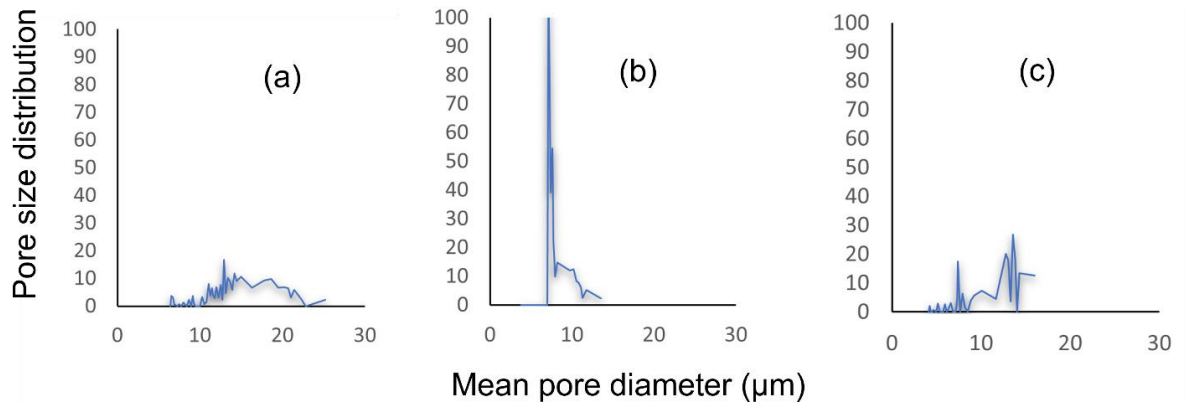


Figure 3.4. Pore size distribution vs pore diameter for (a) PP500-BX, (b) PP1550-RI and (b) PP1550-Vista-RI.

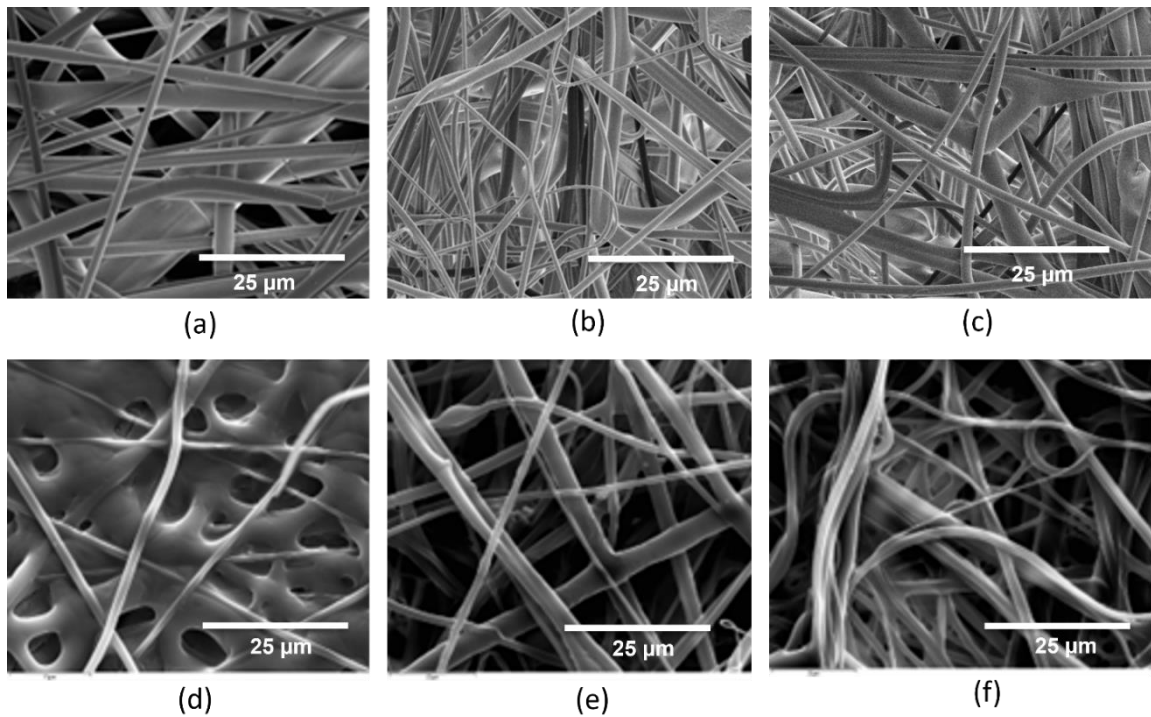


Figure 3.5. Topography of PP500-BX, PP1550-RI, and PP1550-Vista-RI before modification (a, b, and c, respectively) and after modification with 5 w/v % aqueous pluronic solution (d, e, and f respectively).

**Table 3.4** Surface properties of PP meltblown nonwovens loaded with the Pluronic copolymer.

Nonwovens	Properties		
	% w/v Pluronic addition	RMS roughness ( $R_q$ ), $\pm$ SD $\mu\text{m}$	Water Contact angle ( $^\circ$ ) $\pm 1.5$
PP500-BX	0	$11.21 \pm 0.44$	137.9
	1	$9.04 \pm 0.44$	129
	3	$7.89 \pm 0.44$	128.8
	5	$7.5 \pm 0.44$	121.9
PP1550-RI	0	$7.31 \pm 2.74$	143
	1	$7.52 \pm 3.01$	121.5
	3	$8.01 \pm 2.25$	120.8
	5	$8.24 \pm 2.25$	109.3
PP1550-Vista-RI	0	$8.41 \pm 0.05$	140.2
	1	$8.86 \pm 1.09$	119.6
	3	$8.5 \pm 1.05$	105.6
	5	$7.23 \pm 3.01$	126.1

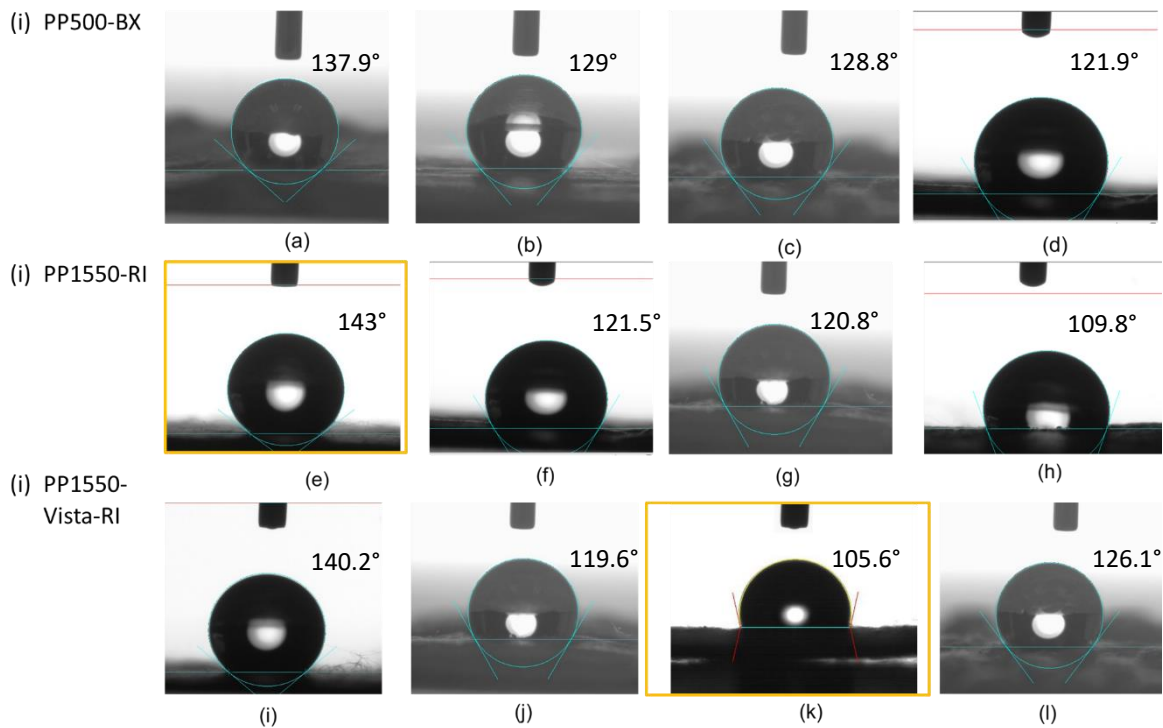


Figure 3.6. Water contact angles of (i) PP500-BX, (ii) PP1550-RI and (iii) PP1550-Vista-RI before and after 0, 1 %, 3 % and 5 % Pluronic treatment; highlighted panels indicate most hydrophobic (PP1550-RI,  $\sim 143^\circ$ ) and most hydrophilic (PP1550-Vista-RI  $\sim 105.6^\circ$ ) surfaces.

### 3.4.2 Effect of PP Nonwoven Structure on Bacterial Adhesion

#### Under Static Conditions

Between *E. coli* and *B. cereus*, the latter is found to attach on nonwovens in greater quantity than *E. coli*. There were more *B. cereus* adhered to PP1550-Vista-RI than PP1550-RI and PP500-BX. This can be due to the similar fiber length of nonwoven fibers (1.5 – 1.8  $\mu\text{m}$ , **Table 3.3**) to that of *B. cereus* which can be as large as (1.0–1.2  $\mu\text{m}$  by 3.0–5.0  $\mu\text{m}$ )<sup>24</sup> (Figure 3.7). PP1550-Vista-RI has almost double bacteria than PP500-BX after incubation with *B. cereus* (**Table 3.5**). This increase in cell attachment can be explained by the rougher surface of PP1550-Vista-RI (**Table 3.3**). The differences in bacterial attachment among the nonwoven surfaces containing both PP500-BX and PP1550-RI for *E. coli* were all significant at  $p < 0.05$  based on t-test.

**Table 3.5** *E. coli* and *B. cereus* (log cfu/cm<sup>2</sup>) cells adhered to nonwovens under static conditions.

Sample ID	48 hr of incubation (log cfu/cm <sup>2</sup> ) $\pm$ SD	
	<i>E. coli</i>	<i>B. cereus</i>
PP500-BX	0.51 $\pm$ 0.56	1.6 $\pm$ 0.44
PP1550-RI	0.51 $\pm$ 0.67	1.9 $\pm$ 0.53
PP1550-Vista-RI	0.72 $\pm$ 0.53	3.1 $\pm$ 0.69

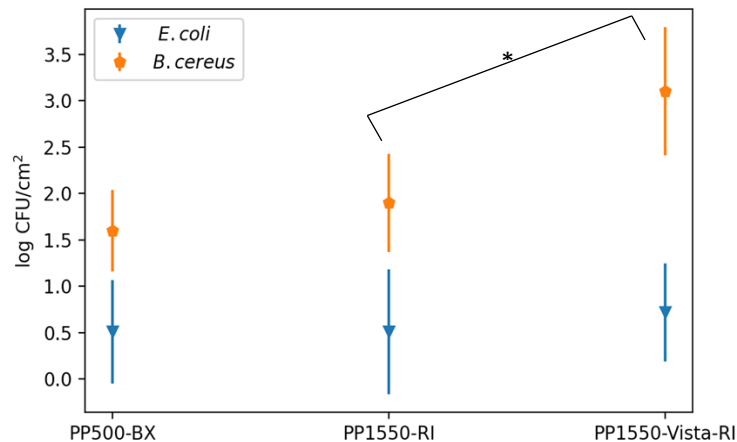


Figure 3.7. *E. coli* and *B. cereus* (log cfu/cm<sup>2</sup>) cells adhered to nonwovens under static conditions (aerobic incubation at 80 rpm at 30 °C for about 48 h), error bars indicate standard deviation, \* $p < 0.05$ .



The numbers of bacterial adhesion between PP1550-Vista-RI and PP1550-RI were compared by t-test. Under static conditions (aerobic incubation at 80 rpm at 30 °C for about 48 h), there is a significant difference in bacterial adhesion between the samples of PP1550-RI and PP1550-Vista-RI (as shown in Figure 3.7). There are more bacteria adhered to PP1550-Vista-RI than PP1550-RI.

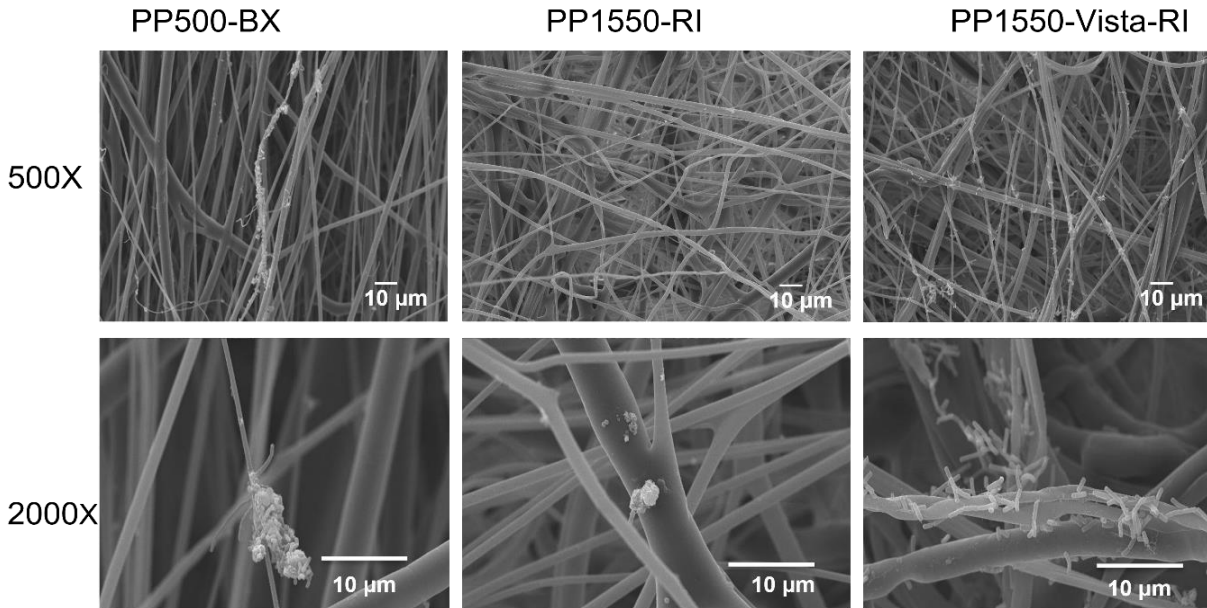


Figure 3.8. Scanning electron micrographs of PP meltblown nonwovens after 48 h of static incubation with *E. coli*: (a), (d): PP500-BX, 17 gsm; (b), (e): PP1550-RI, 25 gsm; (c), (f): PP1550-Vista-RI, 25 gsm.

PP500-BX was more porous ( $15.04 \pm 0.4 \mu\text{m}$ ) with higher RMS roughness of  $11.21 \pm 0.44 \mu\text{m}$  than both PP1550-RI and PP1550-Vista-RI (**Table 3.3**). Also, larger size pores were distributed within PP500-BX, having a mean diameter of  $15.4 \pm 0.4 \mu\text{m}$  (Figure 3.4). PP1550-RI had moderate size pores ( $7.3 \pm 0.5 \mu\text{m}$ ) and moderate RMS roughness with maximum standard deviation ( $7.31 \pm 2.74 \mu\text{m}$ ). Since we could count only the colonies present on the surface and not those falling into grooves between BIAx and Reicofil samples, higher adhesion was found to be on Reicofil samples with moderate porosity. But in case of similar roughness and porosity, surface chemistry was found to govern bacteria adhesion on Reicofil samples. Both PP1550-Vista-RI and PP1550-RI are structurally similar except the presence of Vistamaxx. The presence of Vistamaxx was found to increase surface roughness of PP-Vista-RI and hence can be the reason behind higher bacterial adhesion under static conditions. Significantly higher adhesion was also confirmed by the SEM

images as shown in Figure 3.8 on PP1550-Vista-RI. Hydrophobic polypropylene backbone with 20 % comonomer of polyethylene might have slightly decreased hydrophobicity ( $\sim 140^\circ$ ) than the PP-1550-RI ( $\sim 143^\circ$ ). Under static conditions, adhesion is mainly governed by the surface geometry and surface chemistry of the nonwoven fibers.

### Under Continuous Media Flow

The numbers of *E. coli* and *B. cereus* colonies ( $\log \text{cfu/cm}^2$ ) adhered to nonwovens (PP500-BX, PP1550-RI, and PP1550-Vista-RI) at definite time intervals are reported in **Table 3.6**. A similar quantity of *E. coli* ( $\sim 2.10 \log \text{cfu/cm}^2$ ) is attached to both PP500-BX and PP1550-RI fabrics after 24 h of incubation (Figure 3.9). But PP1550-Vista-RI has the highest quantity of *E. coli*, and this can be explained by the larger fiber diameter and larger pore diameter (**Table 3.3**) of PP1550-Vista-RI as fiber diameter increases, surface area decreases for the initial attachment of bacteria (Figure 3.6).

**Table 3.6** *E. coli* and *B. cereus* ( $\log \text{cfu/cm}^2$ ) cells adhered to nonwovens at a shear rate of  $50 \text{ s}^{-1}$ .

Experiments	<i>E. coli</i> ( $\log \text{cfu/cm}^2$ ) $\pm$ SD	<i>B. cereus</i> ( $\log \text{cfu/cm}^2$ ) $\pm$ SD
PP500-BX (0.5 hr)	$0.31 \pm 0.55$	$0.50 \pm 0.67$
PP500-BX (2 hr)	$0.51 \pm 0.56$	$0.55 \pm 0.63$
PP500-BX (4 hr)	$0.66 \pm 0.44$	$0.66 \pm 0.78$
PP500-BX (6hr)	$0.65 \pm 0.57$	$1.50 \pm 0.59$
PP500-BX (12 hr)	$0.86 \pm 0.44$	$1.60 \pm 0.44$
PP500-BX (24hr)	$2.10 \pm 0.24$	$2.30 \pm 0.34$
PP1550-RI (0.5 hr)	$0.25 \pm 0.53$	$0.23 \pm 0.53$
PP1550-RI (2 hr)	$0.51 \pm 0.67$	$0.56 \pm 0.78$
PP1550-RI (4 hr)	$0.90 \pm 0.23$	$1.30 \pm 0.23$
PP1550-RI (6hr)	$1.60 \pm 0.31$	$1.70 \pm 0.45$

**Table 3.6** (continued).

PP1550-RI (12 hr)	1.50 ± 0.53	1.90 ± 0.53
PP1550-RI (24hr)	2.10 ± 0.86	2.50 ± 0.56
PP1550-Vista-RI (0.5 hr)	0.35 ± 0.55	0.36 ± 0.55
PP1550-Vista-RI (2 hr)	0.72 ± 0.53	0.67 ± 0.55
PP1550-Vista-RI (4 hr)	0.95 ± 0.61	0.95 ± 0.68
PP1550-Vista-RI (6hr)	3.10 ± 0.85	2.90 ± 0.85
PP1550-Vista-RI (12 hr)	3.50 ± 0.66	3.10 ± 0.69
PP1550-Vista-RI (24hr)	3.80 ± 0.53	3.50 ± 0.53

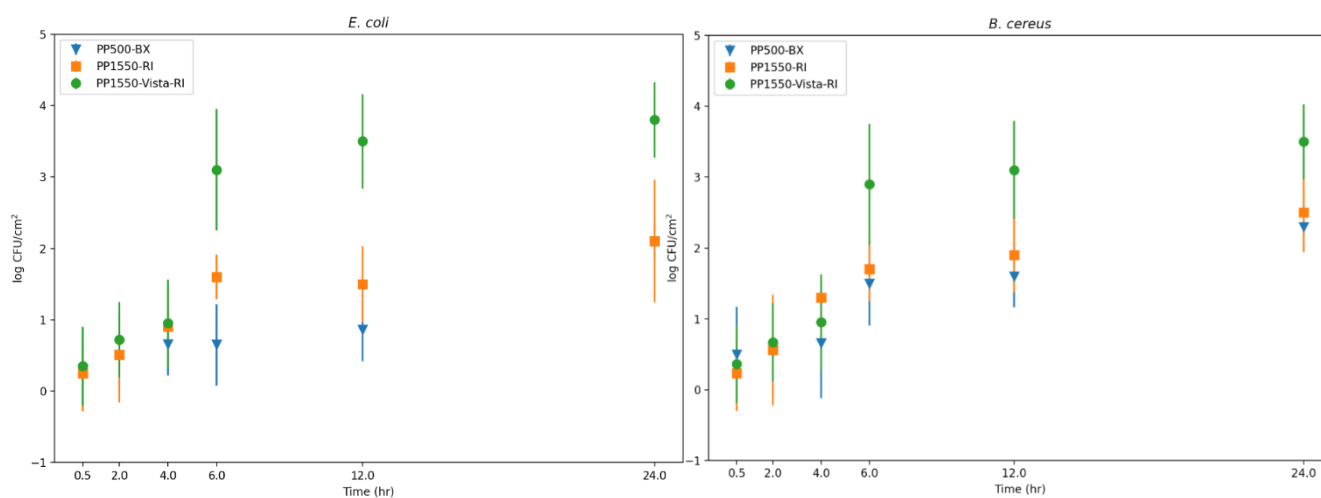


Figure 3.9. *E. coli* and *B. cereus* (log cfu/cm<sup>2</sup>) cells adhered to nonwovens at a shear rate of 50 s<sup>-1</sup>, error bars indicate standard deviation.

### 3.4.3 Characterization of Pluronic Treated Meltblown PP Nonwovens

The presence of Vistamaxx™ 8880 additive improved the surface roughness of PP1550-Vista-RI. SEM images showed maximum surface coverage after coating with 5 w/v % Pluronic (Figure 3.5(d)). This resulted in pore blocking and decrease in RMS roughness by 33 % and also a decrease in water contact angles from 137.9 ° to 121.9 ° (**Table 3.4**). The SEM images of PP1550-RI and

PP1550-Vista-RI showed an increase in roughness due to wrinkling on the fibers (Figure 3.5 (e, f)) after the Pluronic modification. This increase in surface roughness and moderate pore blockage after modification also resulted in a slight decrease in water contact angles (**Table 3.4**). The RMS roughness value associated with this 3%-plu-PP1550-Vista-RI was intermediate ( $8.5 \pm 1.05 \mu\text{m}$ ) between roughness values for untreated and treated nonwovens (**Table 3.4**). PP500-BX showed maximum drop in RMS roughness after 5w/v % Pluronic Treatment ( $7.5 \pm 0.44 \mu\text{m}$ ).

The water contact angles decreased for nonwoven fabrics after treatment with 1 w/v % aqueous pluronic solution as shown by the water contact angles in **Table 3.4**. But with an increase in the concentration of pluronic in solution, water contact angle measurements were unchanged for PP1550-Vista-RI upon modification. No significant differences existed between the structures of PP1550-RI and PP1550-Vista-RI except for the Vistamaxx™ 8880 additive. Therefore, changes in roughness and hydrophilicity after modification with 5 w/v % aqueous Pluronic solution can be explained by the presence of Vistamaxx™ 8880 in PP1550-Vista-RI.

Pluronic modification was found to improve hydrophilicity while decreasing the roughness of PP1550-Vista-RI. PP1550-Vista-RI showed the maximum drop in water contact angle ( $\sim 28^\circ$ ) due to treatment with 3 w/v % of Pluronic (Figure 3.6).

XPS C 1s peaks for treated fabrics are shown in Figure 3.10 in comparison to untreated fabrics. C 1s peak of untreated nonwovens showed only one C-C peak at 285 eV. After Pluronic treatment, C-O peaks at 287 eV were determined for all the samples. Although XPS revealed the presence of Pluronic at the surface of meltblown PP nonwovens, the presence of representative C-O groups was not consistent across all fabric surfaces. For Pluronic treated surfaces, there was a decrease in intensity for C-C peaks whereas increase in C-O peaks. The strongest interaction was observed for PP-1550-RI as shown by the increase in intensity of C-O peak after 5 w/v % Pluronic modification. This may be due to the strongest interaction of hydrophilic parts of Pluronic molecules with the PP-1550-RI sample.

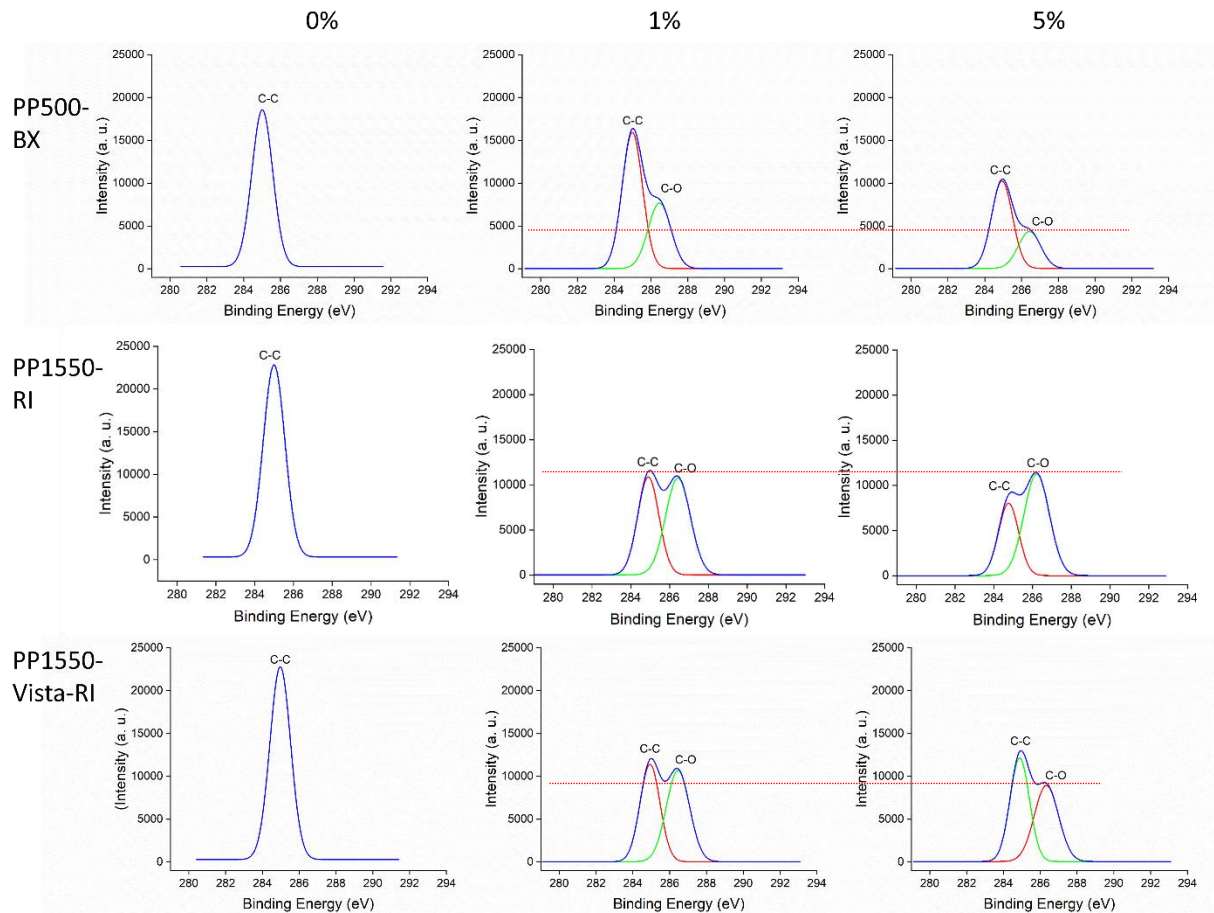


Figure 3.10. Representative XPS spectra of nonwoven fabrics (PP500-BX, PP1550-RI, PP1550-Vista-RI) after a) 0 %, b) 1 % and c) 5 % Pluronic treatment.

### 3.4.4 Effect of Pluronic Treatment on Bacterial Adhesion

Before Pluronic treatment and under static condition, PP1550-Vista-RI had the maximum colony forming units (cfu) of both *E. coli* and *B. cereus* as confirmed by **Table 3.5** and Figure 3.7. Higher resolution SEM image also confirmed the presence of higher cfu of *E. coli* on unmodified PP1550-Vista-RI (Figure 3.8).

Under continuous flow conditions, the same trend for *E. coli* and *B. cereus* colonies on PP1550-Vista-RI was observed (**Table 3.6**). Irrespective of the type of bacteria, PP-1550-Vista-RI had the maximum bacterial accumulation over time ( $\sim 3.80$  cfu/cm<sup>2</sup>) (Figure 3.9).

After pluronic treatment, between *E. coli* and *B. cereus*, the growth of the latter was more influenced by the Pluronic treatment (**Table 3.7**). Figure 3.11 shows the colony count at static

conditions for Pluronic treated nonwovens. PEO blocks of Pluronic copolymers tend to hinder the cell attachment<sup>127</sup> and hence with 5 w/v % Pluronic in aqueous solution, PP1550-Vista-RI has almost negligible amount of bacteria (Figure 3.12). However, there was no significant difference for all types of fabrics for adhesion of both the bacteria. Figure 3.12 shows the photographs of Pluronic treated nonwovens incubated for 48 h with *E. coli* at static conditions. From the highlighted pictures, it is evident that highest growth was found on 5%-PP1550-RI in comparison to 1%-PP1550-RI. This drastic increase in *E. coli* growth may be due to the highest decrease in water contact angle (**Table 3.4**: from 143 ° to 109 °). Also, there was negligible amount of *E. coli* (Figure 3.12) on both 1 w/v % and 5 w/v % treated PP-1550-Vista-RI. Whereas 3%-plu-PP1550-Vista-RI has the maximum amount of *E. coli* among all three treated samples which again can be explained by the decrease in water contact angle after treatment with Pluronic solution (**Table 3.3**: ~ 105 °). Tahmineh et al. found wettability is the primary factor to be responsible for considerably higher adhesion on porous textiles.<sup>92</sup> They also found that hydrophobic textiles with smaller pores would promote *E. coli* adhesion. All the nonwoven samples were still hydrophobic (lowest contact angle achieved ~ 105 °) even after 5 % Pluronic modification, but the combined effect of reduced pore sizes on modified nonwovens also contributed to more bacterial adhesion irrespective of the type of bacteria.

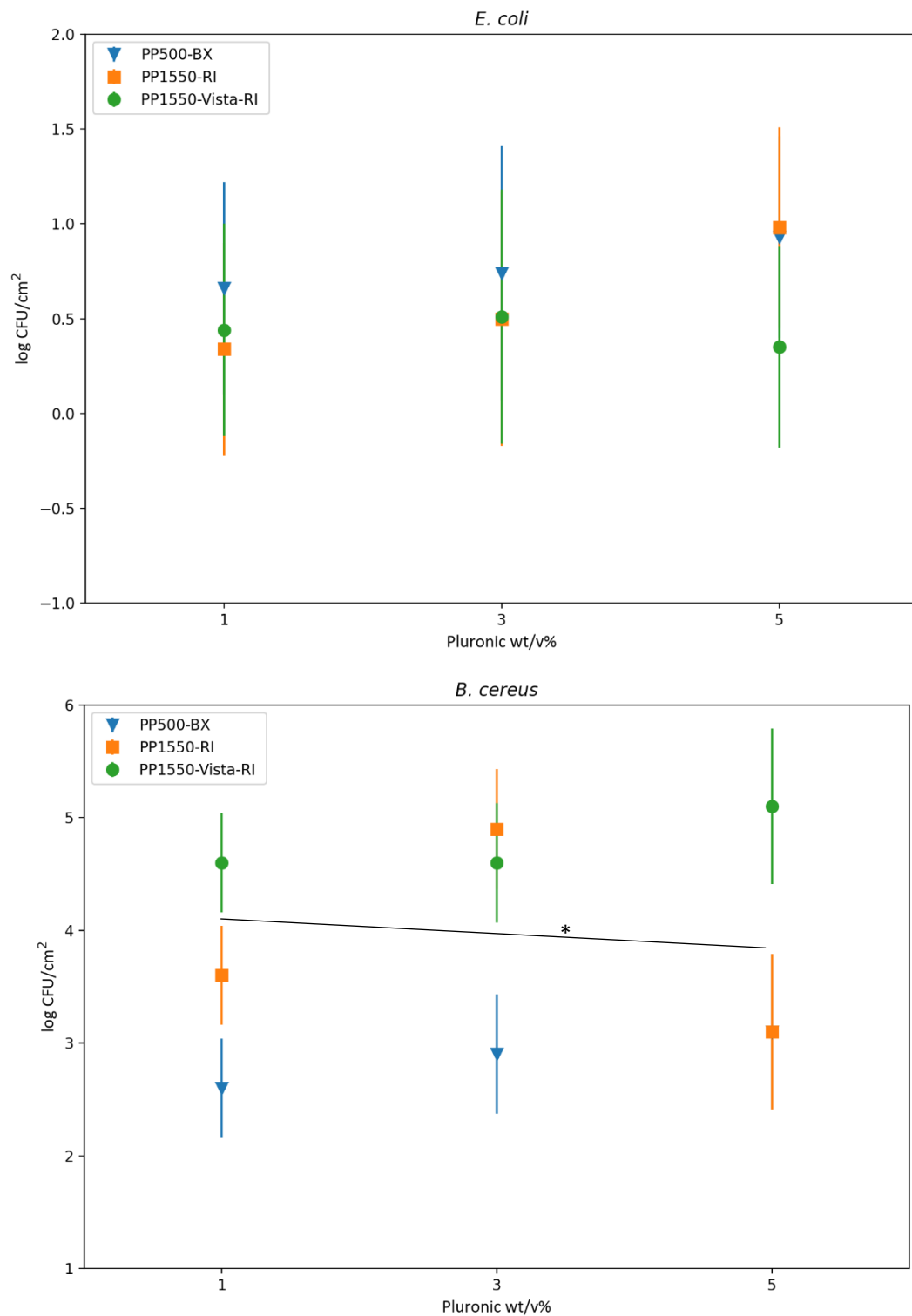


Figure 3.11. *E. coli* and *B. cereus* attachment to modified nonwovens under static conditions, error bars indicate standard deviation, \*p < 0.05.

Figure 3.11 shows the count of colony forming units at static conditions for Pluronic treated nonwovens. Significant differences were observed based on a t-test performed at 95 % confidence interval between *E. coli* and *B. cereus* but there was no substantial difference among nonwoven samples for *E. coli* attachment. *B. cereus* was found to attach significantly on Pluronic treated PP1550-Vista-RI (**Table 3.7**) than Pluronic treated PP500-BX.

**Table 3.7** Mean colony forming units attached to modified nonwovens under static conditions.

Sample ID	48 hr of incubation (log cfu/cm <sup>2</sup> ) ± SD	
	<i>E. coli</i>	<i>B. cereus</i>
1%-plu-PP500-BX	0.66 ± 0.56	2.6 ± 0.44
3%-plu-PP500-BX	0.74 ± 0.67	2.9 ± 0.53
5%-plu-PP500-BX	0.93 ± 0.53	3.1 ± 0.69
1%-plu-PP1550-RI	0.34 ± 0.56	3.6 ± 0.44
3%-plu-PP1550-RI	0.5 ± 0.67	4.9 ± 0.53
5%-plu-PP1550-RI	0.98 ± 0.53	3.1 ± 0.69
1%-plu-PP1550-Vista-RI	0.44 ± 0.56	4.6 ± 0.44
3%-plu-PP1550-Vista-RI	0.51 ± 0.67	4.6 ± 0.53
5%-plu-PP1550-Vista-RI	0.35 ± 0.53	5.1 ± 0.69



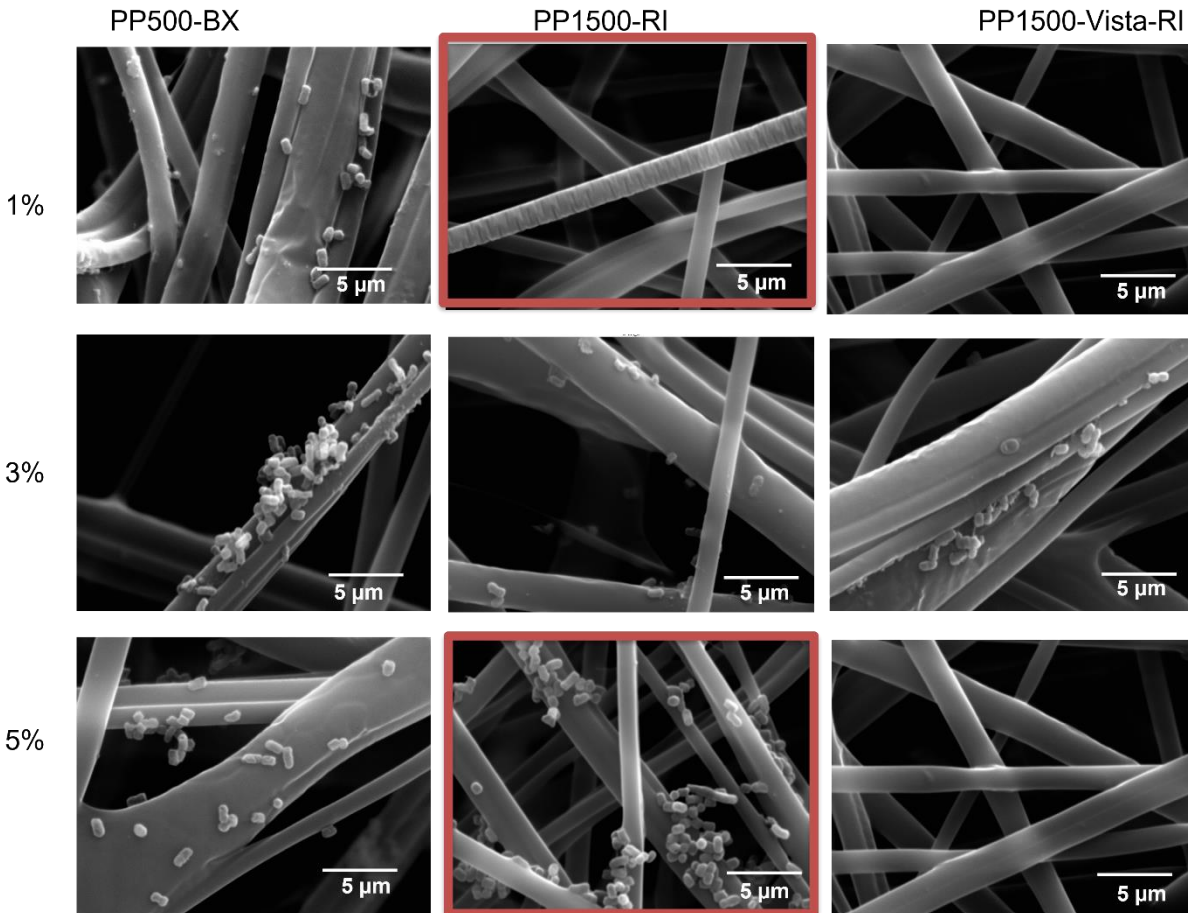


Figure 3.12. Scanning electron micrographs of Pluronic treated PP meltblown nonwovens after 48 h of static incubation with *E. coli* (highlighted: lowest ( $0.34 \text{ cfu/cm}^2$ ) and highest ( $0.98 \text{ cfu/cm}^2$ ) count on 1%-PP1550-RI and 5%-PP1550-RI respectively).

### 3.5 Conclusions

PP500-BX has higher porosity and surface roughness than PP1550-RI and PP1550-Vista-RI. But higher number of *E. coli* was found on PP1550-Vista-RI with a randomly distributed Vistamaxx additive. Unmodified nonwovens were more easily approached by hydrophilic bacteria *E. coli* and *B. cereus* (refer to Chapter 2) than the modified nonwovens for adhesion. Hydrophilic modified nonwovens showed a poor affinity for *E. coli*. But Pluronic modification influenced cell attachment between PP1550-RI and PP1550-Vista-RI. With the increase in Pluronic concentration, *E. coli* adhered to PP1550-Vista-RI in higher quantity with a larger surface area.

Both the surface chemistry and surface topography helped to accumulate *E. coli* on hydrophobic PP1550-Vista-RI.

*B. cereus* bacteria showed a maximum affinity for 5%-plu-PP1550-Vista-RI. Surface irregularities may provide protection to entrapped bacterial cells due to lower shear forces and larger surface area available for adhesion and thus cause cell proliferation.<sup>145</sup> In this case, the size of *B. cereus* bacteria may also played an important role in cell accumulation.

Surface tensions of untreated PP nonwoven fabrics ranged from 31 mN/m and could not prevent the initial attachment of hydrophilic *E. coli* and *B. cereus* bacteria (refer chapter 2) from the environment. Though after Pluronic treatment, the combined change in both the hydrophilicity and roughness influenced adhesion. But overall roughness and fiber diameter contributed more than the surface chemistry in reducing adhesion. Between nonwovens with similar morphologies, the presence of additives played a vital role in bacterial adhesion as the presence of additives also influenced surface chemistry. We can conclude that bacterial adhesion on hydrophobic PP nonwovens is affected by the surface tension and morphology before modification. After modification with Pluronic copolymers, the change in surface chemistry was mostly responsible for reduced bacterial adhesion. Further research should be conducted to measure the force of bacterial adhesion to quantify the changes in adhesion energies due to chemical treatment.

### **Acknowledgments**

This research was sponsored by the Nonwovens Institute (NWI 17-212) and the Department of Textile Engineering, Chemistry and Science, Wilson College of Textiles. The authors are greatly indebted to Dr. Shuang Liu and Dr. Juan Frene for their guidance in bacteria studies.

## CHAPTER 4

### BACTERIAL ADHESION ONTO HYDROPHOBIN TREATED MELTBLOWN POLYPROPYLENE NONWOVENS UNDER STATIC AND CONTINUOUS FLOW CONDITION

#### 4.1 Abstract

Bacteria adhesion and their subsequent colonization onto porous fabrics is a critical concern for public health and safety. The performance of nonwoven textiles, per their usage towards applications in health, hygiene, and filtration, is greatly limited by bacterial contamination as bacterial contamination can lead to cross contamination and infection from healthcare and hygiene products and formation of drug and antibiotic resistant biofilm on filter surfaces.<sup>109–113</sup> Owing to their porous structure and roughness, meltblown nonwovens- in particularly those manufactured from polypropylene, PP- are disposed to bacterial adhesion, its growth, and the formation of biofilms. Modification and careful tuning of hydrophobic nonwoven textiles can improve their performance against bacteria contamination. This study is focused on the influence of native protein: hydrophobin (H\* Protein B) modifications in varying concentrations upon bacteria adhesion onto nonwoven surfaces at both the static and continuous flow conditions. As model bacteria gram negative *Escherichia coli* (*E. coli*, rod shaped, 1-2  $\mu\text{m}$ ), was used in this study. *E. coli* was chosen as it is one of the most common bacteria present in the atmosphere and is a common gut microorganism and can be excreted very easily in fecal matter and hence can also be found in soil, water, plant, and food.<sup>91</sup> Nonwoven hydrophilicity and roughness contributed significantly to promote the adhesion of *E. coli* both under static and continuous flow. Continuous flow helped in *E. coli* adhesion both on unmodified and modified PP nonwovens. *E. coli* adhesion increased with the increase in concentration of hydrophobin due to the combined effect of increased surface roughness and wettability. The assembly of hydrophobin onto nonwovens tuned the adhesion as such at 5 w/w % conc., adhesion was more than doubled from the number of initially attached bacteria. The dependence of *E. coli* adhesion with the hydrophobin concentrations in coating solutions can be scaled up to develop products for the wet wipes and water filters industry where bacterial adhesion is desired to clean or filter out bacteria,

respectively. The flowrate and supply of nutrients and type of bacteria can be the limiting factors to reverse the adhesion when is not desirable.<sup>22</sup>

## 4.2 Introduction

Bacteria adhesion and their subsequent colonization onto porous fabrics<sup>92</sup> is a serious concern for public health and safety. The performance of nonwoven textiles, per their usage towards applications in health, hygiene, and filtration, is greatly limited by bacterial contamination as bacterial contamination can lead to cross contamination and infection from healthcare and hygiene products and formation of drug and antibiotic resistant biofilm on filter surfaces.<sup>109–113</sup> Owing to their porous and rough structure, meltblown nonwovens- in particularly those manufactured from polypropylene, PP- are disposed to bacterial adhesion, its growth, and the formation of biofilms<sup>95</sup>. Though in applications like wipes, face masks and filters, one requires to trap bacteria, but in no such cases biofilm is desirable.<sup>108,115,146–153</sup> Biofilm is a complex structure comprising heterogeneous microbial communities which is very difficult to get rid of and usually pose disease and nosocomial infections when in contact with the human.<sup>146</sup> As model bacteria gram negative *Escherichia coli* (*E. coli*) (rod shaped, 1-2  $\mu\text{m}$ )<sup>89</sup>, was used in this study for both the studies under static and flow conditions. *E. coli* is a common gut microorganism and can be excreted very easily in fecal matter and hence can also be found in soil, water, plant, and food.<sup>91</sup> Several strains being pathogenic, *E. coli* is one of the frequent pathogens in hospital-related and healthcare associated infections.<sup>137</sup>

Microbial contamination leads to biofilm formation which can occur on all types of surfaces exposed to aqueous environments such as rocks in the river, ship hulls, tooth surfaces, soft tissues, implanted biomaterials, beverage filters.<sup>154</sup> To understand bacteria contamination, one approach is understanding their adhesion at static and flow conditions. Previous studies found shear flow promotes biofilm formation by increasing the exopolymeric substance production.<sup>155,156</sup> At static condition bacteria deposition depends on mainly bacteria properties whereas surface properties (wettability, porosity, roughness etc.) and fluid properties are more prominent under flow.<sup>19</sup> Most common industrial applications for nonwovens i. e. wet wipes<sup>86</sup>,

air filters<sup>53</sup>, masks<sup>95</sup> etc. deal with hydrodynamic flow conditions such as shear rates<sup>157</sup> and the flow type<sup>107</sup> - laminar and turbulent flow.<sup>19</sup> Under flow conditions, the rate of adhesion depends on mass transport towards substrate surface and the wall shear rates. Increased fluid flow leads to faster adhesion due to higher mass transport<sup>158</sup> but when fluid flow exceeds a critical limit, wall shear rates are more prominent.<sup>159</sup> Wall shear rates of 6000 – 8000 s<sup>-1</sup> was found to prevent adhesion of *Pseudomonas fluorescens* to stainless steel but wall shear rate of 12000 s<sup>-1</sup> caused the detachment of adhering microorganisms.<sup>154</sup> Adhesion of *Staphylococcus aureus* to collagen coated glass plates was increased at a wall shear rate of 50 – 300 s<sup>-1</sup> and after wall shear rate exceeded the critical limit, the adhesion was decreased at wall shear rate > 500 s<sup>-1</sup>.<sup>160</sup>

Tahmineh et al.<sup>92</sup> found hydrophilic surfaces resulted in higher adhesion of both the gram positive *S. aureus* and gram negative *E. coli* bacteria onto polystyrene (PS) and polylactic acid (PLA) fibers. Though high surface roughness of electrospun PS and PET web promoted bacteria adhesion but it has been found the combined effect of lower pore volume and the smaller fiber-to-fiber gap led to a lower bacteria adhesion as it prevented penetration of bacteria into the structure and hence reversed the adhesion.<sup>92</sup> Several studies are done in static conditions though bacteria adhesion and growth on porous substrates is highly dependent on the hydrodynamic conditions.<sup>93</sup> As the fluid flows, both the deposition and reversibility of bacterial adhesion can occur as the results of the shear rate and flow displacement. Desorption of *Staphylococcus epidermidis* HBH<sub>2</sub> 169, *Acinetobacter calcoaceticus* RAG-1, *Streptococcus thermophilus* from different substrate surfaces was found to be stimulated under flow conditions (Flow volume 0.11 cm<sup>3</sup> and wall shear rate 50 s<sup>-1</sup>) mainly due to the collisions between flowing and adhering bacteria.<sup>93</sup> Researchers found that the secondary interaction minimum (an energy barrier at longer separation distance of several hundred Ångstroms) to be mainly responsible for both the deposition and reversibility of bacterial adhesion on inert polystyrene surface, whereas both the adsorption and desorption phases are influenced by the acid-base interactions for a hydrophobic substrate like fluoroethylenepropylene.<sup>93</sup>

Modification and careful tuning of hydrophobic nonwoven textiles can improve their performance against bacteria contamination as hydrophobic surfaces are more susceptible to bacterial attachment.<sup>161–163</sup> To investigate bacteria adhesion on hydrophobic nonwoven textiles,

we chose to modify their surfaces with a native protein called hydrophobin. Hydrophobins having special bifunctional nature can influence both the roughness and hydrophilicity of nonwovens and have been found to reduce bacterial attachment in previous research.<sup>164, 165</sup> The biofilm formation by *Staphylococcus epidermidis* (nosocomial pathogen) on PS surfaces was reduced by self-assembly of two class I hydrophobins (Vmh2 and Pac3).<sup>166</sup>

Hydrophobins are small proteins of about 100 to 150 amino acids, derived from filamentous fungi, for example *Schizophyllum commune* filamentous fungi.<sup>164</sup> The order of the eight cysteine residues in the hydrophobin primary structures forms a characteristic pattern as all cysteine-residues form disulfides located inside the structure and are clustered into two parts of the structure. Both clusters contain four cysteine-residues each and form extended covalent linkages that span the entire structure and conserve the structure.<sup>164</sup>

Bacterial and fungal microbes release these amphiphilic, hydrophobin proteins to aid their attachment onto hydrophobic surfaces and from the bulk of liquid media. They have unique properties of stability against pH, temperature, solvents, detergents, and ability to modify surfaces and interphases (Teflon, Carbon, PP, PE, PET, Al, wood, SiO<sub>2</sub>). Even under in vitro or technical conditions hydrophobins can reverse the surface polarity by easily self-assembling at interfaces in aqueous solution and under mild conditions, immediately suggest potential applications for these surface active proteins.<sup>167</sup> At the air-water interface the SC3 hydrophobin from *Schizophyllum commune* self-assembles to form an amphiphilic coating which lowers the surface tension and allows the fungus to grow through it.<sup>43</sup> Hydrophobin surface layers also seem to mediate the attachment of pathogenic fungi to the host surface, such as plant or insect cuticle.<sup>44</sup> The SC3 hydrophobin has been found to form very stable coatings on hydrophobic materials such as Teflon and Parafilm, and thereby make them more hydrophilic.<sup>43</sup> Self-assembly of hydrophobins change a surface from hydrophilic to hydrophobic, while hydrophobic material becomes hydrophilic. The water contact angle of the hydrophobic and hydrophilic side of the assembled hydrophobin was found to be in between 60° and 120° and between 22° and 60°, respectively.<sup>45</sup>

Unique combination of amphiphilic and self-assembling nature made these proteins suitable for modification of various such as textiles, polymers, glass surface etc.<sup>168</sup> Their self -assembling capacity depends on their patterns of clustering hydrophobic and hydrophilic parts in solution. From natural sources, hydrophobins are available only in milligram amounts, while BASF succeeded in a recombinant production process, up scaled to pilot plant production in kilogram scale. The optimization by modulation of gene expression as well as the generation of various fusion proteins finally lead to two artificial hydrophobins variants called H\*Protein A and H\*Protein B.<sup>169</sup>

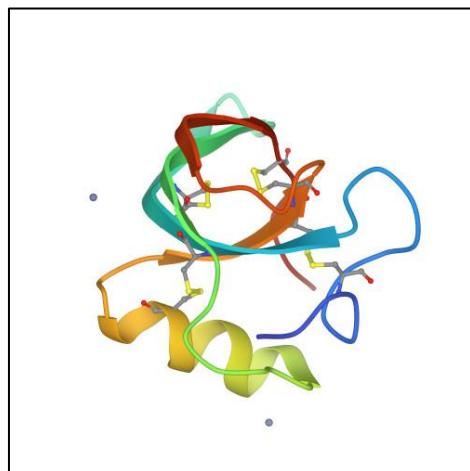


Figure 4.1. Crystal structure of hydrophobin.<sup>170</sup>

US 2006/0040349 A1 patent invented a hydrophobin derived from the thermophilic fungus *Talaromyces thermophiles*.<sup>48</sup> This patent also mentioned numerous applications of hydrophobins which include tissue engineering, drug delivery, stable foam formation etc. Another patent revealed a novel method for coating surfaces with hydrophobin.<sup>49</sup> These proteins have highly conserved structure of eight cysteine residues conserved by strong disulfide linkages which compensate for their agglomerates in solution and can form up to tetramers in solution.<sup>164</sup> Von Vacano, B. *et al* reported that an adsorbed layer of the H\* Protein B (class I hydrophobin) on a model hydrophobic surface (octadecane thiol on gold) prevents the adsorption of secondary proteins bovine serum albumin, casein, or collagen at low-salinity conditions and at pH 8.<sup>167</sup> Nonwovens are mostly hydrophobic polypropylenes and may have the similar phenomenon in the adsorption process of the H\* Protein B hydrophobin in similar conditions. Their structural

arrangements on nonwoven surface actually help to tune bacterial attachment. In this study we will investigate the influence of hydrophobin modifications in varying concentrations upon bacteria adhesion onto nonwoven surfaces at both the static and continuous flow conditions.

### **4.3 Materials and Methods**

#### **4.3.1 Materials**

Achieve™ Advanced PP6936G2 polymer was used to produce meltblown PP nonwoven.

The aqueous solutions of hydrophobin H\* protein B (20 kDa) were made using 1%, 3% and 5% w/v hydrophobin in distilled water. Ninhydrin reagent suitable for amino acid detection and acetic acid were obtained from Sigma Aldrich.

*E. coli* stock culture was a gift from the Department of Crop and Soil Science at NCSU and was subcultured twice from the frozen stock before each experiment. ATCC Medium: 3 Nutrient Agar/Broth from Difco Laboratories, was used as growth media for all three bacteria. Phosphate buffer (pH 7.3) was obtained from Sigma Aldrich. Ethanol (CH<sub>3</sub>CH<sub>2</sub>OH, 99.9 %, 64-17-5) was obtained from Sigma Aldrich and ethanol was diluted to 70 % with distilled water for cleaning purposes.

#### **4.3.2 Methods**

##### **4.3.2.1 Meltblowing of PP Nonwoven Fabrics**

In this research, polypropylene (PP) nonwoven fabric was meltblown nonwoven fabric (basis weight 25 gsm) from Achieve™ Advanced PP6936G2 polymer with melt flow rate of 1550. Melt flow rate (MFR) is the flow rate of material (2.16 kg for polypropylene) extruded at a standardized temperature (230 °C for polypropylene) through a die under pressure from a set mass over a period of 10 min. These fabrics were produced on the Reifenhauer Reicofil™ meltblown pilot line. The width of the Reicofil™ meltblown die is 1 m with 35 capillary holes per inch as shown in Figure 4.2(c) at these conditions: setback/air gap of 1.2 mm, DCD of 25 cm and throughput of 0.4 g/(h·m).



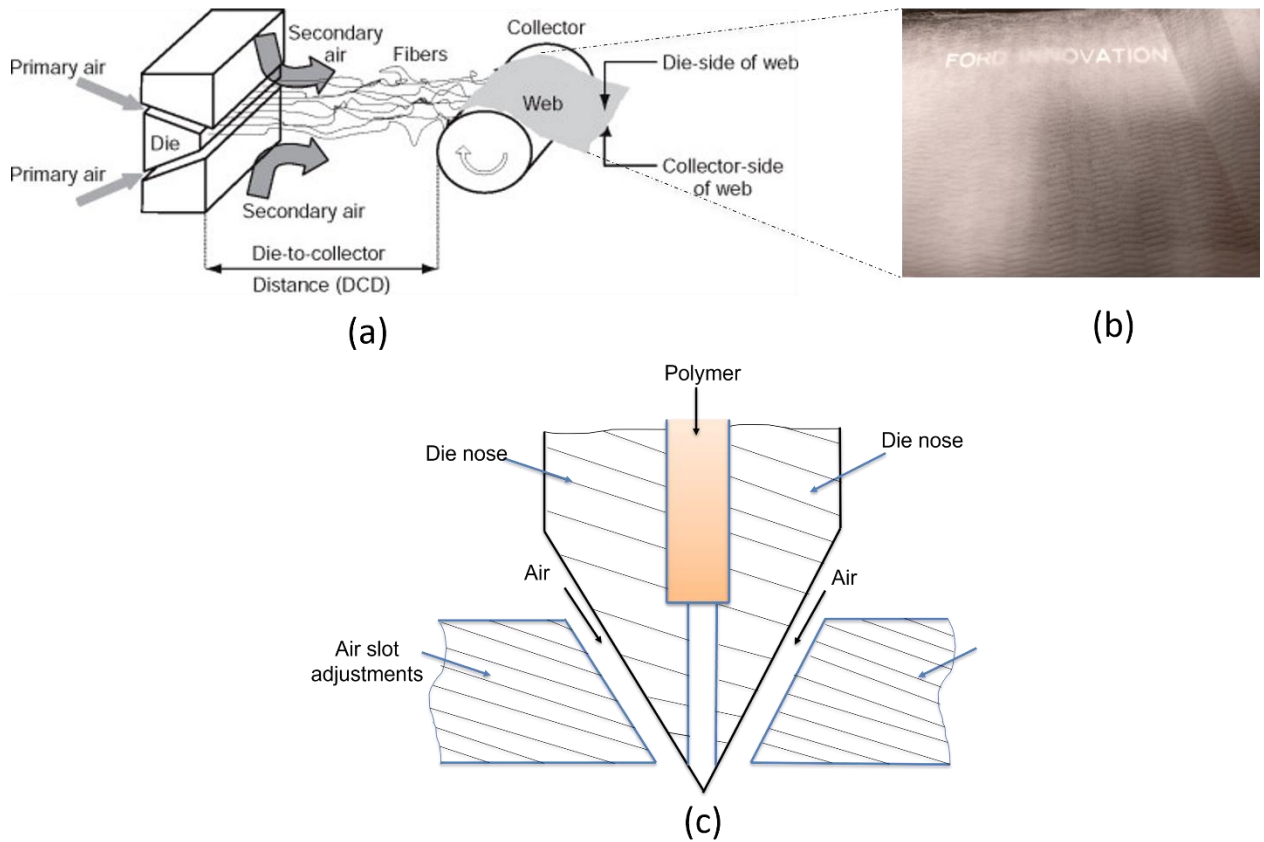


Figure 4.2. The (a) meltblowing process<sup>138</sup>, (b) a meltblown PP nonwoven, and (c) the cross-section of a Reifenhauser Reicofil™ die<sup>140</sup>.

#### 4.3.2.2 Characterization of Meltblown PP Nonwovens

The surface roughness of the modified and unmodified nonwoven fabrics was measured by confocal microscopy. The root means square average ( $R_q$ ) of the profile heights over an evaluation length of 0.4 mm were determined on the LEXT-O-SL4000 3D confocal laser microscope. The 50X objective lens was used for measuring image sizes of 720  $\mu\text{m}$  over a minimum of five readings per sample and at least 3 samples of each type of nonwoven. The wettability of nonwovens was measured by water contact angle. Static contact angles on unmodified and modified nonwoven fabrics were measured using a contact angle goniometer (FTA1000) at room temperature. Three measurements were taken for each sample and the average contact angle value was recorded.

#### **4.3.2.3 Bacteria Count on PP Nonwovens at Static Conditions**

To analyze the possible interactions between microbial cells and the nonwoven polypropylene fabric, the fabrics were incubated with cells of the *E. coli*. Before incubation with the fabrics, bacterial cultures from agar plates were pre-cultured (30 ml) overnight in nutrient broth media. Aliquots of bacteria pre-cultured cells were inoculated in Erlenmeyer flasks containing 25 ml of Nutrient broth to obtain a suspension of  $0.8 \pm 0.02 \times 10^6$  colony forming units (cfu) per ml. The interaction of cells with PP fabrics was then assessed by placing 1 cm<sup>2</sup> pieces of fabric mats into the inoculated flasks and incubating them aerobically and under orbital shaking (80 rpm) in the dark at 30 °C for about 20 h. After 30, 120 and 240 minutes, the fabric mats were removed and rinsed with sterilized water to remove planktonic cells. Afterward each fabric sample was placed into petri dishes and all the Petri dishes were incubated for 24 h in a 37 °C incubator. After incubation, the number of viable cells (colonies) was counted using a Quebec Colony Counter. The results after multiplication with the dilution factor were expressed as mean cfu/ml after averaging the duplicate counts.

#### **4.3.2.4 Bacteria Count on PP Nonwovens Under Flow Conditions**

A flow cell containing three parallel plate flow chambers of 7.7cm<sup>3</sup> (24mm x 40mm x 8mm) with air bubble traps, supply bottle and a damping bottle connected with a pump was used for continuous flow testing (Figure 4.3). During experiments, suspensions of bacteria were made to flow through a circuit, first passing through the flow chambers and then going into the dampening bottle. Pump speed can be adjusted to adjust shear rate and flow volume. Flow volume was set at 0.11 cm<sup>3</sup>s<sup>-1</sup> and wall shear rate was 50s<sup>-1</sup>. The deposition was continued for 4 h. A control fluid of nutrient broth without bacteria was first passed through the flow cell initially to purge air from the system. The number of adhering microorganisms were counted from the images captured by a phase contrast microscope using a 40X objective lens and each image is analyzed using ImageJ image analysis software.<sup>144</sup>

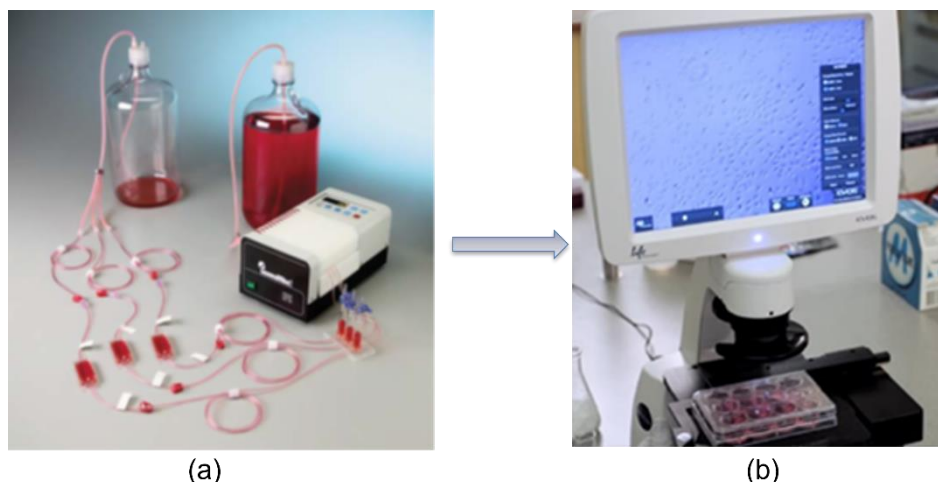


Figure 4.3. (a) Convertible flow cell assembly, (b) phase contrast microscope, 40X objective lens.

T-test was performed to determine significant differences between experimental data sets. The arithmetic mean and standard deviation for the number of bacteria in each medium were calculated. The t-test at 95 % confidence interval was used to determine if two populations have different means and differences were considered significant at  $p < 0.05$ . All data were analyzed using the Origin 2022 statistical software program.

#### 4.3.2.5 Modification of Meltblown PP Nonwovens with Hydrophobin

10 g of the fabric was placed in an Erlenmeyer flask containing the hydrophobin solution (at either 1, 3 and 5 % (w/v of hydrophobin in water). After immersion, fabric was dried for 15 min at 150 °C.

Five samples of each type of nonwoven were weighed before and after each modification with aqueous hydrophobin solution. To confirm the protein deposition on fabrics, ninhydrin test was used. Modified fabrics were wetted with a 3 g/L ninhydrin solution in acetic acid and were heated for 10 min at 160 °C. In the presence of amino groups, the samples turned violet confirming the presence of hydrophobin proteins.

#### 4.3.2.6 Surface Characterization of Modified PP Nonwovens

X-ray photoelectron spectroscopy (XPS) was used to investigate the surface chemistry of nonwoven fabrics, especially those treated with hydrophobin solutions. XPS on the PHOBIOS 150

hemispherical energy analyzer (SPECS GmbH) was equipped with a monochromatic Mg K $\alpha$  excitation source (1253.6 eV). Carbon (C 1s) and oxygen (O 1s) peaks were deconvoluted using Gaussian distributions through Origin 2022 software.

#### 4.4 Results and Discussion

##### 4.4.1 Hydrophobin on Structure of Meltblown PP Nonwovens

After the thermal fixation of hydrophobins the mass change (weighing) and the presence of proteins (ninhydrin test) were characterized. The corresponding data are summarized in **Table 4.1**. To qualitatively prove the protein deposition, the samples were wetted with a ninhydrin solution and in the presence of amino groups the samples turn violet, indicating the successful modification of PP nonwovens with hydrophobin.

**Table 4.1** Change in mass and ninhydrin test before and after hydrophobin modification.

ID	Nonwoven	$\Delta m$ [%]	Ninhydrin Test
PP1550-RI	Without hydrophobin (control)	- 0.2 ( $\pm$ 0.01)	-
1%-HB-PP1550-RI	1% hydrophobin	+ 0.5 ( $\pm$ 0.01)	+
3%-HB-PP1550-RI	3% hydrophobin	+ 1.2 ( $\pm$ 0.03)	+
5%-HB-PP1550-RI	5% hydrophobin	+ 4.2 ( $\pm$ 0.01)	+

##### 4.4.1.1 Surface Wettability and Roughness of Modified Nonwovens

As already mentioned in the introduction, hydrophobins are able to hydrophilize hydrophobic surfaces significantly. Therefore, the water contact angles on the inherently hydrophobic PP were investigated (**Table 4.2**). Water contact angles decreased with an increase in hydrophobin from 1% to 5% w/v. Moreover, the RMS roughness values showed an increase in roughness with the increase in hydrophobin concentration in the treatment. This change in roughness can be explained by the wrinkling introduced onto the surface of the fibers after hydrophobin modification<sup>168</sup> as can be seen in SEM images in Figure 4.4 Individual fibers were found to

combine together and make larger fibers resulting in larger fibers. Géza R. Szilvay showed that both hydrophobin I and hydrophobin II adsorbed onto hydrophobic Teflon surface more readily than hydrophilic quartz surface within seconds via their hydrophobic patches of 4 nm<sup>2</sup> area.<sup>171</sup> This study also mentions that hydrophobin II forms films with a self-assembled hexagonally ordered structure whereas hydrophobin I forms a mosaic of rod like structure called rodlets (5-10 nm in width and several 100 nm in length).<sup>171</sup> H\* protein B being a class I hydrophobin might form nanostructures readily onto hydrophobic PP nonwovens. The change in morphology after hydrophobin modification might be in nanometer scale and might incorporate nanoscale roughness which could increase the adhesion of *E. coli*. Though we have found RMS roughness to increase in micrometer scales and contribute to *E. coli* adhesion in a larger scale under static condition (**Table 4.4**).

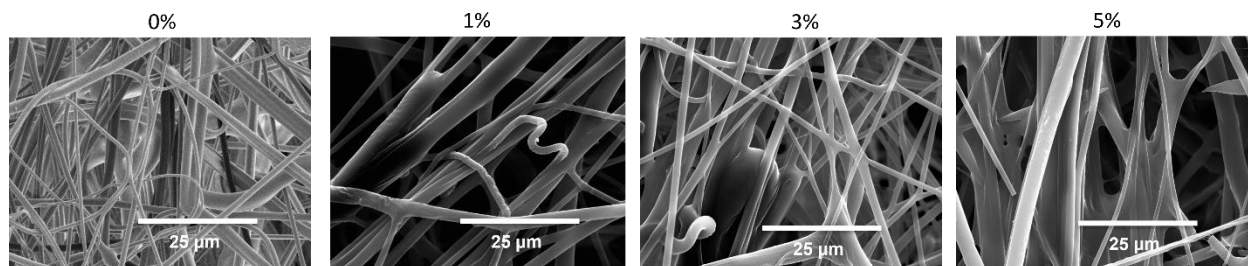


Figure 4.4. SEM images of nonwoven fabrics PP1550-RI before and after hydrophobin treatment.

**Table 4.2** Mean Surface hydrophobicity and RMS roughness of Meltblown PP nonwovens before and after hydrophobin treatment.

Substrate	Water contact angle (°) ± SD	RMS roughness* ( $R_q$ ), μm ± SD
<i>Escherichia coli</i>	30.7 ± 2.8	----
PP1550-RI	143 ± 1.5	7.3 ± 2.7
1%-HB-PP1550-RI	105.3 ± 1.1	9.2 ± 2.3
3%-HB-PP1550-RI	104 ± 1.1	9.5 ± 2.1
5%-HB-PP1550-RI	100 ± 2.1	10.3 ± 1.4

#### 4.4.2 Bacteria Count on PP Nonwovens Under Static and Flow Conditions

The number of *E. coli* colonies attached to the PP nonwoven decreased with time as recorded in **Table 4.3**. After treatment with hydrophobin, the adhesion of *E. coli* increased with the concentration of hydrophobin in solution (w/v %) and time. This trend can be explained by the surface wettability of hydrophobin treated PP nonwovens (**Table 4.2**). With an decrease in water contact angle and increase in roughness, hydrophilic *E. coli* bacteria could attach onto PP nonwovens in agreement with results obtained from Tahmineh et al.<sup>92</sup> Busscher et al. also found that hydrophilic microorganisms adhered most reversibly on hydrophobic substrata.<sup>172</sup> After more than 240 minutes passed, the stationary phase of *E. coli* bacteria reached, and no more adhesion and growth could occur at static conditions (Figure 4.5).

**Table 4.3** Mean *E. coli* attachment at static conditions on unmodified and modified PP nonwovens.

Substrate	PP1550-RI	1%-HB-PP1550-RI	3%-HB-PP1550-RI	5%-HB-PP1550-RI
Time (Minute)	Number of <i>E. coli</i> ( $10^6$ /cm <sup>2</sup> ) $\pm$ SD			
30	0.25 $\pm$ 0.036	0.35 $\pm$ 0.05	0.85 $\pm$ 0.05	1.4 $\pm$ 0.039
120	0.51 $\pm$ 0.046	0.4 $\pm$ 0.046	2.1 $\pm$ 0.045	3.5 $\pm$ 0.049
240	0.9 $\pm$ 0.034	1.5 $\pm$ 0.049	2.5 $\pm$ 0.048	6.5 $\pm$ 0.05

In case of continuous flow, growth continued until there was supply of nutrients even after 240 minutes. But for comparison, data for up to 240 minutes time interval is shown here under continuous flow conditions (**Table 4.4**). The number of colonies of *E. coli* was much higher in case of continuous flow than in static study. This can be explained by the facts established in a study<sup>171</sup> where affinity of hydrophobin I for an air-water interface is much higher than self-association into multimers which means the hydrophilic moieties of H\* protein B are more available to welcome more bacterial cells under continuous flow (Figure 4.6).

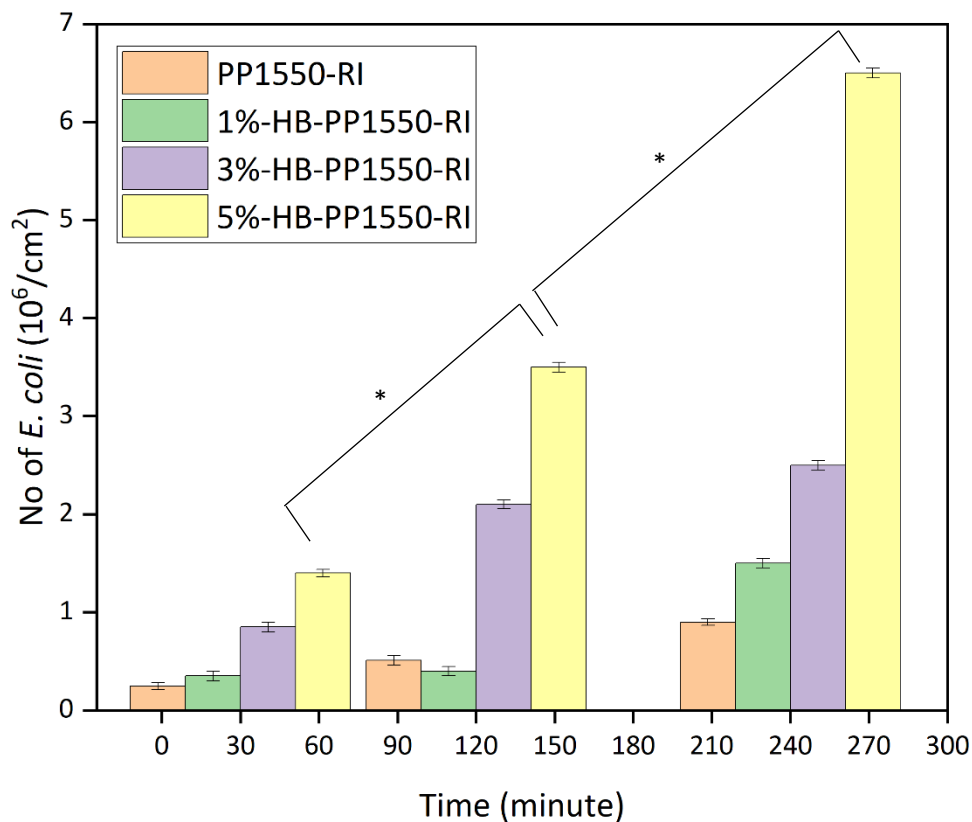


Figure 4.5. *E. coli* adhesion by No of *E. coli* ( $10^6 / \text{cm}^2$ )  $\pm 0.05$  as influenced by the hydrophobin treatment at static conditions, error bars indicate standard deviation, \* $p < 0.05$ .

**Table 4.4** Mean *E. coli* attachment at  $0.11 \text{ cm}^3 \text{ s}^{-1}$  shear rate inside flow cell at time intervals.

Substrate	PP1550-RI	1%-HB-PP1550-RI	3%-HB-PP1550-RI	5%-HB-PP1550-RI
<b>Time (Minute)</b>	<b>Number of <i>E. coli</i> (<math>10^6 / \text{cm}^2</math>) <math>\pm</math> SD</b>			
30	$1.8 \pm 0.045$	$0.7 \pm 0.05$	$3 \pm 0.05$	$5 \pm 0.048$
60	$4 \pm 0.049$	$1.5 \pm 0.045$	$5.5 \pm 0.048$	$6.2 \pm 0.045$
90	$4.9 \pm 0.05$	$2.2 \pm 0.049$	$7 \pm 0.049$	$8.2 \pm 0.049$
120	$8 \pm 0.048$	$3 \pm 0.048$	$9.5 \pm 0.045$	$10.4 \pm 0.048$
180	$9 \pm 0.05$	$3.5 \pm 0.05$	$10.5 \pm 0.05$	$11.2 \pm 0.045$
240	$11 \pm 0.048$	$4 \pm 0.048$	$12 \pm 0.048$	$13.5 \pm 0.05$

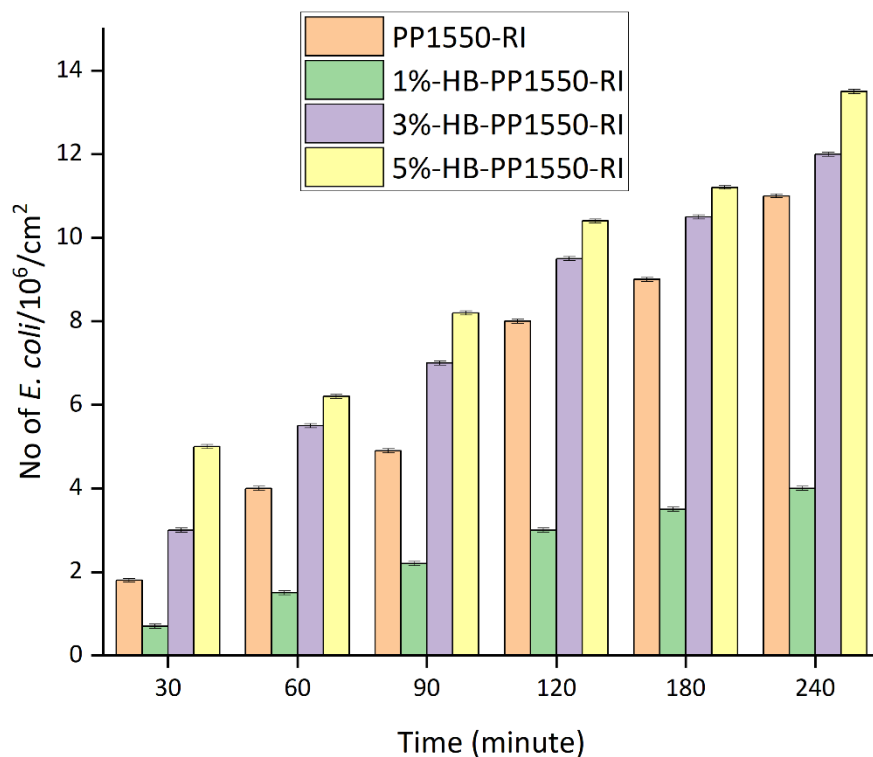


Figure 4.6. The number of *E. coli* adhering to PP meltblown nonwovens as a function of time in a 40 mM potassium phosphate buffer (pH 7.0) during exposure to 50 s<sup>-1</sup> shear rate in a flow chamber, error bars indicate standard deviation.

**Table 4.5** Comparison of static vs continuous study via t-test.

Sample	Time	Significant difference	p-value
PP1550-RI	0 min	+++	< 0.002
	240 min	+++	< 0.001
1%-HB-PP1550-RI	0 min	+++	< 0.004
	240 min	+++	< 0.002
3%-HB-PP1550-RI	0 min	+++	< 0.003
	240 min	+++	< 0.004
5%-HB-PP1550-RI	0 min	+++	< 0.005
	240 min	+++	< 0.005



**Table 4.5** indicates statistical significance between the data from five sets of modified and unmodified nonwoven samples tested at static and continuous flow. Based on a *t*-test at the 95% confidence interval, continuous flow caused significantly ( $p < 0.05$ ) more bacteria adhesion than static condition irrespective of the type of fabric and time of flow. Bacteria adhesion under flow is the initial step before biofilm growth to a host surface. Nutrient flow and passage of air-liquid might help to colonize hydrophobic polypropylene surfaces even better. With passing time increase in bacteria quantity is directly correlated to the availability of nutrients and after the plateau is reached, the colonization is affected by the mass transport. Under flow, a conditioning layer might have generated on the nonwoven surfaces which promoted further bacteria adhesion and hence we could see significant increase in number of colonies after 240 minutes. Formation of conditioning layer will be dependent on the surface chemistry of the host nonwoven surface. The combined effect from increased roughness and wettability (**Table 4.2**) after hydrophobin treatment can explain the significant decrease in initial attachment from 1.8 cfu to 0.7 cfu after 1 % treatment as conditioning layer might not have formed after 30 minutes. As soon as the concentration of hydrophobin in the treatment increased, further improvement in wettability ( $\sim 42^\circ$ ) in favor of conditioning layer formation might have promoted colonization from 1.8 cfu to 5 cfu after 240 minutes. Therefore *E. coli* can attach onto hydrophobic nonwovens treated with 5% hydrophobin as a result of improvement in wettability and mass transport can lead to colonization due to the formation of conditioning layer on the host surface at  $50 \text{ s}^{-1}$  shear rate.

#### **4.4.1.2 Characterization of Hydrophobin Modification by XPS**

Both continuous flow and hydrophobin treatment promoted *E. coli* adhesion on PP nonwovens as shown by Figure 4.7.

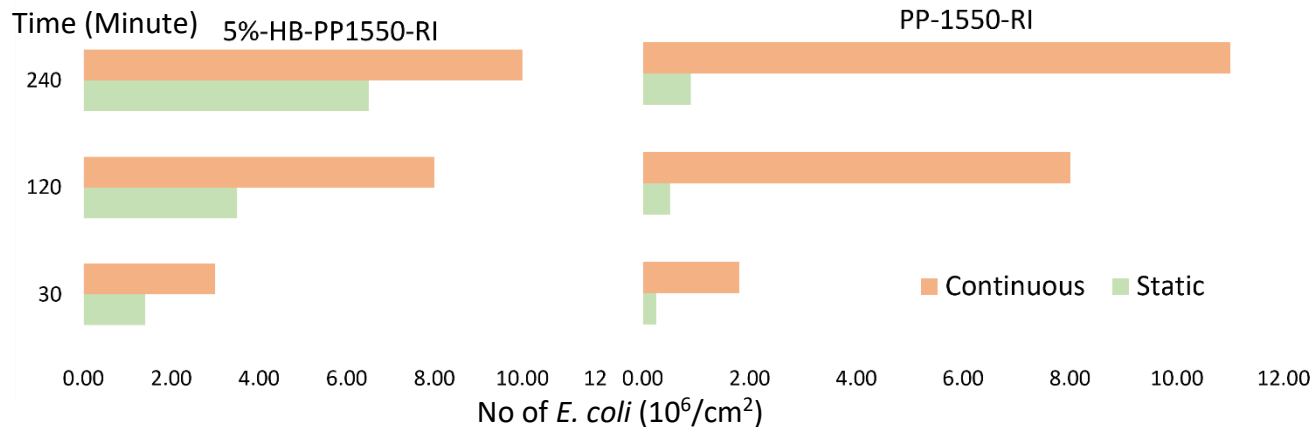


Figure 4.7. *E. Coli* adhesion onto meltblown PP nonwovens (a) with (i. e. 5%-HB-PP1550-RI) and (b) without 5% hydrophobin under static and continuous flow conditions.

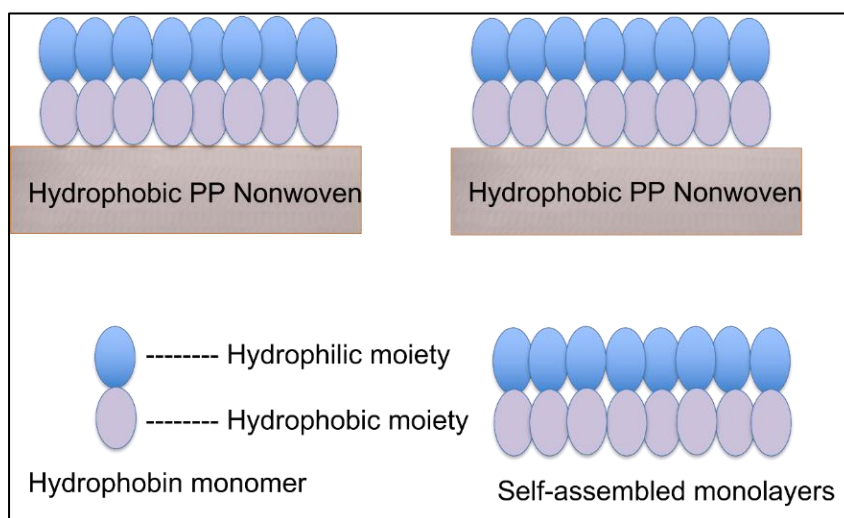


Figure 4.8. Schematic of hydrophobin coated PP nonwovens.

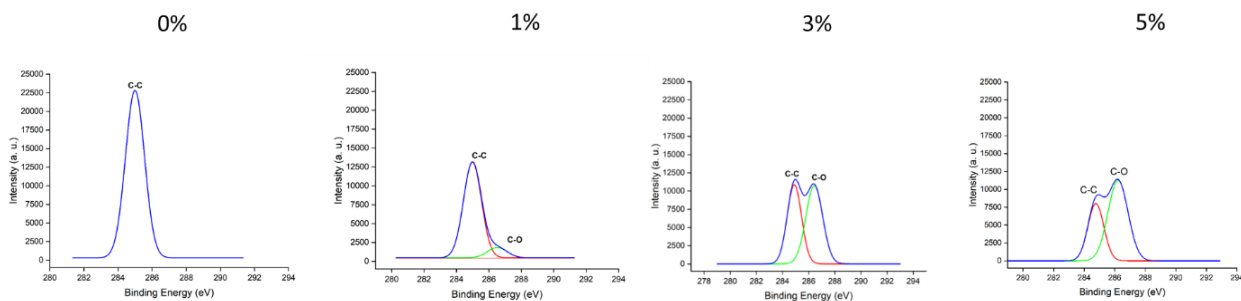


Figure 4.9. XPS spectra of nonwoven fabrics PP1550-RI after hydrophobin treatment.

The modification of nonwoven surfaces with hydrophobin was characterized by XPS (Figure 4.9 and **Table 4.6**). The high intensity C 1s peak decreased as hydrophobin protein coated the nonwoven's surface. Nitrogen (N), oxygen (O), and sulfur (S) peaks are all associated with the amino acid found along the surface of assembled proteins. Thus, the intensities of N 1s, O 1s and S 2p peaks all increased with the amount of hydrophobin at the surface of modified nonwovens. Upon treatment with hydrophobin, the intensity of the N 1s peak at a binding energy of 400 eV increased dramatically from 0 % to 0.75 %.

**Table 4.6** Elemental composition of the unmodified and modified PP nonwovens.

Substrate	C (%)	N (%)	O (%)	S (%)
PP1550-RI	65.56	0	0	0
1%-HB-PP1550-RI	40.06	0.35	20.14	0.53
3%-HB-PP1550-RI	39.03	0.45	22.16	0.64
5%-HB-PP1550-RI	38.06	0.75	23.06	0.84

#### 4.5 Conclusions

This work investigated the influence of hydrophobin assembly upon bacterial adhesion onto hydrophobic meltblown PP nonwovens. Nonwoven roughness contributed significantly to promote the adhesion of *E. coli* both under static and continuous flow. Continuous flow helped in *E. coli* adhesion both on unmodified and modified PP nonwovens. *E. coli* adhesion increased with the increase in concentration of hydrophobin due to the combined effect from increased roughness (~ 41 %) and wettability (~ 42 °). The assembly of hydrophobin onto nonwovens tuned the adhesion as such at 5 w/w %, adhesion was more than doubled from the number of initially attached bacteria. Both hydrophobin modification and continuous flow increased *E. coli* adhesion than the control. The dependence of *E. coli* adhesion with the hydrophobin concentrations in coating solutions can be scaled up to produce products for the wet wipes and water filters industry where bacterial adhesion is required to clean or filter out bacteria. The flowrate and

supply of nutrients and type of bacteria can be the limiting factors to reverse the adhesion when is not desirable.

### **Acknowledgements**

Polypropylene (PP) nonwoven fabrics were supplied from Exxon Mobil. Commercial hydrophobin H\* protein B (10 KDa) is provided by BASF.

## CHAPTER 5

### SUMMARY & CONCLUSIONS

Biofouling is initiated by adhesion and attachment of bacteria on a solid substrate. Transmission of bacteria involves three major components: 1) a source, 2) a susceptible host and 3) a transmission medium. The factors promoting bacterial adhesion will be obviously related to the aforementioned components. This dissertation focused on analyzing properties of sources (which can also serve as medium) such as infected blood, urine, cough, contaminated surface and also properties of host like porous textiles used in healthcare products or respiratory filters. Variables related to sources like surface tension and hydrophilicity were analyzed. Properties of transmission medium like fluid flow, surface tension, chemical nature were also studied with respect to both gram negative and gram positive bacteria strains. Bacteria adhesion to a porous surface and subsequent colonization will depend on both the nature of the bacteria and the environment. The presence of very thick peptidoglycan (long strand of alternating N-acetylmuramic acid (NAM) and N-acetylglucosamine) layer reacts with gram stain in case of gram positive cells while gram negative cells have very thin peptidoglycan layer.<sup>88</sup> In order to consider the effect of bacteria structure on adherence both gram negative *Escherichia coli* (*E. coli*) (rod shaped, 1-2  $\mu\text{m}$ )<sup>89</sup>, and gram positive *Bacillus cereus* (*B. cereus*) (rod shaped, 3–5  $\mu\text{m}$  in length and 1  $\mu\text{m}$  in width)<sup>90</sup> were used in this study. *E. coli* was chosen as it is one of the most common bacteria present in the atmosphere and is a common gut microorganism and can be excreted very easily in fecal matter and hence can also be found in soil, water, plant, and food.<sup>91</sup> *E. coli* is a common pathogen for wound and urinary tract infections in humans.<sup>84,92</sup> *B. cereus* is mainly found in marine and freshwater, vegetables from which soil and food products are easily contaminated.<sup>93</sup> *B. cereus* is also a human pathogen and can cause gastrointestinal diseases by secreting wide array of toxins.<sup>94</sup> Factors related to the host like pore size, roughness, wettability, and surface chemistry are analyzed for commercially produced nonwoven textiles.

From chapter 2 we can conclude that bacterial growth depends on the hydrophilic nature of the carrier solvent. Also, growth is independent of concentration of different solvents irrespective of the type of bacteria. Nutrient broth media surface tension is suppressed negligibly (0.057 N/m to 0.055 N/m) by the addition of chloroform which might increase the growth of *E. coli*. Maximum

growth of *B. cereus*, occurred in nutrient broth mixed with ethyl acetate, which may be due to the polar basic behavior of its cell wall. Adhesion to nonwoven fabrics will depend on the difference of surface energies of carrier fluid and bacteria, the higher the surface energy difference between carrier and bacteria, the higher will be the growth in the carrier, hence the adhesion will be lower on a substrate.

From chapter 3 we can predict that unmodified nonwovens will be more easily approached by polar acidic *E. coli* than the polar basic *B. cereus* as hydrophilic modified nonwovens showed overall poor affinity for *E. coli* than *B. cereus*. Both PP1550-RI and PP-1550-Vista-RI had no trend for adhesion with the increase in Pluronic conc. from 3- 5 w/v % irrespective of the bacteria. With the increase in Pluronic concentration, *E. coli* tend to attach more onto PP1550-RI mainly due to the improved wettability by 34 °. *B. cereus* bacteria showed a maximum affinity for 5%-plu-PP1550-Vista-RI due to the larger fiber diameter and larger pore diameter under flow conditions. The main factors influencing bacteria adhesion are listed in **Table 5.1**.

**Table 5.1** Varying degrees of bacterial adhesion on polypropylene nonwoven fabrics.

PP500-BX	P1550-RI	P1550-Vista-RI
No trend of adhesion under static	No trend of adhesion under static	No trend of adhesion under static
		Highest quantity of <i>E. coli</i> and <i>B. cereus</i> due to the larger fiber diameter and larger pore diameter under flow
<b>Before modification</b>		<b>After modification</b>
Fiber diameter and roughness		Change in wettability
<b>Static condition</b>		<b>Continuous flow condition</b>
Surface roughness		Surface area

Chapter 4 summarized that nonwoven roughness contributed significantly to promote the adhesion of *E. coli* both under static and continuous flow. Continuous flow promoted *E. coli* adhesion both on unmodified and modified PP nonwovens. The assembly of hydrophobin onto nonwovens tuned the adhesion as such at 5 w/v %, adhesion was more than doubled from the number of initially attached bacteria. Both hydrophobin modification and continuous flow increased *E. coli* adhesion than the control. In overall conclusion we can say after hydrophobin modification, there was a definite trend of increase in bacterial adhesion whereas Pluronic treatment offered no such trend. This can be explained by the gradual and definite increase in C-O interaction with an increase in hydrophobin concentration.

The overall objective of this work was to develop a fundamental knowledge of nonwoven surface phenomena occurring when exposed to microbial environments. Three main chapters studied the behaviors that explain varying degrees of bacterial adhesion to modified nonwovens. We could analyze and predict the extent of bacterial adhesion on nonwovens as a function of nonwoven properties.

## APPENDICES

### APPENDIX A. Surface tension of PP Nonwovens through Contact Angle Determination

Static contact angles on unmodified and modified nonwoven fabrics were measured using a contact angle goniometer (FTA1000) at room temperature. Three measurements were taken for each sample and the average contact angle values were recorded. Water, ethylene glycol, DMSO, and diiodomethane were used as probe liquids. The data for surface tension components of the probe liquids are listed in **Table A1**. A droplet of distilled water with a constant volume of 5  $\mu\text{l}$  was dispensed using a micro-syringe. Measurements were taken at 5 s intervals for the unmodified hydrophobic nonwoven surface because water droplets remain stable on the surface. Conversely, measurements were taken at 1 s intervals for the Pluronic modified nonwoven surface, because water droplets get absorbed immediately by the modified nonwoven surfaces. The contact angle values for the other three liquids were taken at intervals from 0 to 5 s.

**Table A1** Probe liquids and their surface tension components from literature.<sup>173</sup>

Surface tension data (dynes/cm)	Total, $\gamma_L$	Dispersion, $\gamma_{LW}$	Polar, $\gamma_L^P$
Water, H <sub>2</sub> O	72.8	21.8	51.0
Ethylene glycol, C <sub>2</sub> H <sub>6</sub> O <sub>2</sub>	48.0	29.0	19.0
Dimethyl sulfoxide, C <sub>2</sub> H <sub>6</sub> OS	44.0	36.0	8.0

### APPENDIX B. Surface Tension of PP Nonwovens

Thermodynamic theory<sup>16</sup> is the physicochemical approach that considers Van der Waals, electrostatic or dipole interactions but expresses them collectively in terms of free energy. This approach determines the extent of bacterial adhesion which depends on the interfacial free energy of adhesion ( $\Delta F_{adh}$ ) and bacterial adhesion is energetically favorable if  $\Delta F_{adh} < 0$ .

$$\Delta F_{adh} = \gamma_{SB} - \gamma_{SL} - \gamma_{BL}$$

$\gamma_{SB}$  = the substratum-bacteria interfacial free energy



$\gamma_{SL}$  = is the substratum-liquid interfacial free energy

$\gamma_{BL}$  = the bacteria-liquid interfacial free energy.

Through Young's equation, experimental data can be obtained for surface tensions<sup>174</sup> of three interacting species -

$$\gamma_{SV} - \gamma_{SL} = \gamma_{LV} \cos\theta$$

Where  $\gamma_{SV}$  is the interfacial tension between a solid substratum S and the vapor phase V,  $\gamma_{SL}$  the interfacial tension between S and the liquid L and  $\gamma_{LV}$  the interfacial tension between L and V and  $\theta$  represents the contact angle of the liquid L on the solid S.

Determination of the surface tension ( $\gamma_{SV}$ ) of the nonwovens was performed by means of contact angle measurements via Zisman theory. For non-polar surfaces like polypropylene, nonpolar test liquids and surface energy theories which do not emphasize specific molecular interactions were chosen. According to Zisman theory, if contact angle data is plotted in the form of liquid surface tension versus cosine of contact angle ( $\cos\theta$ ) and extrapolated to  $\cos\theta = 1$  ( $\theta = 0^\circ$ ), a surface tension value is obtained for the highest surface tension liquid that will completely wet polypropylene nonwovens with a contact angle of  $0^\circ$ . This value (typically reported in units of dynes/cm) is equal to the surface energy of polypropylene in  $\text{mJ/m}^2$ . Such plots are commonly called "Zisman plots".

**Table B1** Nonwoven surface tensions measured from the contact angle study show no trend.

Fiber ID	Surface Tension (mN/m)
PP500-BX	$30.1 \pm 0.05$
PP1550-RI	$30.7 \pm 0.04$
PP1550-Vista-RI	$30.9 \pm 0.05$

## REFERENCES

1. Visser, J. Particle Adhesion and Removal: a Review. *Part. Sci. Technol. An Int. J.* **13**, 169–196 (1995).
2. Visser, J. Van der Waals and other cohesive forces affecting powder fluidization. *Powder Technol.* **58**, 1–10 (1989).
3. Banerjee, I., Pangule, R. C. & Kane, R. S. Antifouling coatings: Recent developments in the design of surfaces that prevent fouling by proteins, bacteria, and marine organisms. *Adv. Mater.* **23**, 690–718 (2011).
4. El-Khatib, E. M. For Authors Antimicrobial and Self-cleaning Textiles using Nanotechnology. *Res. J. Text. Appar. Iss Downloaded by Univ. LIVERPOOL AtPT) RJTA* **16**, 156–17401 (2012).
5. Duckworth, O., Andrews, M., Mitchell, E., Gardner, T., Sombers, L., Santelli, C., & Polizzotto, M. Reactivity of biogenic manganese oxides associated with an environmental remediation system at a Superfund site. *Abstr. Pap. Am. Chem. Soc. (Vol. 250)*,.
6. Duckworth, O. W. *et al.* Environmental Science Processes & Impacts a superfund site treatment system †. *Environ. Sci. Process. Impacts* **00**, 1–9 (2016).
7. Physico-chemistry of initial microbial adhesive interactions – its mechanisms and methods for study. *FEMS Microbiol. Rev.* **23**, 179–230 (1999).
8. Tenke, P. *et al.* Bacterial biofilm formation on urologic devices and heparin coating as preventive strategy. *Int. J. Antimicrob. Agents* **23**, 67–74 (2004).
9. Kroes, I., Lepp, P. W. & Relman, D. A. Bacterial diversity within the human subgingival crevice. *Proc. Natl. Acad. Sci. U. S. A.* **96**, 14547–52 (1999).
10. Dufrêne, Y. F., Boonaert, C. J. P. & Rouxhet, P. G. Adhesion of *Azospirillum brasilense*: Role of proteins at the cell-support interface. *Colloids Surfaces B Biointerfaces* **7**, 113–128 (1996).
11. Barboza, M. *et al.* Glycosylation of human milk lactoferrin exhibits dynamic changes during early lactation enhancing its role in pathogenic bacteria-host interactions. *Mol. Cell. Proteomics* **11**, 1–10 (2012).
12. Maga, E. A., Weimer, B. C. & Murray, J. D. Dissecting the role of milk components on gut microbiota composition. *Gut Microbes* **4**, 136–139 (2013).
13. Ferreyra, J. A. *et al.* Gut microbiota-produced succinate promotes *C. Difficile* infection after antibiotic treatment or motility disturbance. *Cell Host Microbe* **16**, 770–777 (2014).
14. Weimer, B. C., Chen, P., Desai, P. T., Chen, D. & Shah, J. Whole cell cross-linking to discover host-microbe protein cognate receptor/ligand pairs. *Front. Microbiol.* **9**, 1–13 (2018).

15. I, J. W. E. Evaluating Filtration A Comparison of Polymeric Membranes and Nonwovens. (1988).
16. Myrvik, Q. on orthopaedic implant materials. **10**, 325–328 (1989).
17. Ong, Y. L., Razatos, A., Georgiou, G. & Sharma, M. M. Adhesion forces between E. coli bacteria and biomaterial surfaces. *Langmuir* **15**, 2719–2725 (1999).
18. Ly, M. A. D. The effects of culture concentration and age, time, and temperature on bacterial attachment to polystyrene. *Canadian J. Microbiol.* **23**, (1977).
19. Zheng, S. *et al.* Implication of Surface Properties, Bacterial Motility, and Hydrodynamic Conditions on Bacterial Surface Sensing and Their Initial Adhesion. *Front. Bioeng. Biotechnol.* **9**, 1–22 (2021).
20. Kim, B. R., Bae, Y. M., Hwang, J. H. & Lee, S. Y. Biofilm formation and cell surface properties of Staphylococcus aureus isolates from various sources. *Food Sci. Biotechnol.* **25**, 643–648 (2016).
21. Dufregne, Y. F. & Rouxhet, P. G. Surface composition , surface properties , and adhesiveness of Azospirillum brasilense-variation during growth. (1994).
22. Krsmanovic, M. *et al.* Hydrodynamics and surface properties influence biofilm proliferation. *Adv. Colloid Interface Sci.* **288**, (2021).
23. Friedlander, R. S. *et al.* Bacterial flagella explore microscale hummocks and hollows to increase adhesion. *Proc. Natl. Acad. Sci. U. S. A.* **110**, 5624–5629 (2013).
24. Siddiquie, R. Y., Gaddam, A., Agrawal, A., Dimov, S. S. & Joshi, S. S. Anti-Biofouling Properties of Femtosecond Laser-Induced Submicron Topographies on Elastomeric Surfaces. *Langmuir* **36**, 5349–5358 (2020).
25. Chien, H. W., Chen, X. Y., Tsai, W. P. & Lee, M. Inhibition of biofilm formation by rough shark skin-patterned surfaces. *Colloids Surfaces B Biointerfaces* **186**, 110738 (2020).
26. Epperlein, N. *et al.* Influence of femtosecond laser produced nanostructures on biofilm growth on steel. *Appl. Surf. Sci.* **418**, 420–424 (2017).
27. Xu, L. C. & Siedlecki, C. A. Staphylococcus epidermidis adhesion on hydrophobic and hydrophilic textured biomaterial surfaces. *Biomed. Mater.* **9**, (2014).
28. Morgan, T. D. & Wilson, M. The effects of surface roughness and type of denture acrylic on biofilm formation by Streptococcus oralis in a constant depth film fermentor. *J. Appl. Microbiol.* **91**, 47–53 (2001).
29. Zhao, C. Q., Xu, X. C., Li, R. Y., Chen, J. & Yang, F. L. Highly effective permeability and antifouling performances of polypropylene non-woven fabric membranes modified with graphene oxide by inkjet printing and immersion coating methods. *Water Sci. Technol.* **67**,

- 2307–2313 (2013).
30. Wang, C. *et al.* High flux and antifouling filtration membrane based on non-woven fabric with chitosan coating for membrane bioreactors. *Bioresour. Technol.* **101**, 5469–5474 (2010).
  31. Feng, R. *et al.* Highly effective antifouling performance of N-vinyl-2-pyrrolidone modified polypropylene non-woven fabric membranes by ATRP method. *J. Memb. Sci.* **369**, 233–242 (2011).
  32. Zhang, C. H., Yang, F. lin, Wang, W. J. & Chen, B. Preparation and characterization of hydrophilic modification of polypropylene non-woven fabric by dip-coating PVA (polyvinyl alcohol). *Sep. Purif. Technol.* **61**, 276–286 (2008).
  33. Hsiao, S. W., Venault, A., Yang, H. S. & Chang, Y. Bacterial resistance of self-assembled surfaces using PPOm-b-PSBMAz zwitterionic copolymer - Concomitant effects of surface topography and surface chemistry on attachment of live bacteria. *Colloids Surfaces B Biointerfaces* **118**, 254–260 (2014).
  34. C, B. W. and N. Purity of the sacred lotus, or escape from contamination in biological surfaces. *Planta* 1–8 (1997).
  35. Anselme, K. *et al.* The interaction of cells and bacteria with surfaces structured at the nanometre scale. *Acta Biomater.* **6**, 3824–3846 (2010).
  36. Cappelletti, M. *et al.* Growth of *Rhodococcus* sp. strain BCP1 on gaseous n-alkanes: New metabolic insights and transcriptional analysis of two soluble di-iron monooxygenase genes. *Front. Microbiol.* **6**, 1–15 (2015).
  37. Davis, R. Microfiltration and ultrafiltration: Principles and applications Leos J. Zeman and Andrew L. Zydney, Marcek Dekker, New York, 1996. *J. Memb. Sci.* **134**, 273–274 (1997).
  38. Huisman, I. H., Prádanos, P. & Hernández, A. The effect of protein-protein and protein-membrane interactions on membrane fouling in ultrafiltration. *J. Memb. Sci.* **179**, 79–90 (2000).
  39. Gholap, S. G., Badiger, M. V. & Gopinath, C. S. Molecular origins of wettability of hydrophobic poly(vinylidene fluoride) microporous membranes on poly(vinyl alcohol) adsorption: Surface and interface analysis by XPS. *J. Phys. Chem. B* **109**, 13941–13947 (2005).
  40. Yoon, K. *et al.* High flux ultrafiltration membranes based on electrospun nanofibrous PAN scaffolds and chitosan coating. *Polymer (Guildf).* **47**, 2434–2441 (2006).
  41. Von Vacano, B. *et al.* Hydrophobin can prevent secondary protein adsorption on hydrophobic substrates without exchange. *Anal. Bioanal. Chem.* **400**, 2031–2040 (2011).
  42. Wohlleben, W. *et al.* Recombinantly produced hydrophobins from fungal analogues as

- highly surface-active performance proteins. *Eur. Biophys. J.* **39**, 457–468 (2010).
43. Linder, M. *et al.* The hydrophobins HFBI and HFBI from *Trichoderma reesei* showing efficient interactions with nonionic surfactants in aqueous two-phase systems. *Biomacromolecules* **2**, 511–517 (2001).
  44. Kershaw, M. J. & Talbot, N. J. Hydrophobins and Repellents: Proteins with Fundamental Roles in Fungal Morphogenesis. *Fungal Genet. Biol.* **23**, 18–33 (1998).
  45. Wösten, H. A. B. & De Vocht, M. L. Hydrophobins, the fungal coat unravelled. *Biochim. Biophys. Acta - Rev. Biomembr.* **1469**, 79–86 (2000).
  46. Zampieri, F., Wösten, H. A. B. & Scholtmeijer, K. Creating surface properties using a palette of hydrophobins. *Materials (Basel)*. **3**, 4607–4625 (2010).
  47. Scholtmeijer, K., Wessels, J. G. H. & Wösten, H. A. B. Fungal hydrophobins in medical and technical applications. *Appl. Microbiol. Biotechnol.* **56**, 1–8 (2001).
  48. Flash, F. O. R. A., Controller, M., Valley, E. & Group, L. A. W. (19) United States (12). **1**, (2009).
  49. Lisa Edelmann; Bronx; NY (US); Robert J. Desnick; New York. United States (12). *US Pat. Appl. Publ.* **1**, 1–38 (2014).
  50. Russell, S. J. *Handbook of nonwovens*. (2007).
  51. Shailer, L. *Introduction. The Nonwoven Fabrics Industry*. (1959).
  52. Hassan, M. A. A. Structure Property Process Relationships for Meltblown Fibrous Media. (*Doctoral Diss. North Carolina State Univ. Raleigh, USA*). (2013).
  53. Maus, R., Goppelsröder, A. & Umhauer, H. Survival of bacterial and mold spores in air filter media. *Atmos. Environ.* **35**, 105–113 (2001).
  54. Bockmuhl, D. *et al.* (19) United States (12). **1**, (2008).
  55. Drabek, J. & Zatloukal, M. Meltblown technology for production of polymeric microfibers/nanofibers: A review. *Phys. Fluids* **31**, (2019).
  56. Lee, Y. E., & Wadsworth, L. C. Fiber and web formation of melt-blown thermoplastic polyurethane polymers,. *J. Appl. Polym. Sci.* **105(6)**, 3724–3727 (2007).
  57. Begenir, A. Structure-Process-Property Relationships in Elastic Nonwovens Made From Multi-Block Elastomers. (*Doctoral Diss. North Carolina State Univ. Raleigh, USA*) (2008).
  58. Malkan, S. R. An overview of spunbonding and meltblowing technologies,. *TAPPI J.* **78**, 185-185. (1995).
  59. Lee, Y., & Wadsworth, L. C. Effects of melt-blowing process conditions on morphological

- and mechanical properties of polypropylene webs. *Polymer (Guildf)*. **33(6)**, 1200-1209. (1992).
60. Wente, V. A. Superfine thermoplastic fibers. *Ind. Eng. Chem.* **48(8)**, 1342-1346. (1956).
  61. Sun, Q., & Zhang, D. Analysis and simulation of non-Newtonian flow in the coathanger die of a meltblown process. e, . *J. Appl. Polym. Sci.* **67(2)**, 193–200 (1998).
  62. Lee, Y., & Wadsworth, L. C. Structure and filtration properties of melt blown polypropylene webs. *Polym. Eng. Sci.* **30(22)**, 1413-1419.e (1990).
  63. Ellison, C. J., Phatak, A., Giles, D. W., Macosko, C. W., & Bates, F. S. Melt blown nanofibers: Fiber diameter distributions and onset of fiber breakup. *Polymer*, **48(11)**, 3306-3316. (2007).
  64. Zhang, D., Sun, Q., & Liu., Y. Comparison of different air gap/setback of die on Reifenhauser bicomponent meltblown line. *Beltwide Cott. Conf. Nashville, TN.* (2003).
  65. Drabek, J. Applied rheology for melt blown technology. (2011).
  66. Pu, Y. *et al.* Preparation of polypropylene micro and nanofibers by electrostatic-assisted melt blown and their application. *Polymers (Basel)*. **10**, 1–12 (2018).
  67. Yesil, Y. & Bhat, G. S. Porosity and barrier properties of polyethylene meltblown nonwovens. *J. Text. Inst.* **108**, 1035–1040 (2017).
  68. Virk, R. K., Ramaswamy, G. N., Bourham, M. & Bures, B. L. Plasma and Antimicrobial Treatment of Nonwoven Fabrics for Surgical Gowns. *Text. Res. J.* **74**, 1073–1079 (2004).
  69. Huang, W. & Leonas, K. K. Evaluating a One-Bath Process for Imparting Antimicrobial Activity and Repellency to Nonwoven Surgical Gown Fabrics. *Text. Res. J.* **70**, 774–782 (2000).
  70. Mittal, K. L. (2004). *Polymer Surface Modification: Relevance to Adhesion.* (2003).
  71. Jinka, S. *et al.* Atmospheric pressure plasma treatment and breathability of polypropylene nonwoven fabric. *J. Ind. Text.* **42**, 501–514 (2013).
  72. Tsai, P. P., Wadsworth, L. C. & Roth, J. R. Surface Modification of Fabrics Using a One-Atmosphere Glow Discharge Plasma to Improve Fabric Wettability. *Text. Res. J.* **67**, 359–369 (1997).
  73. Pane, S., Tedesco, R. & Greger, R. Acrylic Fabrics Treated with Plasma for Outdoor Applications. *J. Ind. Text.* **31**, 135–145 (2001).
  74. Bures, B. L. E. E. Plasma and Antimicrobial Treatment. *Text. Res. J.* **74**, 1073–1079 (2004).
  75. Chen, K. S. *et al.* Surface grafting polymerization of JV-Vinyl-2-pyrrolidone onto a poly(ethylene terephthalate) nonwoven by plasma pretreatment and its antibacterial

- activities. *J. Appl. Polym. Sci.* **100**, 803–809 (2006).
76. Wang, C., Yang, F. & Zhang, H. Fabrication of non-woven composite membrane by chitosan coating for resisting the adsorption of proteins and the adhesion of bacteria. *Sep. Purif. Technol.* **75**, 358–365 (2010).
  77. Kayaoglu, B. K. Plasma Surface Treatments of Nonwovens. *Non-woven Fabr.* (2016) doi:10.5772/61307.
  78. Wertheimer, M. R. Plasma surface modification of polymers for improved adhesion — a critical review . *J Adhes Sci.* (2017) doi:10.1163/156856193X00600.
  79. Sauperl, O. Textiles for protection against microorganism. *AIP Conf. Proc.* **1727**, (2016).
  80. Abreu, M. J., Silva, M. E., Schacher, L. & Adolphe, D. Designing surgical clothing and drapes according to the new technical standards. *Int. J. Cloth. Sci. Technol.* **15**, 69–74 (2003).
  81. Verbeek, J. H. *et al.* Personal protective equipment for preventing highly infectious diseases due to exposure to contaminated body fluids in healthcare staff. *Emergencias* **33**, 59–61 (2021).
  82. Anderson, D. J. *et al.* The antimicrobial scrub contamination and transmission (ASCOT) trial: A three-arm, blinded, randomized controlled trial with crossover design to determine the efficacy of antimicrobial-impregnated scrubs in preventing healthcare provider contamination. *Infect. Control Hosp. Epidemiol.* **38**, 1147–1154 (2017).
  83. Why use nonwovens in medical and healthcare? <https://www.edana.org/nw-related-industry/nonwovens-in-daily-life/medical-and-healthcare>.
  84. Hsieh, Y. -L & Merry, J. The adherence of *Staphylococcus aureus*, *Staphylococcus epidermidis* and *Escherichia coli* on cotton, polyester and their blends. *J. Appl. Bacteriol.* **60**, 535–544 (1986).
  85. Majchrzycka, K., Okrasa, M., Szulc, J., Brycki, B. & Gutarowska, B. Time-dependent antimicrobial activity of filtering nonwovens with gemini Surfactant-based biocides. *Molecules* **22**, 1–13 (2017).
  86. Edwards, N. W. M. *et al.* Role of surface energy and nano-roughness in the removal efficiency of bacterial contamination by nonwoven wipes from frequently touched surfaces. *Sci. Technol. Adv. Mater.* **18**, 197–209 (2017).
  87. Jones, N., Ray, B., Ranjit, K. T. & Manna, A. C. Antibacterial activity of ZnO nanoparticle suspensions on a broad spectrum of microorganisms. *FEMS Microbiol. Lett.* **279**, 71–76 (2008).
  88. Bajpai, I. & Basu, B. Strategies to Prevent Bacterial Adhesion on Biomaterials. *Biomimetics* 163–202 (2013) doi:10.1002/9781118810408.ch7.

89. Subramanian, B., Anu Priya, K., Thanka Rajan, S., Dhandapani, P. & Jayachandran, M. Antimicrobial activity of sputtered nanocrystalline CuO impregnated fabrics. *Mater. Lett.* **128**, 1–4 (2014).
90. Senesi, S. & Ghelardi, E. Production, Secretion and Biological Activity of *Bacillus cereus* Enterotoxins. *Toxins* vol. 2 1690–1703 (2010).
91. Blount, Z. D. The unexhausted potential of *E. coli*. *Elife* **4**, 1–12 (2015).
92. Hemmatian, T., Lee, H. & Kim, J. Bacteria adhesion of textiles influenced by wettability and pore characteristics of fibrous substrates. *Polymers* vol. 13 1–14 (2021).
93. Meinders, J. M., van der Mei, H. C. & Busscher, H. J. Deposition Efficiency and Reversibility of Bacterial Adhesion under Flow. *J. Colloid Interface Sci.* **176**, 329–341 (1995).
94. Bottone, E. J. *Bacillus cereus*, a volatile human pathogen. *Clin. Microbiol. Rev.* **23**, 382–398 (2010).
95. Majchrzycka, K., Okrasa, M., Szulc, J., Jachowicz, A. & Gutarowska, B. Survival of microorganisms on nonwovens used for the construction of filtering facepiece respirators. *International Journal of Environmental Research and Public Health* vol. 16 (2019).
96. Absolom, D. R. *et al.* Surface thermodynamics of bacterial adhesion. *Appl. Environ. Microbiol.* **46**, 90–7 (1983).
97. Properties, T. Datasheet dpg. (2019).
98. Endo, Y., Mune, M. & Usukura, J. Factors affecting reduction in preservative efficacy in nonwoven fabrics. *Biocontrol Sci.* **25**, 149–157 (2020).
99. Dataphysics. Surface tension values of some common test liquids for surface energy analysis Surface tension values of some common test liquids for surface energy analysis. **49**, 0–4 (2020).
100. Road, S. & Lincolnshire, N. SeaQuantum X200 - 2 ( UK ) SECTION 1 : Identification of the substance / mixture and of the company / SECTION 2 : Hazards identification SECTION 2 : Hazards identification. **2006**, 1–15 (2014).
101. Pogorzelski, S., Watrobska-Swietlikowska, D. & Sznitowska, M. Surface tensometry studies on formulations of surfactants with preservatives as a tool for antimicrobial drug protection characterization. *J. Biophys. Chem.* **03**, 324–333 (2012).
102. Bellon-Fontaine, M. N., Rault, J. & Van Oss, C. J. Microbial adhesion to solvents: A novel method to determine the electron-donor/electron-acceptor or Lewis acid-base properties of microbial cells. *Colloids Surfaces B Biointerfaces* **7**, 47–53 (1996).
103. Volkmer, B. & Heinemann, M. Condition-Dependent cell volume and concentration of *Escherichia coli* to facilitate data conversion for systems biology modeling. *PLoS One* **6**, 1–



- 6 (2011).
104. Pakpour, N. & Horgan, S. General Microbiology Lab Manual. *Hayden-McNeil, LLC* 117–120 (2019).
  105. Reynolds, J. Serial Dilution Protocols. *Am. Soc. Microbiol.* 1–7 (2005).
  106. Anjum, N., Bellon-Fontaine, M. N., Heny, J. M. & Riquet, A. M. A novel process to develop modified polymeric surfaces for the analysis of bacterial adhesion: Surface properties and adhesion test. *J. Appl. Polym. Sci.* **109**, 1746–1756 (2008).
  107. Fink, R., Oder, M., Rangus, D., Raspor, P. & Bohinc, K. Microbial adhesion capacity. Influence of shear and temperature stress. *Int. J. Environ. Health Res.* **25**, 656–669 (2015).
  108. Edwards, N. W. M., Best, E. L., Goswami, P., Wilcox, M. H. & Russell, S. J. Factors affecting removal of bacterial pathogens from healthcare surfaces during dynamic wiping. *Text. Res. J.* **89**, 580–589 (2019).
  109. Banu, A., Anand, M. & Nagi, N. White coats as a vehicle for bacterial dissemination. *J. Clin. Diagnostic Res.* **6**, 1381–1384 (2012).
  110. Bajpai, V., Dey, A., Ghosh, S., Bajpai, S. & Jha, M. K. Quantification of bacterial adherence on different textile fabrics. *Int. Biodeterior. Biodegrad.* **65**, 1169–1174 (2011).
  111. Sailo, C. V. *et al.* Pathogenic microbes contaminating mobile phones in hospital environment in Northeast India: Incidence and antibiotic resistance. *Trop. Med. Health* **47**, 1–11 (2019).
  112. Gupta, P. *et al.* Bacterial contamination of nurses' white coats made from polyester and polyester cotton blend fabrics. *J. Hosp. Infect.* **94**, 92–94 (2016).
  113. Bajpai, P. ". The control of microbiological problems. in *Pulp and Paper Industry* 103–195 (2015).
  114. Ajmeri, C. J. & Ajmeri, J. R. *Application of Nonwovens in Healthcare and Hygiene Sector. Medical Textiles and Biomaterials for Healthcare: Incorporating Proceedings of MEDTEX03 International Conference and Exhibition on Healthcare and Medical Textiles* (Woodhead Publishing Limited, 2005). doi:10.1533/9781845694104.2.80.
  115. Majchrzycka, K., Okrasa, M., Skóra, J. & Gutarowska, B. Evaluation of the survivability of microorganisms deposited on filtering respiratory protective devices under varying conditions of humidity. *Int. J. Environ. Res. Public Health* **13**, (2016).
  116. Rai, M., Yadav, A. & Gade, A. Silver nanoparticles as a new generation of antimicrobials. *Biotechnol. Adv.* **27**, 76–83 (2009).
  117. Yasuyuki, M. *et al.* Antibacterial properties of nine pure metals: A laboratory study using *Staphylococcus aureus* and *Escherichia coli*. *Biofouling* **26**, 851–858 (2010).

118. Ren, H. *et al.* A Review on Recent Achievements and Current Challenges in Antibacterial Electrospun N-halamines. *Colloids Interface Sci. Commun.* **24**, 24–34 (2018).
119. Batrakova, E. V. & Kabanov, A. V. Pluronic block copolymers: Evolution of drug delivery concept from inert nanocarriers to biological response modifiers. *J. Control. Release* **130**, 98–106 (2008).
120. Kalantari, K., Afifi, A. M., Jahangirian, H. & Webster, T. J. Biomedical applications of chitosan electrospun nanofibers as a green polymer – Review. *Carbohydr. Polym.* **207**, 588–600 (2019).
121. Jiao, Y. *et al.* Quaternary ammonium-based biomedical materials: State-of-the-art, toxicological aspects and antimicrobial resistance. *Prog. Polym. Sci.* **71**, 53–90 (2017).
122. Marambio-Jones, C. & Hoek, E. M. V. A review of the antibacterial effects of silver nanomaterials and potential implications for human health and the environment. *J. Nanoparticle Res.* **12**, 1531–1551 (2010).
123. Zhang, X., Wang, L. & Levänen, E. Superhydrophobic surfaces for the reduction of bacterial adhesion. *RSC Adv.* **3**, 12003–12020 (2013).
124. Valdiglesias, V. Cytotoxicity and Genotoxicity of Nanomaterials. *Nanomaterials* **12**, 279–290 (2022).
125. Gupta, A. & Silver, S. Silver as a biocide: Will resistance become a problem? *Nature Biotechnology* vol. 16 888 (1998).
126. American Society for Testing & Mater. Standard test methods for mass per unit area (weight) of woven fabric. (1985) doi:10.1520/D3776.
127. Bridgett, M. J., Denyer, S. P. & Davies, M. C. The control of staphylococcal adhesion to poly(styrene) surfaces by polymer surface modification with pluronic surfactants. *J. Pharm. Pharmacol. Suppl.* **43**, 23 (1991).
128. Morra, M. & Cassinelli, C. Bacterial adhesion to polymer surfaces: A critical review of surface thermodynamic approaches. *J. Biomater. Sci. Polym. Ed.* **9**, 55–74 (1997).
129. Arthur W. Adamson, Alice P. Gast - Physical Chemistry of Surfaces, 6th Edition-Wiley-Interscience (1997).pdf.
130. Roosjen, A., Kaper, H. J., van der Mei, H. C., Norde, W. & Busscher, H. J. Inhibition of adhesion of yeasts and bacteria by poly(ethylene oxide)-brushes on glass in a parallel plate flow chamber. *Microbiology* **149**, 3239–3246 (2003).
131. Bridgett, M. J., Davies, M. C. & Denyer, S. P. Control of staphylococcal adhesion to polystyrene surfaces by polymer surface modification with surfactants. *Biomaterials* **13**, 411–416 (1992).

132. Hsu, L. C., Fang, J., Borca-Tasciuc, D. A., Worobo, R. W. & Moraru, C. I. Effect of micro- and nanoscale topography on the adhesion of bacterial cells to solid surfaces. *Appl. Environ. Microbiol.* **79**, 2703–2712 (2013).
133. Busscher, H. J., Doornbusch, G. I. & Van Der Mei, H. C. Adhesion of Mutans Streptococci to Glass With and Without a Salivary Coating as Studied in a Parallel-plate Flow Chamber. *J. Dent. Res.* **71**, 491–500 (1992).
134. Pitt, W. G., McBride, M. O., Barton, A. J. & Sagers, R. D. Air-water interface displaces adsorbed bacteria. *Biomaterials* **14**, 605–608 (1993).
135. Lyklema, J., Norde, W., van Loosdrecht, M. C. M. & Zehnder, A. J. B. Adhesion of bacteria to polystyrene surfaces. *Colloids and Surfaces* **39**, 175–187 (1989).
136. Mittal K. L. *Advances in Contact Angle, Wettability and Adhesion*. (John Wiley & Sons, 2015).
137. Kasuga, E. *et al.* Bactericidal activities of woven cotton and nonwoven polypropylene fabrics coated with hydroxyapatite-binding silver/titanium dioxide ceramic nanocomposite ‘Earth-plus’. *Int. J. Nanomedicine* **6**, 1937–1943 (2011).
138. Hutten, I. M. *Processes for Nonwoven Filter Media. Handbook of Nonwoven Filter Media* (2007). doi:10.1016/b978-185617441-1/50020-2.
139. Producing, M. D. E. F. O. R. (45) July 23, 1974. 1–6 (1974).
140. Eckhard C. A. Schwarz. APPARATUS AND PROCESS FOR MELT-BLOWING AFBERFORMING THERMOPLASTC POLYMER AND PRODUCT PRODUCED THEREBY. (1983).
141. American Society for Testing & Mater. Standard test methods for mass per unit area (weight) of woven fabric. 7–11 (1985) doi:10.1520/D3776.
142. Method, S. T. Standard method of test for air permeability of textile fabrics. 1–5 (1975) doi:10.1520/D0737-18.2.
143. Jena, A. & Gupta, K. Liquid Extrusion Techniques for Pore Structure Evaluation of Nonwovens. *Int. Nonwovens J.* **os-12**, 1558925003os–12 (2018).
144. Zhang, J. *et al.* A comprehensive review of image analysis methods for microorganism counting: from classical image processing to deep learning approaches. *Artificial Intelligence Review* vol. 55 (Springer Netherlands, 2022).
145. Muhammad, M. H. *et al.* Beyond Risk: Bacterial Biofilms and Their Regulating Approaches. *Front. Microbiol.* **11**, 1–20 (2020).
146. Song, X., Vossebein, L. & Zille, A. Efficacy of disinfectant-impregnated wipes used for surface disinfection in hospitals: A review. *Antimicrob. Resist. Infect. Control* **8**, 1–14 (2019).

147. Edwards, N. W. M., Best, E. L., Goswami, P., Wilcox, M. H. & Russell, S. J. Recontamination of healthcare surfaces by repeated wiping with biocide-loaded wipes: “One wipe, one surface, one direction, dispose” as best practice in the clinical environment. *Int. J. Mol. Sci.* **21**, 1–11 (2020).
148. Edwards, N. W. M. *et al.* Role of surface energy and nano-roughness in the removal efficiency of bacterial contamination by nonwoven wipes from frequently touched surfaces. *Science and Technology of Advanced Materials* vol. 18 (2017).
149. Salama, P., Gliksberg, A., Cohen, M., Tzafrir, I. & Ziklo, N. Why are wet wipes so difficult to preserve? Understanding the intrinsic causes. *Cosmetics* **8**, (2021).
150. Brosseau LM, McCullough NV, V. D. BACTERIAL SURVIVAL ON RESPIRATOR FILTERS AND SURGICAL MASKS Lisa M. Brosseau, Sc.D., CIH, Nicole Vars McCullough, and Donald Vesley University of Minnesota, School of Public Health, Minneapolis, Minnesota. *J. of the Am. Biol. Saf. Assoc.* **2**, 32–43 (1997).
151. Majchrzycka, K., Okrasa, M., Jachowicz, A., Szulc, J. & Gutarowska, B. Microbial growth on dust-loaded filtering materials used for the protection of respiratory tract as a factor affecting filtration efficiency. *Int. J. Environ. Res. Public Health* **15**, (2018).
152. Bonnevie Perrier, J. C., Le Coq, L., Andrès, Y. & Le Cloirec, P. SFGP 2007 - Microbial growth onto filter media used in air treatment devices. *Int. J. Chem. React. Eng.* **6**, (2008).
153. Majchrzycka, K., Okrasa, M., Szulc, J., Jachowicz, A. & Gutarowska, B. Survival of microorganisms on nonwovens used for the construction of filtering facepiece respirators. *Int. J. Environ. Res. Public Health* **16**, (2019).
154. Busscher, H. J. & Van Der Mei, H. C. Microbial adhesion in flow displacement systems. *Clin. Microbiol. Rev.* **19**, 127–141 (2006).
155. Hou, J., Veeregowda, D. H., van de Belt-Gritter, B., Busscher, H. J. & van der Mei, H. C. Extracellular polymeric matrix production and relaxation under fluid shear and mechanical pressure in *Staphylococcus aureus* biofilms. *Appl. Environ. Microbiol.* **84**, 1–14 (2018).
156. Thomen, P. *et al.* Bacterial biofilm under flow: First a physical struggle to stay, then a matter of breathing. *PLoS ONE* vol. 12 (2017).
157. Zhu, J. *et al.* Effects of Hydrophilicity, Adhesion Work, and Fluid Flow on Biofilm Formation of PDMS in Microfluidic Systems. *ACS Appl. Bio Mater.* **3**, 8386–8394 (2020).
158. Sjollema, J., Busscher, H. J. & Weerkamp, A. H. Deposition of oral streptococci and polystyrene latices onto glass in a parallel plate flow cell. *Biofouling* **1**, 101–112 (1988).
159. Yu Liu, J.-H. T. The essential role of hydrodynamic shear force in the formation of biofilm and granular sludge. *Water Res.* **36**, 1653–1665 (2002).
160. Nehal Mohamed, Thomas R. Rainier, Jr., J. M. R. Novel Experimental Study of Receptor-

- Mediated Bacterial Adhesion Under the Influence of Fluid Shear. *Biotechnol. Bioeng.* **68**, 628–636 (2000).
161. Lorenzetti, M. *et al.* The influence of surface modification on bacterial adhesion to titanium-based substrates. *ACS Appl. Mater. Interfaces* **7**, 1644–1651 (2015).
  162. Verhorstert, K. W. J. *et al.* In Vitro Bacterial Adhesion and Biofilm Formation on Fully Absorbable Poly-4-hydroxybutyrate and Nonabsorbable Polypropylene Pelvic Floor Implants. *ACS Appl. Mater. Interfaces* **12**, 53646–53653 (2020).
  163. Møllebjerg, A., Palmén, L. G., Gori, K. & Meyer, R. L. The Bacterial Life Cycle in Textiles is Governed by Fiber Hydrophobicity. *Microbiol. Spectr.* **9**, (2021).
  164. Linder, M. B., Szilvay, G. R., Nakari-Setälä, T. & Penttilä, M. E. Hydrophobins: The protein-amphiphiles of filamentous fungi. *FEMS Microbiol. Rev.* **29**, 877–896 (2005).
  165. Scholtmeijer, K. *et al.* Surface Modifications Created by Using Engineered Hydrophobins. **68**, 1367–1373 (2002).
  166. Artini, M. *et al.* Hydrophobin coating prevents *Staphylococcus epidermidis* biofilm formation on different surfaces. *Biofouling* **7014**, 1–11 (2017).
  167. Von Vacano, B. *et al.* Hydrophobin can prevent secondary protein adsorption on hydrophobic substrates without exchange. *Anal. Bioanal. Chem.* **400**, 2031–2040 (2011).
  168. Opwis, K. & Gutmann, J. s. Surface modification of textile materials with hydrophobins. *Text. Res. J.* **81**, 1594–1602 (2011).
  169. Wohlleben, W. *et al.* Recombinantly produced hydrophobins from fungal analogues as highly surface-active performance proteins. *Eur. Biophys. J.* **39**, 457–468 (2010).
  170. Hakanpaa, J. Two crystal structures of *Trichoderma reesei* hydrophobin HFBI--The structure of a protein amphiphile with and without detergent interaction. *Protein Sci.* **15**, 2129–2140 (2006).
  171. Grunér, M. S. *et al.* Self-assembly of class II hydrophobins on polar surfaces. *Langmuir* **28**, 4293–4300 (2012).
  172. Busscher, H. J., Uyen, M. H. M. J. C., Weerkamp, A. H., Postma, W. J. & Arends, J. Reversibility of adhesion of oral streptococci to solids. *FEMS Microbiol. Lett.* **35**, 303–306 (1986).
  173. Good, R. J. Contact angle, wetting and adhesion. *J. Adhes. Sci. technol.* **6**, 1269–1302 (1992).
  174. Adamson, A. W., & Gast, A. P. *Physical Chemistry of Surfaces*. New York: Interscience publishers. vol. 150 (1967).